Recombinant expression of cytochrome P450-2D6 and its application in tamoxifen metabolism

By

Munyai Vukosi Edwin
3699407

SUBMITTED TO THE UNIVERSITY OF WESTERN CAPE
In fulfilment of the requirements for the degree,

M.Sc. in Biotechnology

Faculty of Natural Sciences
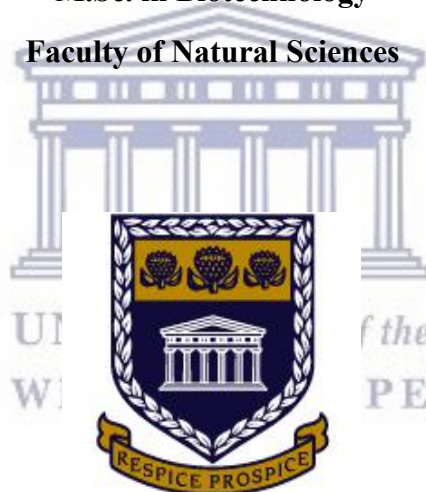
UNIVERSITY *of the*
WESTERN CAPE

Supervisor: Dr Takalani Mulaudzi-Masuku

Co-supervisor: Prof Emmanuel Iwuoha

MAY 2018

DECLARATION

I, …………………………….., declare that the content in this thesis or dissertation is my actual work (unless where it is indicated by references) and that neither the whole work nor any part of it has been, is being, or is to be submitted for another degree in this or any other university.

I support that the university may utilise this work, whole or any portion of the content, for the purpose of research.

Signature: …………………………………

Date: ……………………………………..

I

ACKNOWLEDGEMENTS

ABBREVIATIONS

ACS	American Cancer Society
Amp	Ampicillin
BCPI	Breast Cancer Prevention Institute
BSA	Bovine serum albumin
BRCA 1/2	Breast cancer gene 1/2
CPS	Counts per second
CYP	Cytochrome 450 enzyme
CV	Cyclic voltammetry
DNA	Deoxyribonucleic acid
E. coli	*Escherichia coli*
ER	Oestrogen receptors
FAD	Flavin adenine dinucleotide
FMN	Flavin mononucleotide
FDA	Food and Drug Administration
GE	Gold electrode
IARC	International Agency Research of Cancer
IPTG	Isopropylthiogalactosidase
kDA	Kilo Dalton
LOD	Limit of detection
MCF-7	Michigan cancer foundation 7
NaCl	Sodium chloride
NADPH	Nicotinamide adenine dinucleotide phosphate
NCBI	National Center for Biotechnology Information
NCI	National Cancer Institute
OD	Optical density
PCR	Polymerase chain reaction
RLU	Relative light units
SDS-PAGE	Sodium dodecylsulphate polycrylamide gel electrophoresis

SNRIs   Selective noradreline reuptake inhibitors

SERMs   Selective oestrogen receptor modulators

SSRIs   Selective serotonin reuptake inhibitors

SWV   Square wave voltammetry

TABLE OF CONTENTS

LIST OF TABLES

UNIVERSITY *of the*
WESTERN CAPE

LIST OF FIGURES

UNIVERSITY *of the*
WESTERN CAPE

Summary

Breast cancer is regarded as the most common form of cancer in women and it comprises of approximately 23 % of female cancers, while affecting women at any age range. For oestrogen receptor positive patients, tamoxifen is used as a prescribed medication for breast cancer therapy. However, tamoxifen in its natural form is not active to achieve the required treatment and prevention of breast cells proliferation. Since tamoxifen is a prodrug, it need to be converted into its active form, endoxifen, for which it is achieved by the action of the cytochrome P450 enzymes. Cytochrome P450 2D6 (CYP2D6) is a member of cytochrome P450 enzymes for which are superfamily of heme enzymes characterised by their ability to catalyse the oxidative reactions of compounds, including the pathway of tamoxifen metabolism. However, due to polymorphism that lead to inactive phenotypes of CYP2D6 in this gene, there is a challenge of diagnosing if a patient can metabolise tamoxifen or not. The current diagnostic tool, Amplichip® CYP450, for CYP2D6 is based on genotypes, and it lead to uncertainness as to whether the presence of functionalCYP2D6 alleles of CYP2D6 may lead to coding of active protein, thus leading to wrong treatment measures and overdose of tamoxifen. Electrochemical techniques have provided reliable, simple, quick, and sensitive methods for the determination of drug metabolism by enzymes. Therefore, it is important to develop a CYP2D6 phenotype-based sensor to detect and tell whether a particular individual can metabolise the drug or not.

This study was designed with the aim to clone the human CYP2D6, express and purify the recombinant protein in large quantities and at a cheaper way. Lastly, to design CYP2D6 based sensor and conduct electrochemical characterisation of tamoxifen metabolism. To achieve this aim, *in silico* studies have characterised CYP2D6 as a 50.05397 kDa molecular weight and insoluble transmembrane protein, with isoelectric point of pI = 6.21. A 1375 bp

amplicon of CYP2D6 was successfully cloned to generate pTrcHis-TOPO-CYP2D6 expression construct that was expressed as a 6x His fusion protein of ~ 68 kDa (including the Xpress TOPO and 6x His-tag). The protein was then purified under denaturing conditions using the Ni-NTA affinity system followed by its refolding. Finally, the activity of the protein was tested using the P450-GLO™ CYP2D6 assay, which indicated that the enzyme was successfully refolded and active to be used for post-expression applications. Analysis of the absorbances using UV-Vis spectroscopy, indicated that CYP2D6 has a sorbet absorbance band at 216 nm, and it shifted upon the additions of tamoxifen, which implied the binding of tamoxifen to CYP2D6. Analysis of emission using fluorescence spectroscopy showed undefined fluctuation shifts upon the addition of tamoxifen with emission characteristics. The binding of tamoxifen to the heme site of CYP2D6 was also monitored electrochemically by detecting shifts in the potential that occurred upon addition of tamoxifen. The observed shifts in both unfolded and folded proteins correlate to the differential binding of the tamoxifen molecules to the reduced states of the heme (redox active site). Further, it was observed that the electrochemical response of both proteins was also influenced by the structure conformation (folded or unfolded). Cloning and electrochemical characterisation of the CYP2D6 gene provides a promising means to study and develop a CYP based biosensor for breast cancer therapy at low cost. However, there is a need to study more and to use a molecular linker when immobilising the protein on gold electrode in order to improve the electron transfer in the electrochemical system.

CHAPTER 1: LITERATURE REVIEW

1.1 Introduction

Breast cancer is globally health challenge and the most common one in females, comprising approximately 23% of female cancers (Parkins and Fernández, 2006; Ramathuba *et al*., 2015). It is the second most common cancer behind skin cancer (Ferlay *et al*, 2012), affecting women in any age range (Omotara *et al*, 2012). However, breast cancer risk increases with age and it has been the main cause of mortality in women aged over 40 years (Omotara *et al*., 2012; Ramathuba *et al*., 2015). Based on the recent breast cancer statistics by the International Agency for Research on Cancer (IARC) (2012), there were approximately 14.1 million new cancer cases and 8.2 million cancer deaths worldwide. It was also estimated that by 2030, there will be about 21.7 million global new cancer cases and about 13 million cancer deaths, for which will be influenced mainly by population growth and aging (Torre *et al*., 2016). The oestrogen hormone is responsible for stimulation and progression of breast cancer proliferation (Chang, 2012). The hormone binds to the breast cells through oestrogen receptors, thus stimulating nuclear DNA to proliferate the breast cells into cancerous cells (Travis and Key, 2003). The biological action of oestrogen is mediated by the presence of oestrogen receptors for which nearly 70 % of breast tumours expresses the oestrogen receptors and also progesterone receptors (Chang, 2012; Roy and Vadlamudi, 2012).

Breast cancer treatment depends on the patient's specific type of breast cancer, whether is oestrogen dependent or non-oestrogen dependent (ACS, 2017). There are 5 types of breast cancer treatment namely; hormonal therapy, aromatase inhibitors, lumpectomy, radiation, and chemotherapy. Selective oestrogen-receptor modulators (SERMs: Tamoxifen or Raloxifene) and aromatase inhibitors (anastrozole, exemestane, and letrozole) are also used after surgery, radiation or chemotherapy in order to decrease the possibility of breast cancer recurrence.

1

Hormonal therapy by the use of tamoxifen is the most common prescribed measure for oestrogen receptor positive breast cancer (NCCN, 2013).

Liver cytochrome P450s are involved in metabolism of tamoxifen into its active form, endoxifen, necessary for prevention or stopping breast cancer proliferation (Cronin-Fenton *et al.*, 2014). CYP2D6 and CYP3A4/5 enzymes are the main enzymes in the conversion of tamoxifen into its more active metabolites (Lee *et al.*, 2005; Borges *et al.* 2006; Dean, 2016). However, CYP2D6 is of more significance since it is highly polymorphic with alleles that are metabolically inactive (Ingelman-Sundberg *et al.*, 2007; Pinto and Dolan 2011). Therefore, it is believed that there is an association between CYP2D6 genotyping and phenotyping for drug metabolism purpose (Fleeman *et al.,* 2010). Since CYP2D6 is a heme containing enzyme and it confers electron exchange in association to drugs, this has brought interest in designing a CYP2D6 based electrochemical biosensor which will focus on the phenotypic function of CYP2D6. This review will focus on breast cancer, its treatment with tamoxifen, brief discussion on the enzymes responsible for tamoxifen metabolism, and finally electrochemical biosensor used for testing tamoxifen metabolism.

1.2 Breast cancer and its development

Breast cancer is regarded as a clonal disease that occurs when somatic cells undergo the process of abnormal growth and to express full malignant potential (Balmain *et al*., 2003; Mohanty *et al*., 2012). Most breast cancers begin to develop in breast tissues, milk glands such as lobules, and ducts that connect the lobules to the nipple (ACS, 2016). According to Mohanty *et al*., (2012), breast cancer was originally a single disease of the breast, for which through extensive research and clinical studies it was then defined as a breast tumour. Hence, it is important that patients receive therapy that is specific to the breast cancer type. Breast cancer is known to be a hormone responsive type of cancer (Folkerd and Dowsett, 2010).

Factors such as age, family history, clinical history, a late first pregnancy, prolonged exposure to hormones, and life style (overweight or obesed after menopause, physical inactivity, alcohol consumption) can play a role in the development of breast cancer (Roche, 2016).

Breast cancer is regarded as a hormone-dependent tumorous condition by which the hormone binds to hormone response elements on the nuclear DNA, activating or suppressing specific sequences in the regulatory regions of breast cancer genes thus causing uncontrolled cell growth and differentiation (Clemons and Goss, 2001; Travis and Key, 2003). Hormone such as oestrogen is commonly known to be responsible for stimulation and progression of breast cancer (Chang, 2012). The biological action of oestrogen is mediated by the presence of oestrogen receptors for which are expressed on their surfaces (Chang, 2012; Roy and Vadlamudi, 2012). Therefore, breast cancer cells which express oestrogen receptors are referred to as oestrogen receptor positive. Oestrogen causes the stimulation of breast cancer by binding to the oestrogen receptor thus leading to cell proliferation, mutation and expression of breast cancer gene 1 (BRCA1) and breast cancer gene 2 (BRCA2) which result to breast cancer (Goetz et al., 2008; Kitagishi et al., 2013). After oestrogen binds to oestrogen receptors, a quick induction of mitosis takes place with mutations in each generations and there is a shorter time for DNA to undergo repair processes (BCPI, 2007). The mechanism of stimulating the development of breast cancer by oestrogen is shown below in Figure 1.1. Therefore, the reliable therapeutic measure for all stages of the disease in highly susceptible woman (at pre- and postmenopausal stages) need to target the oestrogen receptors by using antioestrogens (Chang, 2012).
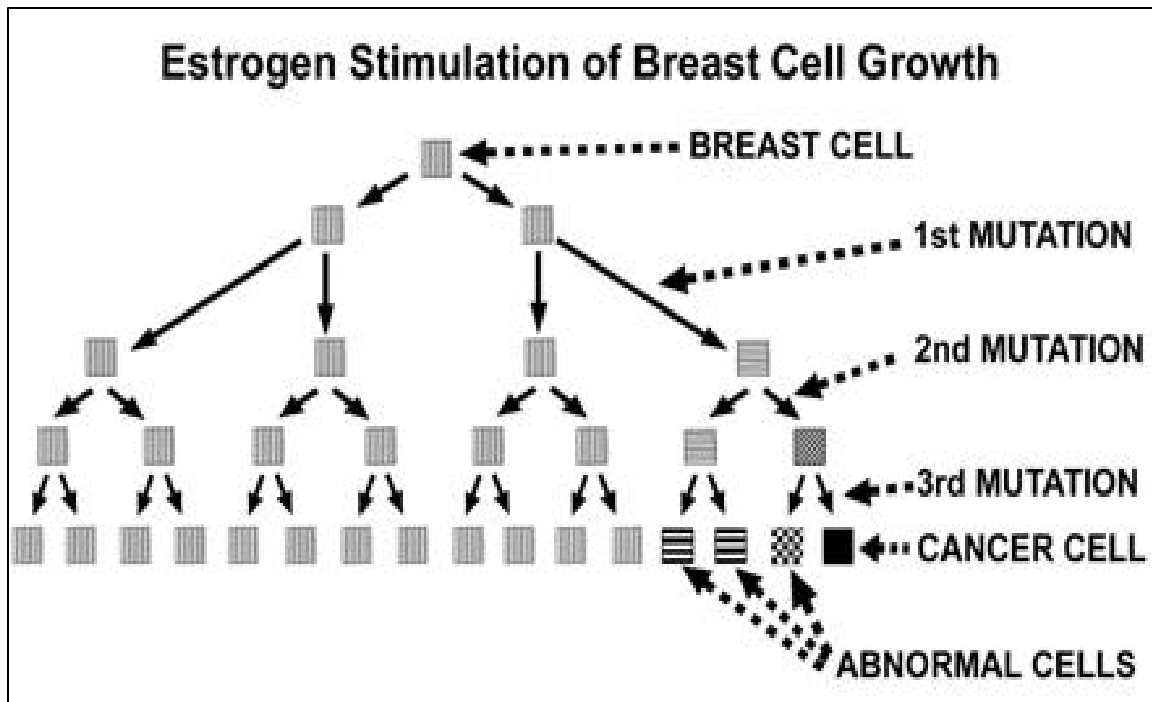
Figure 1.1: The development of breast cancer abnormal cells. Through oestrogen binding to the breast cells, a quick induction of mitosis takes place and DNA synthesis takes place with each mitotic doubling of cells. A short doubling time may result in more mutations, because the cell has a shorter resting phase (i.e., a shorter time for DNA repair). (BCPI, 2007). http://www.bcpinstitute.org/onlinepub.htm.
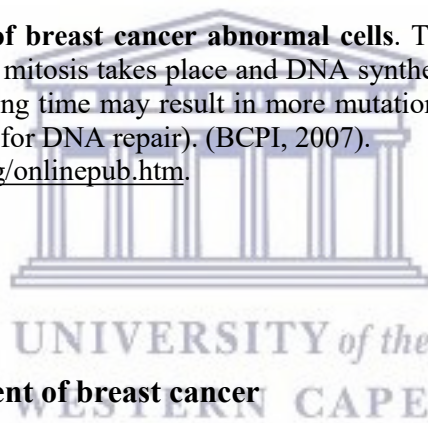
1.3. Tamoxifen

1.3.1 Tamoxifen as a treatment of breast cancer

Tamoxifen is one of the selective oestrogen receptor modulator (SERM); and a standard care for many women with oestrogen receptor positive breast cancer (Fleeman *et al* 2010). Tamoxifen binds to oestrogen receptors and thus block the oestrogen effect of stimulating the growth of breast cancer cells. Tamoxifen blocking action occurs by up-regulating the production of transforming growth factor B (TGFb) for which it inhibits tumour cell growth, while down-regulating the insulin-like growth factor 1 (IGF-1), that is responsible for the stimulation of breast cancer cell growth (NCI, 2018). Since it was approved by Food and Drug Administration (FDA) in 1977 and later years, it has been used for more than 30 years to treat hormone receptor–positive breast cancer (Lukong, 2017). In 1985, FDA approved its

4

use as an adjuvant therapy in postmenopausal women followed by its approval for its use alone in 1986. In 1989-1990, FDA established the approval of tamoxifen use in premenopausal women with oestrogen receptor positive breast cancer and for pre and postmenopausal patients, who had node-positive oestrogen receptor-positive breast cancer. In 1993, FDA approved the indication for tamoxifen use in the treatment of advanced breast cancer in men (MacGregor and Jordan 1998; Goss *et al*., 2005). Tamoxifen is administered orally as a prodrug and it has less effect than its active forms that are formed within the body, therefore its metabolism is important in order to have an impact during breast cancer therapy. Depending on the individual state, the recommended length of time that tamoxifen is taken differs from individual to individual ranging from 5 to 10 years (Sugerman, 2013). The daily dose that is recommended for tamoxifen is between 20 - 40 mg (FDA, 2006).

1.3.2 Tamoxifen metabolism

The pharmacological active forms of tamoxifen, 4-hydroxytamoxifen, N-desmethyl-4-hydroxytamoxifen and endoxifen have 30-100 times more affinity to oestrogen receptors than tamoxifen itself (Cronin-Fenton *et a*l., 2014). Endoxifen as an antagonist of oestrogen, has more affinity for binding to oestrogen receptors due to its similarities to oestrogen, both baring methyl (-CH3) and hydroxyl (-OH) groups (Cronin-Fenton *et a*l., 2014; Kelly *et al*., 2017). Cytochrome P450 enzymes that are abundant in the liver such as CYP3A4/5, CYP2C9, CYP2C19, CYP2B6, and CYP2D6, are responsible for the metabolism of tamoxifen into its active functional form, endoxifen (Cronin-Fenton *et al*., 2014). However, the main enzymes in this conversion process are CYP2D6 and CYP3A4/5 (Lee e*t al*., 2005; Borges *et al*. 2006; Dean, 2016). Therefore, CYP2D6 is of more importance since it is highly polymorphic thus leading to alleles that are metabolically inactive (Desta *et al*., 2004; Ingelman-Sundberg et al., 2007; Pinto and Dolan 2011). The

conversion of tamoxifen into its metabolites is shown in Figure 1.2, indicating two pathways and steps that involve associated cytochrome P450s. Several studies have shown that that there is a clinical evidence linking CYP2D6 metabolising status to tamoxifen metabolism on patients. A clinical trial was conducted by North Central Cancer Treatment Group (Trial 89-30-52), and they treated women with oestrogen receptor positive type of cancer at postmenopausal and thus drew the tamoxifen metabolic statuses in different patients (Goetz *et al*., 2005; Ferraldeschi and Newman, 2010).
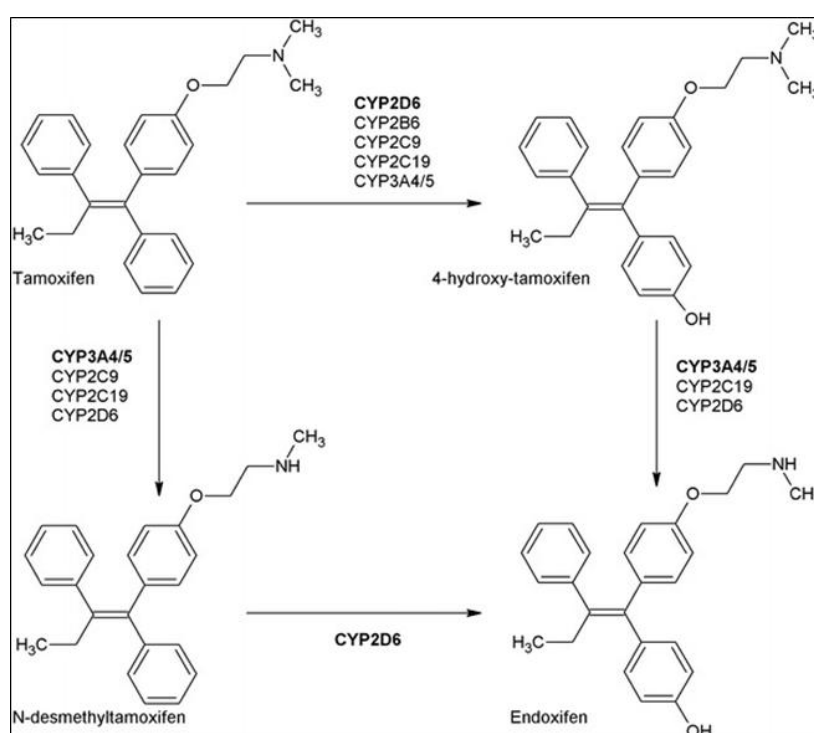
Figure 1.2: Tamoxifen metabolism to its active metabolites. Tamoxifen conversion involves two pathways which involves either CYP2D6 or CYP3A4 in a two-step bi-products (N-desmethltamoxifen and 4-hydroxytamoxifen) to endoxifen. However, other cytochrome p450 enzymes are also involved to assist these main enzymes in converting tamoxifen into endoxifen (Desta *et al*., 2004).

1.3.3 Variation in tamoxifen metabolism

Interindividual variation in human drug response is a huge challenge in therapy (Samer *et al*., 2013). Factors such as age, gender, race/ethnicity, disease states, organ dysfunctions, smoking, diet, and concomitant medications are known to influence variation in drug responses (Franceschi *et al*., 2008; Frere *et al*., (2008). Genetics is another source of

interindividual variability known to influence drug response (Samer *et al*., 2013), hence it is important to know the genetic expression level of CYP2D6 in breast cancer therapy. There are different causes of variations that can result in tamoxifen metabolism and these include; (1) reduction in CYP2D6 activity due to the uptake of inhibitors and (2) polymorphism in the CYP2D6 gene, for which both have shown to reduce the level of endoxifen (Borges *et al*. 2006). Certain drugs such as selective serotonin reuptake inhibitors (SSRIs) and selective noradrenaline reuptake inhibitors (SNRIs) are used to combat stress and depression and at the same time they inhibit the activity of CYP2D6 (Hoskins *et al*., 2009). SSRIs such as fluoxetine and paroxetine are known to have negative impact on the formation of tamoxifen metabolites, therefore negatively impact the efficacy of tamoxifen therapy (Hoskins *et al*., 2009). Polymorphisms in genes responsible for tamoxifen metabolising enzymes, drug receptors, drug transporters production and molecules involved in signal transduction mechanisms they play a major role on the functional reduction of these molecules and thus affect efficacy or toxicity of a drug (Johnson and Lima, 2003). The study by Jin *et al*. (2005) showed that patients with extensive metabolising genotypes whom were taking such CYP2D6 inhibitors, developed low concentrations of plasma endoxifen. A follow up study by Borges *et al*. (2006) showed that 158 patients with breast cancer who were taking adjuvant tamoxifen were examined to have 33 alleles of CYP2D6 including many variants.

1.4 Cytochrome P450-2D6

Cytochrome P450 enzymes are large superfamily of enzymes that are abundant in the liver and are involved in a number of oxidative-reductive reactions of exogenous and endogenous compounds (Cronin-Fenton *et al.*, 2014). Possible redox reactions of cytochrome P450 enzymes are due to the presence of heme centre (iron protoporphyrin IX ring), which achieve electron exchange between a compound and a cytochrome P450 protein (Capece *et al.*, 2008).

Cytochrome P450 enzymes have been identified in all domains of life including animals, plants, fungi, protists, bacteria, archaea, and even in viruses. However, they have not been found in *Escherichia coli* bacterial species (Lamb *et al.*, 2009). Recently, it was discovered that there are more than 21,000 distinct known CYP proteins (Nelson, 2009). Cytochrome P450 enzymes are coloured ("'chrome') cellular " (cyto") with a sorbet peak absorbance of light at wavelengths approximately 450 nm, when the heme iron is reduced and complexed to carbon monoxide thus the name "Cytochrome P450" (Mathew, 2010).
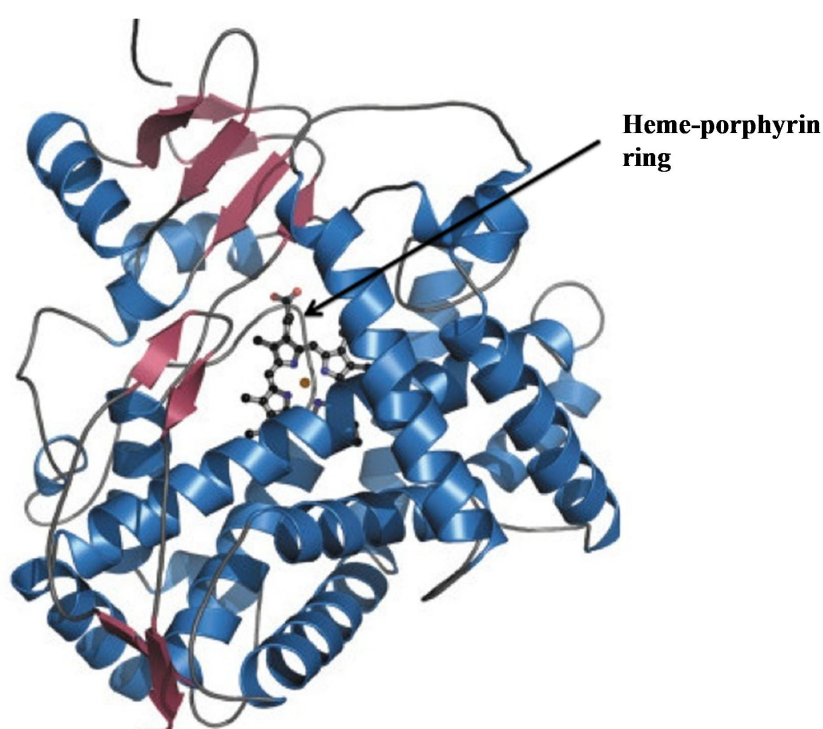
Figure 1.3: The 3D typical structure of cytochrome p450 enzymes (Matthew, 2010). The heme-porphyrin ring provides a site where electrochemical electron exchange takes place and it bared in the centre of protein's main lobes.

Cytochrome P450 2D6 (CYP2D6) as a member of cytochrome P450 enzymes is involved in oxidative-reductive reactions of exogenous and endogenous compounds, including tamoxifen as a drug (Cronin-Fenton *et al.*, 2014). CYP2D6 gene has a number of mutant alleles which are due to polymorphic insertion or deletion of base pairs in the gene sequence (Meyer and Zanger, 1997; Singh *et al.*, 2011). Such genetic change causes variation in the tamoxifen metabolic pathway, thus leading to less or no tamoxifen active metabolites. The allelic

variant distribution differs among different population ethnic groups (Lewis *et al.*, 2004), and it influences different drug metabolism. Patients are classified into four (4) groups based on metabolic activity of CYP2D6 (McGraw *et al* 2012) including (1) Poor metabolisers (with variants that result in poor metabolism), (2) Intermediate metabolisers (with moderate variants), (3) Extensive metabolisers (normal metabolism), and finally (4) Ultra rapid metabolisers (higher metabolism). It has been observed that Caucasians are of more considered and there is approximately 6 - 10 % of individuals which are poor metabolisers, 10 - 15 % which are intermediate metabolisers, and up to 10 - 15 % which are ultra-rapid metabolisers (Horn and Hansten, 2008; Brauch *et al*. 2009).

To date, the alleles of CYP2D6 are reported to be more than 100 variants (*) in humans (Pinto and Dolan, 2011). The most significant and commonly studied variants include CYP2D6*9, CYP2D6*10, CYP2D6*17, CYP2D6*29, and CYP2D6*41, which have reduced functional activity; CYP2D6*3 through CYP2D6*8 as well as CYP2D6*36, which have no functional activity; and duplications of CYP2D6*1xN, CYP2D6*2 or CYP2D6*35 which lead to enhanced functional capacity and the ultra-rapid metaboliser phenotype (Ingelman-Sundberg *et al*., 2007; Pinto and Dolan 2011). Table 1 shows a full summary of all alleles of CYP2D6 gene, duplication of CYP2D6 gene alleles and their associated enzyme activity in metabolising drugs. Study by Ferraldeschi and Newman (2010) have indicated that a huge number of lower frequency polymorphisms in CYP2D6, results in a reduced activity, and may contribute to the extensive inter-individual differences in CYP2D6 metabolic ability.

Table 1.1: Alleles of CYP2D6 and their associated activity (Zhou, 2009)

CYP2D6 alleles	Allele designation	Metabolic status	Enzyme activity
*1,*2, *33. *35	Normal or wild type	Extensive metaboliser	Normal
*3, *4, *5-8, *11-16, *18-21, *36, *38, *42, *44, *56, *62	Null	Poor metaboliser	No protein or inactive
*9, *10, *17, *29, *41 59	Reduced activity	Intermediate metaboliser	Decreased
*22-28, *30-32, *34, *37, *43, *45-55	Unknown activity	Not applicable	Unknown
Duplicated alleles			
*2xN, *2xN *35xN	Multiplication of normal alleles	Ultra-metaboliser	Increased
*10xN, *17xN *29xN *41xN	Multiplication of reduced activity alleles	Intermediate metaboliser	Decreased
*4xN, *6xN, 36xN	Multiplication of null alleles	Poor metaboliser	No protein or inactive
*43xN, *45xN	Multiplication of alleles of unknown activity	Not applicable	Unknown

1.5 Implications of CYP2D6 poor metabolic activity

Human deficiency in CYP2D6 activity has been observed among up to 10% of whites that may have an altered capacity in processing these drug agents (Zanger *et al.*, 2004; Gonzalez and Yu, 2006), which is a problem since these patients may be at high risk of incurable cancer using drugs, particularly tamoxifen in this case. CYP2D6 deficiency is basically connected to the complete defect of the CYP2D6 gene for which a broad range of DNA sequence variations may result (Zanger *et al*., 2004). The breast cancer occurrence can lead to death with about 1 in 36 chance a woman's death (Omotara *et al* 2012; ACS, 2016). Although the death rate has been declining since 1989 (due to the result of earlier detection through screening, increased awareness and improved treatment) (ACS, 2016), the concern lies on the increased breast cancer deaths estimated in 2012 by the International Agency for Research on Cancer that there will be 21.7 million new cases and cancer deaths of about 13 million. Some patients have mutations in certain genes such as breast cancer gene 1 (BRCA1) and breast cancer gene 2 (BRCA2) having various high- and low-risk susceptibility to breast cancer

(Goetz *et al.*, 2008).

1.6 Assessment methods for assaying tamoxifen metabolism

Genetic variants of CYP2D6 have been discovered and studied by a number of cohorts in recent years (Zhou *et al.*, 2012), not just for breast cancer therapy but also for a number of a wide range of drugs and diseases. Therefore, it is necessary that each patient must be tested for the ability to metabolise tamoxifen. Assessment of CYP2D6 gene's presence and activity involves collection of different samples that may be taken *in vivo* or *in vitro* for CYP 450 tests on blood samples, cheek swab and saliva collections (Roche, 2016). The present study involves the bio-electrochemical characterisation of CYP2D6 in tamoxifen metabolism for which it is based on CYP2D6 phenotype itself.

1.6.1 Genotyping of CYP2D6-current method

There was a growing forecast that genotyping of CYP2D6 gene may be used to assist in treatment decision-making in whether patients should take tamoxifen or not (Fleeman *et al.*, 2011). According to Honskins *et al.* (2009) tests for genotyping CYP2D6 were supposed to quicken the identification for proper administration of medications. Based on literature, most studies also helped in clarifying the advice to clinical researchers that CYP2D6 genotyping could guide in selecting the correct anti-oestrogen therapy for postmenopausal women with early-stage breast cancer, and how to best treat patients that are intermediate or poor metabolisers (Goetz *et al.*, 2008; Chang, 2012; Rae, 2013). To date, the FDA have approved the diagnostic tool, Amplichip® CYP450 (the only commercial complete test), which was successful for screening only 33 variants in the CYP2D6 gene (Roche, 2016). CYP2D6 genotyping can help in determining whether tamoxifen is to be administered to patients or not. However, studies that established the clinical utility of CYP2D6 genotyping (using Amplichip® CYP450) in determining treatment choice or dose, in relation to tamoxifen

therapy have not yet been published (Honskins *et al*., 2009). In addition, the presence of CYP2D6 genes that are of functional metabolic activity is not always associated with the expression of protein itself (Isozymes, 2009). A rapid diagnostic tool that will achieve the detection of CYP2D6 activity in metabolising tamoxifen at a phenotypic level is required, such that it will detect if the enzyme is active based on its availability on the blood samples.

1.6.2 Bio-electrochemical testing using biosensors

A biosensor is defined as a device that detects biochemical interaction by generating signals proportional to the amount of an analyte in question (Bhalla *et al*., 2016). According to Sassolas *et al*. (2011), biosensor is composed of two elements, namely: (1) bioreceptor, a sensitive attached biological element such as enzyme, DNA probe, antibody recognising the analyte (e.g. enzyme substrate, complementary DNA, antigen), (2) transducer which is used to convert biochemical signal that occurs due to interaction of analyte with the bioreceptor (Asturias-Arribas *et al* 2014). Electrochemical transducers are used to develop biosensors and have advantageous characteristics such as cost effective and easiness to design. Electrochemical biosensor are characterised by the use of electrochemical cell usually containing three electrodes (working, reference and counter electrodes) (Asturias-Arribas *et al* 2014). The electrochemical cell set up is connected to the potentiostat for electron exchange and the results are monitored in the computer system as shown in Figure 1.4. The reference electrode is used to maintain a known redox potential and is usually made of basically made of Ag/AgCl. The working electrode function as an element in which a reaction in question is focused, while the counter electrode provide a current in and to the electrolytic solution to the working electrode. In order for this setup to be functional, the three electrodes should both be conductive and chemically stable at a pH that favours both elements (Koyun *et al*., 2012). The advantages of electroanalytical sensors are that they

permit the analysis of species with great specificity, they are very rapid, sensitive, highly selective and cost effective. According to literature, it is already implemented for clinical analysis, particularly for glucose level in diabetic patients (Dixon *et al*., 2002; Koyun *et al*., 2012). Good results in the determination of some drugs *in vitro* have been obtained by electrochemical methods and its application has greatly increased over the last few years (Álvarez-Lueje *et al*., 2012; Siddiqui *et al*., 2017).
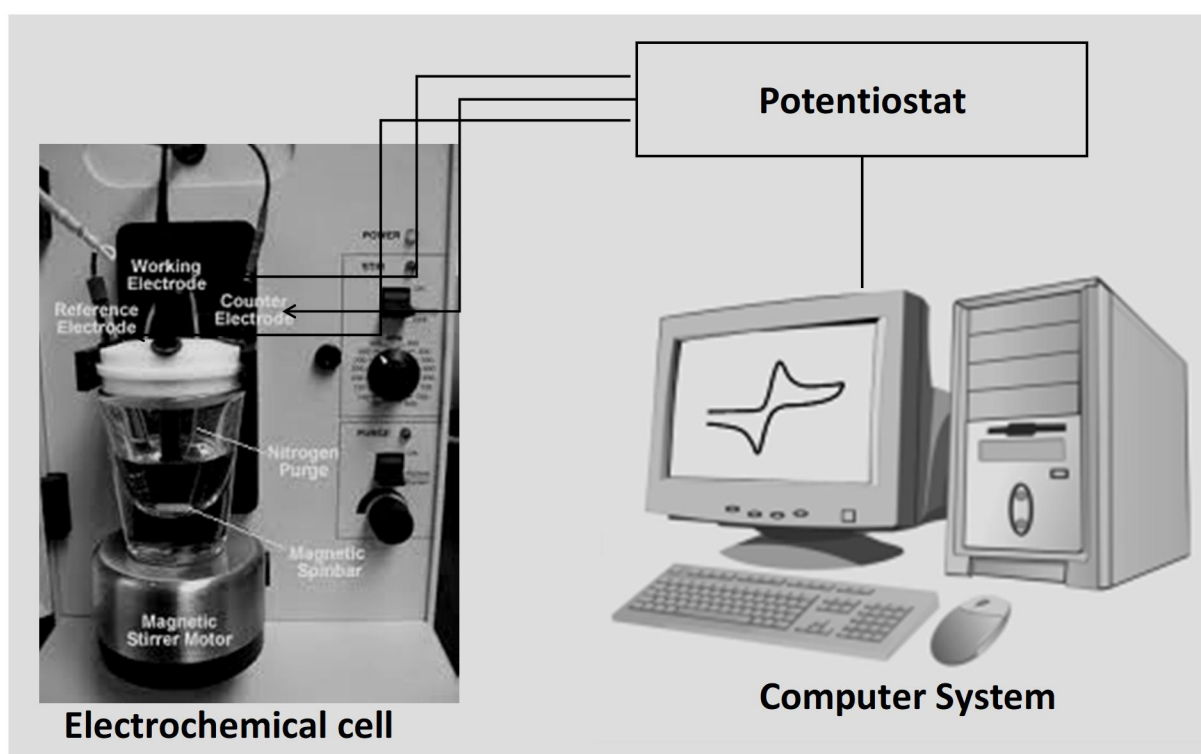
Figure 1.4: The electrochemical analysis set up. The electrochemical cell contains three electrodes (working, counter, and reference) connected to the potentiostat to generate the data and computer system for data monitoring (computed on Microsoft office power point).

The transfer of electrons between proteins and drug is an essential feature, and it is therefore of importance in the mechanism of electron transfer of cytochrome P450 enzymes, where electrons are transferred to and from their substrates (Bistolas *et al*., 2005), Recent researchers have measured tamoxifen and endoxifen plasma *in vivo* concentrations following the administration of tamoxifen in breast cancer therapy (Honskins *et al*., 2009). In this study,

the selective determination of tamoxifen metabolism by CYP2D6 was performed using electrochemical biosensor.

1.7 Study rationale

Breast cancer is the leading cause of most fatal incidences in women and men worldwide, and the most prescribed drug is tamoxifen. However, there is an inter-individual differences in response to tamoxifen treatment for which is linked to drug metabolism classification due to associated polymorphism in the CYP2D6 gene. Tamoxifen metabolism by patients is categorised into four metabolic profile due to CYP2D6 polymorphism and it results in non-active phenotypes of CYP2D6, which cannot metabolise tamoxifen. Therefore, there are challenges with the current diagnostic tool, Amplichip® CYP450, which is genotypic based since it is time consuming, expensive and has inconclusive drug metabolic results. It is therefore important to develop new procedures which will be easy to use at a low cost. In this study, it will be the first time that this gene is cloned, expressed and purified with the purpose to develop a rapid biosensor for screening the metabolic status of patient's tamoxifen metabolism.

1.8 Aim and objectives

The present study was designed with the purpose to develop a simple, low cost CYP2D6 biosensor which will test the tamoxifen metabolism in breast cancer patients, with the specific objectives:

● To conduct *In-Silico* characterisation of CYP2D6.

● To produce a highly purified active recombinant CYP2D6 protein.

● To prepare a biosensor and conduct electrochemical analysis in order to measure the redox potential of recombinant CYP2D6 in metabolising tamoxifen in vitro.

- To conduct electrochemical analysis to measure the redox potential in breast cancer cells in response to tamoxifen treatment (*Future work*).

- And lastly, to develop a prototype, for rapid and simple detection of tamoxifen metabolism in breast cancer patients (*Fututre work*).

CHAPTER 2: *In silico* characterisation, cloning and recombinant expression of cytochrome P450 2D6 (CYP2D6)

ABSTRACT

Cytochrome P450 2D6 (CYP2D6) is a member of the cytochrome P450 enzymes, which catalyse oxidative reactions of exogenous and endogenous compounds, including various drugs. CYP2D6 is one of the main enzymes together with other cytochrome P450 enzymes that are responsible for tamoxifen metabolism. However, it has been observed that not all tamoxifen treated patients are able to metabolise tamoxifen and this is due to the polymorphic behaviour of these enzymes. It is of importance to develop a simple mechanism that will detect and tell whether a particular individual can metabolise tamoxifen or not before given a drug. Enzyme biosensors are an effective and quick way that have been used to study redox reactions and drug metabolism, however due to the high cost of commercial enzymes, thorough investigations are limited. Therefore, this chapter aimed at generating a CYP2D6 expression construct for high throughput expression of recombinant protein at an affordable manner. *In silico* characterisation indicated that CYP2D6 is a 50.05397 kDa insoluble, transmembrane protein that is located mainly in the endoplasmic reticulum and the extracellular space. Its 3D structure is characterised by an iron porphyrin IX ring that is located in the centre. CYP2D6 was cloned successfully into pTrcHis-TOPO® vector, over-expressed as a ~68 kDa protein (including ~4 kDa Xpress TOPO epitope and ~4 kDa 6x His tag and TOPO priming sequences of ~10 kDa), and further purified under denaturing conditions using the Ni-NTA affinity system followed by refolding. Finally the activity of the protein was assayed using P450-GLO CYP2D6 kit, which indicated that the enzyme was successfully refolded and active for post-expression applications.

Key words: Cloning, CYP2D6, Enzyme activity, *In silico,* Over-expression, Purification.
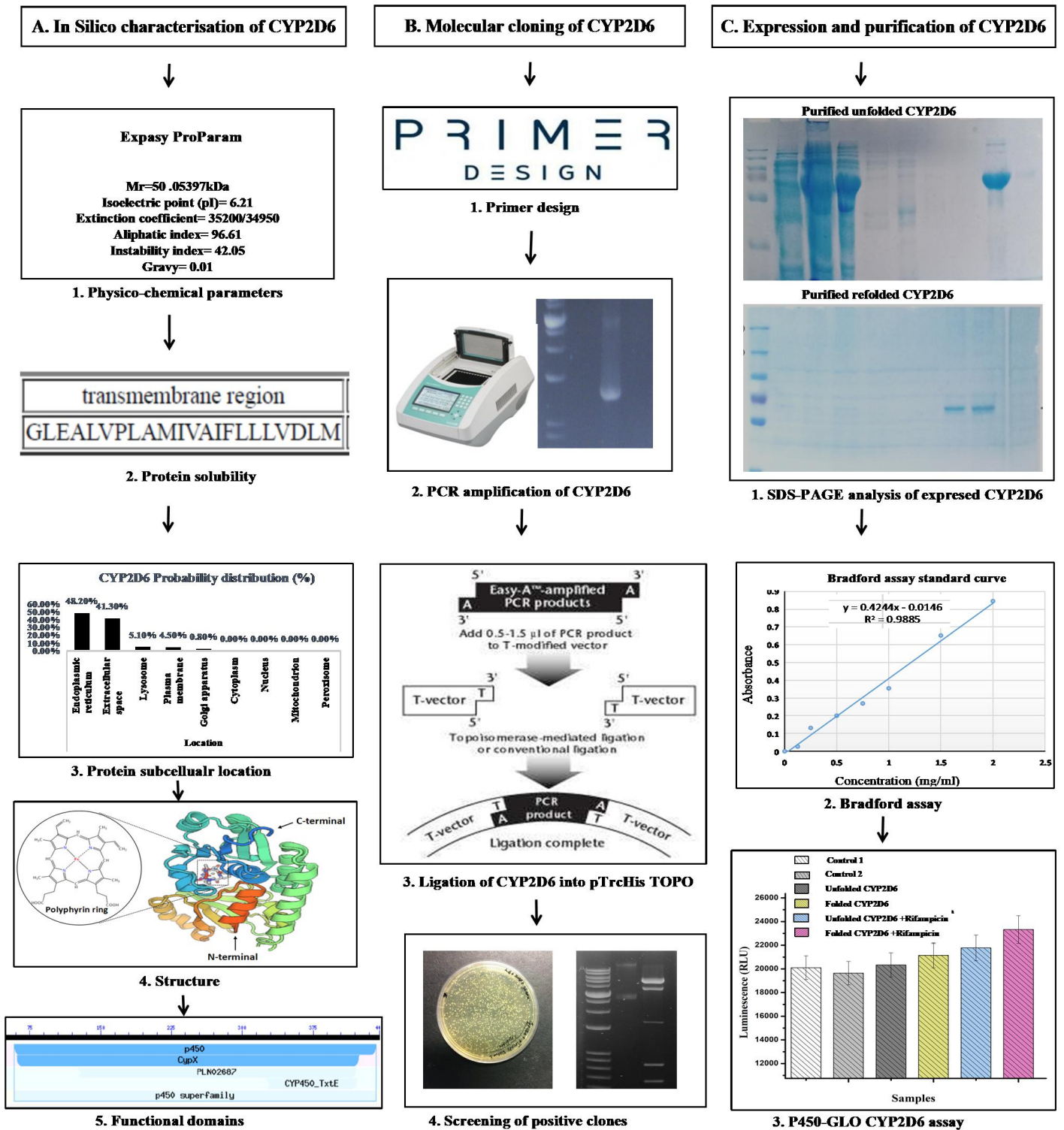
Figure 2.1: Graphical abstract illustrating the *In silico* and molecular characterisation of CYP2D6 (The abstract was computed using Microsoft Power Point).

2.1 Introduction

Cytochrome P450 2D6 (CYP2D6) is a heme-containing enzyme, which is responsible for the catalysis or removal of exogenous and endogenous compounds, including various drugs (Subehan *et al*., 2006). CYP2D6 and CYP3A4/5 are the main and abundant enzymes that are responsible for tamoxifen metabolism into its final most active product, endoxifen (Mathew, 2010). Therefore, these enzymes are of clinical importance during breast cancer therapy using tamoxifen (Zanger *et al*., 2004). CYP2D6 is highly polymorphic thus it leads to many allelic variants that affects tamoxifen metabolism efficiency (Surekha *et al*., 2010; Zhou *et al*., 2012; Wang *et al*., 2015). In order to study the metabolism of tamoxifen using the redox reaction, cytochrome P450 enzymes are required to be used as biosensors. General molecular studies of recombinant proteins require *in silico* characterisation of proteins as a starting point, in order to understand their physico-biochemical behaviour in expression systems especially bacterial cells (Negi *et al.,* 2017). Therefore, bioinformatics techniques are tools of choice to provide information on the protein's characteristics such as protein length, molecular weight, isoelectric point (pI), solubility, subcellular localisation, structure and functional domains (Rehm, 2001).

Recombinant protein production involves genetic manipulation in order to produce a construct of interest to be expressed in a recommended simple expression host such as *E. coli* (Rosano and Ceccarelli, 2014). Engineering of proteins usually involves the use of vectors as expression systems suited to express proteins in different cells (Turanli-Yildiz *et al*., 2012). The expression system usually contains sequences that have important functions in several steps of genetic engineering such as cloning, expression and purification of proteins (Fakruddin *et al*., 2013). There are different types of expression systems with different advantages and disadvantages in the entire protein production process (Liu *et al*., 2012).

Therefore, it is of more significance to choose the best expression system which suits the target protein (Rosano and Ceccarelli, 2014). The pTrcHis-TOPO® TA vector system was chosen as a vector of choice in this study, due its high efficiency, fast-direct insertional way of amplified PCR products for expression in *E. coli* (Yuvaraj, 2007). More advantageously is that the ligation occurs in the absence of DNA ligase and post PCR procedures such as digestion of the insert and plasmid are not neccessary. In addition, PCR primers are not likely to contain specific restriction endonuclease digestion sequences since the plasmid contains its own restriction sites for screening purposes (Chaudhary *et al.*, 2014). The technique has adopted the biological activity of DNA topoisomerase I, which cleave and re-join supercoiled DNA ends to facilitate replication. In order to insert the gene of interest, the topoisomerase is covalently bounded at each end of un-circular plasmid bearing single 3´-thymidine (T) overhangs, and it facilitate the joining of single 5´-Adenosine (A) overhangs of insert to form T-A bonds. Once the gene sequence of interest is inserted into a plasmid, the construct is transformed and expressed in *E. coli*.
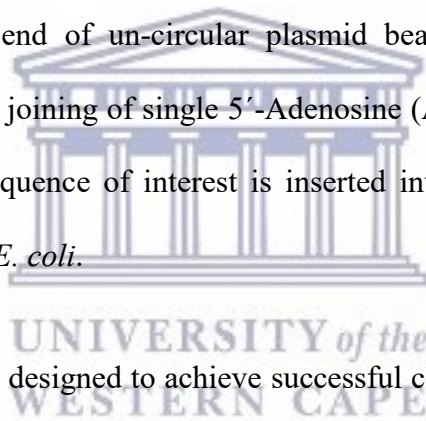
The pTrcHis-TOPO® vector is designed to achieve successful cloning and expression through several features. (1) The trc promoter, a hybrid promoter containing the –35 region from the trpB promoter and the –10 region from the lacUV5 promoter for high-level expression in *E. coli* (Brosius *et al.*, 1985; Amann *et al.*, 1983; Mulligan *et al.,* 1985). (2) The lacO sequence for binding the lac repressor encoded by the lacIq gene. In the absence of IPTG, lac repressor binds to the lacO sequence, repressing transcription, whereas upon addition of IPTG, expression is induced (Jacob and Monod, 1961; Müller-Hill *et al.,* 1968). (3) rrnB antitermination sequence that reduces premature transcription termination (Li *et al.,* 1984). (4) T7 gene 10 translational enhancer sequence for more efficient translational initiation (Olins et al., 1988). (5) A minicistron containing nucleotides that are efficiently translated in

prokaryotic cells for enhanced translational efficiency (Schoner *et al*., 1986). (6) An N-terminal peptide containing the HisG epitope, the Xpress™ epitope and a 6x His-tag for detection and purification of the recombinant protein. (7) An enterokinase recognition site for removal of the N-terminal peptide. Because of its small size and the simplicity that goes with its incorporation, the 6x His-tag is widely used for the purification of recombinant proteins and is less likely to interfere with protein structure and function (Niiranen *et al.*, 2007). All these features of the pTrcHis-TOPO® plasmid are indicated in Figure 2.2.
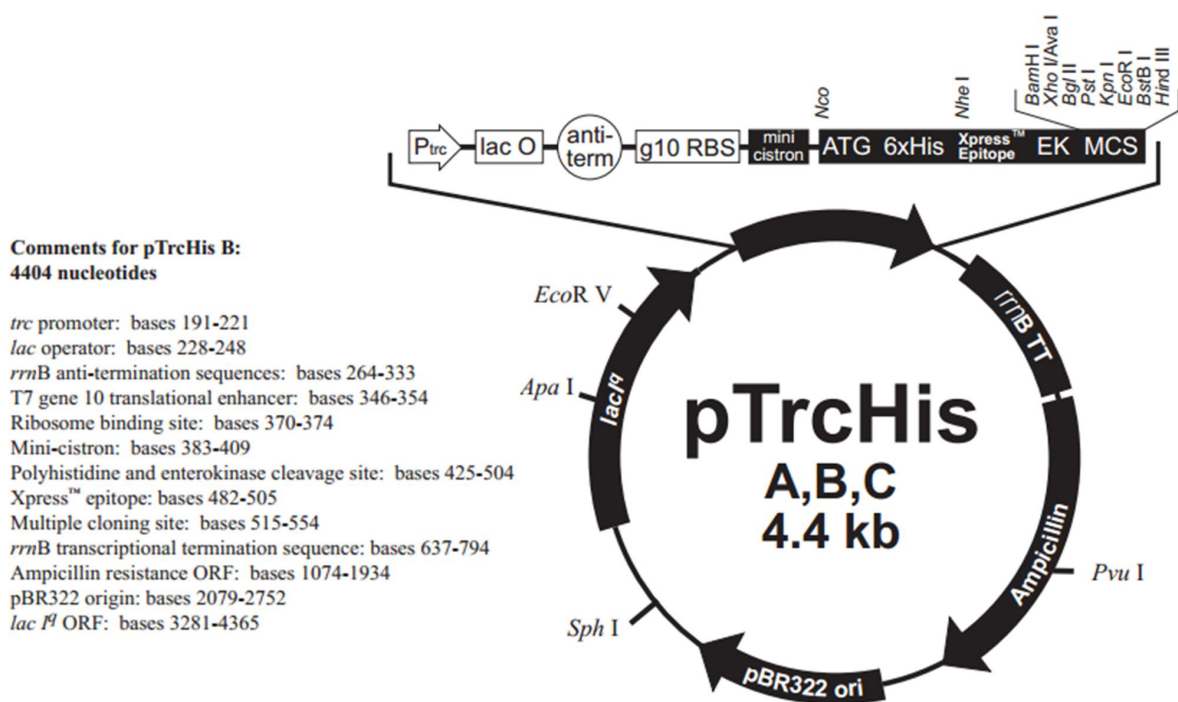
Figure 2.2: Circular map of the pTrcHis-TOPO® expression vector. The map shows the T7 *lac* promoter, which increases expression of high levels of proteins under induction by IPTG, the 6x His-tag, which facilitate purification using the Ni-NTA purification system, Xpress epitope for protein detection, and the multiple cloning site (MCS), which contains different restriction digestion sites (Invitrogen, Life technologies).

The resultant recombinant construct is transformed into bacteria in order to express the protein of interest (Lodish *et al*., 2000). During protein expression different expression conditions such as the concentration of IPTG, temperature and time of induction are screened in order to produce high amount of proteins (Rosano and Ceccarelli, 2014). Following expression is the purification of the protein of interest, which is achieved using

20

chromatography, particularly affinity chromatography in this case. This is a powerful tool for purifying recombinant proteins from crude extracts to a nearly homogeneous preparation in a single step (Kimple, 2013). It allows the biological properties of the sample to be purified through binding and reverse interaction between affinity ligands (Magdeldin and Moser, 2012). However, most naturally occurring proteins lack tags which would allow purification by affinity purification, so they require modification through addition of either N- or C-terminal tags.

After expression of recombinant proteins, the question is raised as whether the target protein is active or not (Rothbauer *et al*., 2008). Therefore, enzyme activity assays are employed to test the functionality before the enzyme is used for future applications (Gräslund *et al*., 2008). Enzyme assays work best in that they are specific catalysed reactions, meaning that the accumulated product is inversely proportional to the enzyme specific-substrate consumed and directly proportional to the enzyme activity (Bisswanger, 2014). The P450-Glo luminescent assays are assay of choice for cytochrome P450 enzymes (Inceoglu *et al*., 2009), and their use can be enhanced based on individual cytochrome P450 enzyme that is specific to a particular pro-luciferin substrate (Cali *et al.,* 2012). In this study, the assay that provides a luminescent method was used for measuring the activity of CYP2D6. It employs a pro-luciferin substrate, luciferin-ME EGE, for which is converted by the reaction of CYP2D6 into *D*-luciferin. *D*-luciferin thus undergo luciferase catalysis to produce light equivalent to the CYP2D6 enzyme activity (Cali *et al*., 2006).

2.2 Material and methods

2.2.1 *In silico* characterisation of physical and biochemical properties of CYP2D6

In silico characterisation of CYP2D6 was conducted in order to understand the physico-biochemical behaviour and structure of CYP2D6 protein using several bioinformatics tools.

2.2.1.1 CYP2D6 sequence retrieval

The human CYP2D6 amino acid sequence (GenBank accession number: CAK54644.1) that is encoded by CYP2D6 gene (Genbank: CU013213.1) was retrieved from the National Centre for Biotechnology Information (NCBI) database in FASTA format. The sequence was used as an input for any subsequent bioinformatics analysis tool used in this study.

2.2.1.2 Prediction of physico-chemical parameters

The physical properties of CYP2D6 including the number of amino acids, Molecular weight (M*r*), Isoelectric point (pI), instability index (Guruprasad *et al*., 1990), total number of negatively (Asp+Glu) and positively (Arg+Lys) charged residues, aliphatic index (Ikai, 1980), extinction coefficient (Gill and von Hippel, 1989), Grand Average of hydropathicity (GRAVY), and the protein's half-life in several organisms were predicted using Expasy ProtPraram tool (Gasteiger *et al*., 2005). In order to understand the physical stability of a protein, the sequence was also submitted to Cys_REC tool from softberry (http://linux1.softberry.com/berry.phtml) to locate the disulphide bonds between the pairs of cysteine residues.

2.2.1.3 Protein solubility and sub cellular localisation

The solubility of CYP2D6 was determined using a web-based protein solubility prediction online server, SOSUI (Hirokawa et *al.*, 1998). SPPRED was used to predict the percentage probability of CYP2D6 expression in *E. coli*. Localisation of the protein was determined using YLoc online server, which is an interpretable prediction system for protein subcellular localisation prediction in *E. coli*, with a confidence value to indicate if the predictions are trust worthy. It also gives the reason why the predictions were made and which properties of the protein sequence are associated with these predictions (Briesameister *et al*., 2010). The high accuracy YLoc+ was chosen for CYP2D6 in order to predict multiple locations of the protein with high accuracy.

2.2.1.4 Protein structure and functional analysis of CYP2D6

In order to determine the structure of CYP2D6 and functionally characterise it, the retrieved sequence was submitted to SWISS model Workspace online server (Arnold *et al*., 2006) in order to build the protein model structure. Workspace allows each user to formulate their personal protein homology models by submitting the protein sequence. The amino acid sequence was also submitted to NCBI conserved domain check in order to determine the different biochemical functions that a protein can perform (Marchler-Bauer *et al.,* 2017).

2.2.2 *In vitro* molecular characterisation of CYP2D6

In vitro characterisation of CYP2D6 was conducted in order to generate the CYP2D6 expression construct and to produce a highly purified CYP2D6 protein for post-expression applications.

2.2.2.1. Primer design and polymerase chain reaction

Primers specific for the human cytochrome P450 CYP2D6 genes were designed manually based on the CYP2D6 sequence retrieved from NCBI (Genbank Accession No. CU 013213.1). The forward and reverse primers were designed such that they include the *BamH*I and *Xho*I sites (as shown in Table 2.1) respectively for the purpose of screening through restriction double digestion. The pTrcHis forward/reverse and Xpress TOPO forward primers were provided as part of the TOPO cloning kit (Invitrogen, Life technologies).

Table 2.1: Primer set used for molecular characterisation of CYP2D6

Primer name	Sequence
CYP2D6 forward	5'-GTACGGATCCATGGGGCTAGAAGCACTGGTG-3'
CYP2D6 reverse	5'-GTACCTCGAGCTAGCGGGGGCACAGCAC-3'
pTrcHis forward	5'-GAGGTATATATTAATGTATCG-3'
pTrcHis reverse	5'-GATTTAATCTGTATCAGG-3'
Xpress TOPO forward	5'-TATGGCTAGCATGACTGGT-3'

Note: Restriction enzymes are underlined and highlighted in blue and brown for *BamH*I and *Xho*I respectively

The pCellFree_G03 plasmid containing CYP2D6 (Cat# 67137) was a gift from Kirill Alexandrov, Addgene (Gagoski *et al*., 2015) and it was used as a DNA template for PCR amplification. The PCR amplification was performed in a final volume of 25 µl and was carried out using the 2x Dream Taq PCR MasteMix, (Cat#K1081, Thermo Scientific, USA) as shown in Table 2.2. PCR reaction was conducted according to the following cycles: pre-denaturation at 96 °C for 3 min followed by 35 cycles of amplification (94 °C for 1 min denaturation; 65 °C for 2 min annealing; 72 °C for 2 min extension) and the final extension at

72 °C for 5 min. Samples were then analysed by running on a 1 % agarose gel and viewed using the Alpha DigiDoc RT 92-12071-00 gel viewer (Innotech Corp, Japan).

Table 2.2: PCR amplification reaction mixture

Initial concentration	Reagents	Control	Experiments	Final concentration
2X	Dream Taq MasterMix	13 µl	13 µl	1X
10 µM	CYP2D6 Forward primer	2 µl	2 µl	0.8 µM
10 µM	CYP2D6 Reverse primer	2 µl	2 µl	0.8 µM
-	dH2O	8 µl	4 µl	-
4.480 µg	Template CellFree CYP2D6	0 µl	4 µl	0.784 µg
	Total	25 µl	25 µl	

2.2.2.2 Purification of PCR amplified CYP2D6 fragment

The PCR product was purified from the agarose gel using the GeneJET Gel Extraction Kit (Cat# K0692, Thermo Fisher Scientific, USA), and all procedures were done according to the manufacturer's instructions. The concentration of the purified CYP2D6 was determined using NanoDrop ND-2000 spectrophotometer (Thermo Fisher Scientific, USA). The purified CYP2D6 was then analysed by running on a 1 % agarose gel and viewed on the Alpha DigiDoc RT 92-12071-00 gel viewer (Innotech Corp, Japan).

2.2.2.3. Generation of the expression construct of CYP2D6

In order to generate the expression construct containing CYP2D6, PCR product purified in section 2.2.2 was cloned into the pTrcHis-TOPO® vector using the TOPO TA cloning kit (Cat# K4410-01, Thermo Fisher Scientific, USA), according to the manufacturer's instructions. In brief, 20 ng/µl of the PCR sample was ligated with the 20 ng/µl pTrcHis-TOPO® vector in a final reaction volume of 5 µl as shown in Table 2.3. The ligation reaction mix was gently mixed and incubated for 5 min at room temperature, followed by transformation into the TOP10 *E. coli* competent cells.

Table 2.3: The ligation reaction mix for generating pTrcHis-CYP2D6 construct.

Initial concentration	Reagents	Experiments	Final concentration
20 ng/µl	**Purified PCR product**	1 µl	4 ng/µl
20 ng/µl	**pTrcHis-TOPO® vector**	1 µl	4 ng/µl
-	**Nuclease free water**	3 µl	-
	Final volume	**5 µl**	

2.2.2.4 Transformation of DNA into competent cells

Competent cells, TOP10 cells, were thawed on ice followed by mixing 2 µl of ligation mix and 50 µl competent cells in a 1.5 ml Eppendorf tube. The mixture was incubated on ice for 30 min followed by heat-shocking at 42 °C for 45 s. Cells were then placed on ice for 2 min followed by the addition of 450 µl SOC media (1.5 % yeast extract, 1 % Bacto-Tryptone, 10 mM NaCl, 2 mM KCl, 10 mM $MgCl_2$, 20 mM glucose). The reaction tubes were incubated with shaking at 37 °C for 1 h. About 100 µl of the transformation mix was plated on LB plates containing 50 µg/ml ampicillin. The plates were incubated overnight at 37 °C.

2.2.2.5 Plasmid DNA isolation

Plasmid DNA isolation was done according to the alkaline lysis method (Birnboim and Doly, 1979). Single colonies from the plate containing *E. coli* TOP10 cells transformed with the ligation mixture were selected and inoculated into 15 ml SOC media supplemented with 50 µg/ml ampicillin. The culture was incubated at 37 °C overnight with shaking (200 rpm). Glycerol stocks were prepared from the overnight culture and stored at -80 °C. The remaining culture was centrifuged at 5500 rpm for 10 min and the supernatant was discarded. The plasmid was then isolated from the pellet using GeneJET Plasmid Miniprep Kit (Cat# K0503, Fermentas, UK) according to the manufacturer's instruction.

2.2.2.6 Screening colonies carrying CYP2D6 construct

In order to determine the positive clones, restriction double digestion and PCR were used to determine the presence of the gene of interest. In brief, a double digestion reaction was set up containing 1 µg of pTrcHis-TOPO® isolated plasmids, 10x Fast Digest Green Buffer®, and FastDigest® *BamH*I and *Xho*I to a final volume of 25 µl as shown in Table 2.4. The PCR was used to further confirm the positive clones by amplifying the gene of interest using the same conditions as described in sectionn 2.2.2.1, with slight modifications on the primer sets. Different primer combinations were used and the set up was as follows: PCR amplification 1 using (X press TOPO forward primer + pTrcHis reverse primer), PCR amplification 2 using (CYP2D6 forward primer + pTrcHis reverse primer) as recommended by the TOPO TA cloning kit, and PCR amplification 3 using gene specific primers (CYP2D6 forward and reverse primers). Sequences of the primers can be found in Table 2.1. Both the double digested reaction mixtures and the PCR samples were then analysed on 1 % agarose gels and viewed using the Alpha DigiDoc RT 92-12071-00 gel viewer (Innotech Corp, Japan).

Table 2.4: Double digest reaction mix.

Initial concentration	Reagents	Volume	Final concentrations
1 µg	Plasmid	10 µl	0.2 µg
10X	10x fast Digest Green Buffer®	5 µl	(1X)
30 U	BamHI	1 µl	0.6 U
20 U	XhoI	1 µl	0.4 U
-	Nuclease free water	33 µl	-
	Total	50 µl	

2.2.2.7 DNA sequencing

The plasmid DNA extracted in section 2.2.2.5 was sent for sequencing at Inqaba biotech (Pretoria, South Africa). In brief, 10 µl of 101 ng/µl plasmid was pipetted into PCR tubes, sealed and stored on ice for transportation. The following primers were used in the entire sequencing trial and their sequences are already shown in Table 2.1: CYP2D6 forward, CYP2D6 reverse, pTrcHis forward, pTrcHis reverse, and Xpress TOPO forward.

2.2.2.8 Expression of the recombinant pTrcHis-CYP2D6 construct

The positive clone (pTrcHis-TOPO-CYP2D6 construct) was expressed in *E. coli* TOP10 cells. In brief, the construct was transformed as described in section 2.2.3. After transformation, a single colony of *E. coli* TOP10 cells transformed with pTrcHis-TOPO-CYP2D6 construct was inoculated into 10 ml Luria broth supplemented with 0.5% glucose and 50 µg/ml ampicillin and incubated at 37 °C with shaking overnight. The following day the overnight culture was then diluted into 1:10 with Luria broth supplemented with the same ingredients as above and the culture was incubated at 37 °C until the cells reached an optical density between 0.4 – 0.6 at a wavelength of 600 nm (OD_{600}). The culture was induced with 2 mM of isopropyl-1-thio-ᴅ-galactopyranosidase (IPTG) for 2, 4 and 16 h for the time course

28

expression at 30 °C and 37 °C. After expression, the best condition for expression was chosen following large scale expression. In brief, the large scale expression was conducted in a final volume of 500 ml and the protein was induced at 30 °C for 4 h. The culture was centrifuged at 5500 rpm for 10 min and the pellet was kept at -20 °C for post-expression procedures.

2.2.2.9 Determination of the solubility of recombinant CYP2D6

The solubility and/or insolubility nature of recombinant CYP2D6 protein was determined as described below. The large scale extracted pellets were re-suspended in lysis buffer [50 mM sodium buffer pH 8.0, 1x Triton-X100, 1 mM dithiolthreitol (DTT), 100 µg/ml of lysozyme, 1 mM phenylmethylsulfonyl fluoride (PMSF)] and urea lysis buffer [200 mM NaCl, 50 mM Tris-Cl; pH 8.0, 500 mM glucose, 0.05 % (w/v) PEG, 20 mM β-mercaptoethanol, 8 M urea, 10 mM imidazole], for soluble and insoluble fractions determination respectively. Firstly the pellet was re-suspended in the lysis buffer without urea and incubated on ice for 30 min while shaking. After incubation, cells were sonicated for 4 cycles (30 s pulsing and 30 s chilling cycles on ice) in order to rupture and solubilise the cell contents. The cellular components (crude lysate) were then centrifuged at 10 000 g at 4 ºC for 30 min and their supernatant (soluble fraction) was transferred into an ice-cold 1.5 ml Eppendorf tube. And the pellet was re-suspended in urea lysis buffer and then lysis was done the same way as described above. In this case the second supernatant from the urea treated pellet contained the insoluble fraction. Both the supernatants containing the soluble and the insoluble protein fractions were then stored at -20 °C until further purification. Portions of both fractions were then analysed by SDS-PAGE in order to determine the presence and relative proportions of the soluble or insoluble fractions of the recombinant CYP2D6.

2.2.2.10 Purification of the recombinant CYP2D6

The Ni-NTA beads were pre-packed into an empty 30 cm XK16 plastic Econo-Column (Bio-Rad Laboratories Inc., California, USA). The cell lysate previously obtained was then purified on a Ni-NTA affinity system under denatured conditions. The column was washed with 3 column volume (CV) of distilled water to remove the ethanol. The affinity gel was then equilibrated with 3 CV of equilibration buffer [50 mM sodium phosphate pH 8.0, 200 mM NaCl, 500 mM glucose, 0.05 % (w/v) PEG, 20 mM β-mercaptoethanol, 8 M urea, 10 mM imidazole]. The protein lysate was added to the equilibrated column and the flow through was collected. The column was washed 4 times with wash buffer 1, 2, 3, 4 [50 mM sodium phosphate buffer, 300 mM NaCl, containing 0, 10, 20, 50 mM imidazole pH 8.0 respectively] and the flow throughs were collected as wash 1, 2, 3, and wash 4. The protein was then eluted with the elution buffer [50 mM sodium phosphate buffer, 300 mM NaCl, 250 mM imidazole] in two fractions as elution 1 and 2. The column was then washed with 3 CV of 2 M NaCl and the beads were stored in 20 % ethanol at 4 °C. The collected flow through, washes and the eluted proteins were then analysed on a 12 % SDS-PAGE. The purified protein was stored as glycerol stocks (950 µl protein containing 50 µl of 100 % glycerol) at -20 °C, and at -80 °C for long term storage.

2.2.2.11 Refolding of the denatured purified recombinant CYP2D6 protein

The purified denatured protein was dialysed before it was refolded in order to reduce the concentration of imidazole, to allow the binding when re-eluted on the column. In brief, 5 ml of 0.5 mg/ml was poured into Snakeskin Dialysis Tubing clipped tube (Cat# 68700, Thermo Fisher Scientific, USA) and then placed in 1 000 ml dialysis buffer [8 M urea, 50mM sodium phoshate pH 8.0, 10 mM Tris-Cl; pH 8.0, 300 mM NaCl, 20 mM β-mercaptoethanol, 5 % glycerol, and 10 mM imidazole], with magnetic stirring at 80 rpm. The dialysis process was

allowed to run for 48 h in the cold room. After dialysis, the Ni-NTA column was pre-equilibrated with 3 CV refolding buffer A [8 M urea, 200 mM NaCl, 50 mM Tris-Cl; pH 8.0, 500 mM glucose, 0.05 % (w/v) PEG, 20 mM β-mercaptoethanol, 10 mM imadazole] and in preparation for refolding. The dialysed purified recombinant CYP2D6 protein was loaded into the column followed by washing four times using 0 M urea refolding buffer B [200 mM NaCl, 50 mM Tris-Cl; pH 8.0, 500 mM glucose, 0.05% (w/v) PEG, 4 mM reduced glutathione, 0.4 mM oxidized glutathione, and 0.5 mM phenylmethanesulfonylfluoride (PMSF)]. The refolded protein was eluted as two fractions using elution buffer [300 mM NaCl, 50 mM sodium phosphate buffer, 250 mM imidazole]. The refolded protein was further analysed on a 12 % SDS-PAGE and then stored as glycerol stocks (950 µl protein containing 50 µl of 100 % glycerol) at -20 °C and at -80 °C for long term storage.

2.2.2.12 Determination of CYP2D6 protein concentrations

Protein concentrations of both unfolded and folded CYP2D6 were determined using the Bradford assay (Bradford, 1976). The Bradford assay depends on the binding of the Coomassie Blue G-250 dye to proteins thus forming a complex with a detectable absorbance (Brunelle et al., 2017). The Bradford standards and sample reactions (Table 2 and 3 in appendix IV) were prepared in a 96 well plate. The absorbances of proteins in reaction with the dye were measured photometrically at 595 nm using the FLUOstar Omega multi-mode plate reader (BMG LABTECH, Germany). To determine the protein concentrations of the original samples a linear regression of the data from the BSA standards (Figure 2 in appendix IV) was conducted and the concentrations were evaluated using the equation given by the slope of the graph.

2.2.2.13 Enzyme activity assay of recombinant CYP2D6

The enzyme activity of CYP2D6 was measured using P450-Glo™ CYP2D6 assay kit (Cat#

V8891, Promega Corp), according to the manufacturer's instructions. In brief, the system contained a recombinant human cytochrome P450, a luminogenic cytochrome P450 substrate, an NADPH regeneration system, KPO4 buffer (pH 7.4), luciferin-free water and a luciferin detection reagent that contained a stabilised recombinant firefly luciferase (UltraGlo^{TM} Luciferase) and ATP. The luminogenic P450-Glo™ substrates, luciferin-ME EGE are derivatives of beetle luciferin (D-luciferin) for which is specific for CYP2D6 enzyme. The P450 reactions of 50 μl were performed in 96 well plates containing 10 min pre-incubated 12.5 μl reaction [0.5 pM of recombinant CYP2D6, 30 μM luciferin-ME EGE, 0.1 M KPO4 buffer pH 7.4]. Equal amount of 12.5 μl rifampin was used as a test inducer compound of CYP2D6. The reaction was initiated by adding 25 μl of 2x NADPH regeneration system (NADP$^+$, glucose-6-phosphate, (G6PDH)) and incubated for 30 min at room temperature. After incubation, luciferin detection reagent of 50 μl was to stop the P450 reaction and initiate the luciferase reaction. In Summary, the enzyme assay reaction mix was conducted as shown in Table 2.5. The luminescence was read after 20 min incubation at room temperature in the absence of light. The signal that is dependent on the amount of luciferin was produced and was equivalent to the amount of luciferin glowing product that was then quantified using FLUOstar Omega multi-mode plate reader (BMG LABTECH, Germany). The measuring conditions were 380 nm excitation and 480 nm emission, with an integration time of 1 second and gain of 150. All experiments were done in triplicates and statistics was determined using origin software.

Table 2.5: The CP450-Glo^{TM} CYP2D6 enzyme assay reaction mix set up.

Components	Control	Unfolded protein	Folded protein
Enzyme (CYP2D6)	-	+	+
Luciferin-ME EGE	+	+	+
KPO4 buffer	+	+	+
2x NADPH regeneration system	+	+	+
Rifampicin (inducer)	-/+	-/+	-/+
Luciferin detection reagent	+	+	+

Note: (+) means added; (-) means not added; and -/+ mean added and not added

UNIVERSITY *of the*
WESTERN CAPE

2.3 Results

2.3.1 *In silico* characterisation of the physical, biochemical and structural properties of cytochrome P450 2D6 (CYP2D6)

2.3.1.1 Prediction of the physical parameters of CYP2D6

In order to conduct *in silico* characterisation of CYP2D6, the primary sequence of CYP2D6 (GenBank: CAK54644.1) was obtained from NCBI database. Protein sequence retrieval of CYP2D6 has shown that the protein of interest consists of 446 amino acids (Figure 2.3) and it was further confirmed by Expasy Protparam tool (Table 2.6.).

>CAK54644.1 CYP2D6

MGLEALVPLAMIVAIFLLLVDLMHRRQRWAARYPPGPLPLPGLG
NLLHVDFQNTPYCFDQLRRRFGDVFSLQLAWTPVVVLNGLAAVRE
ALVTHGEDTADRPPVPITQILGFGPRSQGRPFRPNGLLDKAVSNVIA
SLTCGRRFEYDDPRFLRLLDLAQEGLKEESGFLREVLNAVPVLLHIP
ALAGKVLRFQKAFLTQLDELLTEHRMTWDPAQPPRDLTEAFLAEM
EKAKGNPESSFNDENLCIVVADLFSAGMVTTSTTLAWGLLLMILHP
DVQRRVQQEIDDVIGQVRRPEMGDQAHMPYTTAVIHEVQRFGDIV
PLGVTHMTSRDIEVQGFRIPKGTTLITNLSSVLKDEAVWEKPFRFHP
EHFLDAQGHFVKPEAFLPFSAGRRACLGEPLARMELFLFFTSLLQH
FSFSVPTGQPRPSHHGVFAFLVTPSPYELCAVPR

Figure 2.3: NCBI retrieved sequence of CYP2D6. The highlighted and underlined section on the sequence represent the transmembrane region.

Physical and biochemical parameters of CYP2D6 such as number of amino acids (446), molecular weight (50.05397 kDa), theoretical pI (6.21) total number of positively (43) and negatively (49) charged residues, half-life in *E. coli* cells (>10 h), extinction coefficient (35200/34950), aliphatic index (96.61), instability index (42.05), and GRAVY (0.001), values were computed automatically using Expasy ProtPraram tool. All estimated physico-biochemical parameters of CYP2D6 are represented in Table 2.6 and the entire data is shown at Appendix II. Cys_REC tool was used to characterise CYP2D6 and locate

disulphide bonds between the pairs of cysteine residues for physical stability of the protein. About five cysteines were identified in the CYP2D6 sequence and none of them are SS-bonded as shown in Figure 2.4.

Table 2.6: Predicted physico-chemical parameters of CYP2D6

Parameter	Prediction value
Number of amino acids	446
Molecular Weight	50.05397 kDa
Theoretical pI	6.21
Number of positive residues	43
Number of negative residues	49
Estimated half-life in *E. coli*	>10 h
Extinction coefficient	35200/34950
Aliphatic index	96.61
Instability Index	42.05
GRAVY	0.001

```
5 cysteines are found in positions:   57  140  245  392  442

CYS      57 is probably not SS-bounded   Score= -10.0
CYS     140 is not SS-bounded            Score= -19.5
CYS     245 is not SS-bounded            Score= -26.5
CYS     392 is not SS-bounded            Score= -42.6
CYS     442 is not SS-bounded            Score= -21.4
```

Figure 2.4: Number of cysteine residues and possible disulphide bonds on CYP2D6. Five cysteins were predicted at the protein sequence position 57, 140, 245, 392, and 442, but not are SS – bonded (predicted using CYS-REC tool).

2.3.1.2 Recombinant Protein solubility and subcellular localisation

SOSUI is a tool that predicts a part of the secondary structure of proteins from a given amino acid sequence thus discriminate if the protein is a soluble or a transmembrane protein. SOSUI server predicted that CYP2D6 is an insoluble transmembrane (GLEALVPLAMIVAIFLLLVDLM; 22 length) protein, with a probability percentage 0.0 % (predictred by SPPRED) as highlighted and underlined in Figure 2.3. The YLoc+ parameter was used for subcellular localisation prediction of CYP2D6 as it allows for prediction at multiple cellular locations. The distribution of CYP2D6 in *E. coli* was predicted to be 48 % in the endoplasmic reticulum (ER), 41.3 % in the extracellular space, 5.1 % in the lysosome, 4.5 % in the plasma membrane, 0.8 % in the Golgi apparatus, and 0 % in the rest of the cell locations (Figure 2.5).
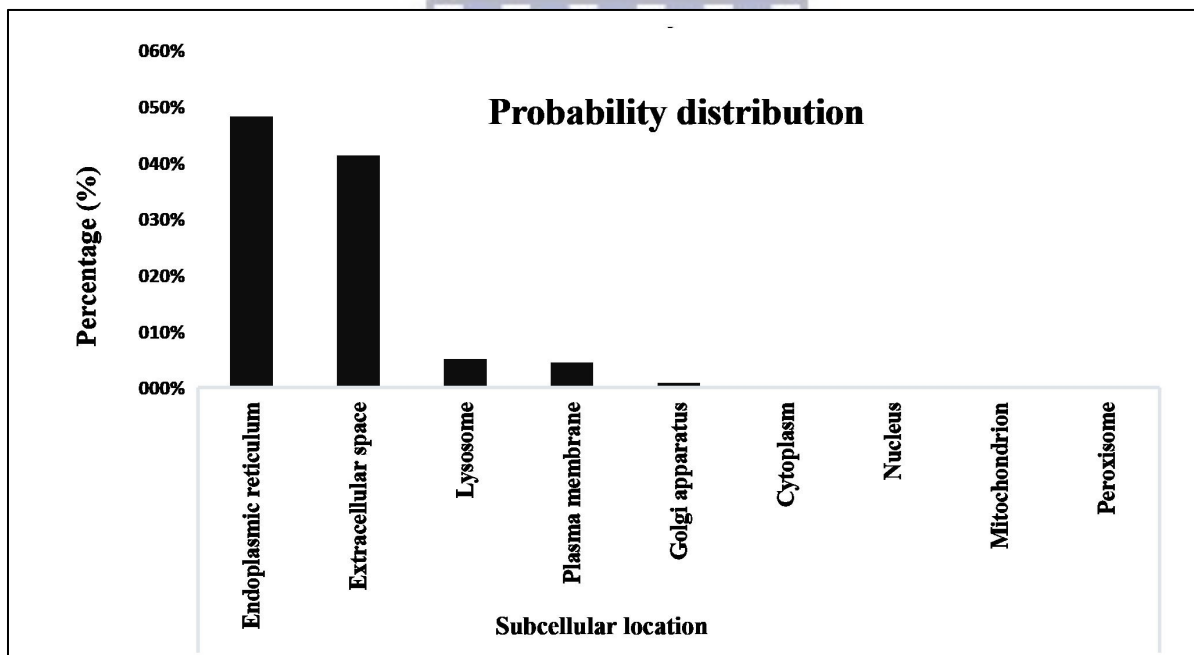
Figure 2.5: Subcellular distribution of CYP2D6 as predicted by YLoc+. Predictions indicate that CYP2D6 is mainly located in the endoplasmic reticulum and extracellular space.

2.3.1.3 Protein structure and functional analysis of CYP2D6

The structure of CYP2D6 was formulated using SWISS model workspace by inserting the FASTA sequence (GenBank: CAK54644.1). Figure 2.6 shows the 3D model structure of CYP2D6 consisting of 4 main protein chains surrounding the porphyrin ring containing the site of the heme and the direction arrangement of terminals (C- and N- terminals). The FASTA sequence was also used to determine the functional conserved domains of CYP2D6 using conserved domain server (Figure 2.7). The protein was observed that it falls within the P450 Superfamily. Within the sequence, there were 4 main functional domains (two specific and two non-specific hits) including the P450, which categorises CYP2D6 as a protein that perform oxidative degradation of various compounds; CypX, which gives the protein a secondary metabolites biosynthesis, transport and catabolism, and defence mechanisms abilities; PLN02687, for flavonoid 3'-monooxygenase; and CYP450 TxtE, for enzymes that convert L-tryptophan into L-4-nitrotryptophan. The other non-specific views are given in full view as shown in Figure 1 in Appendix III.
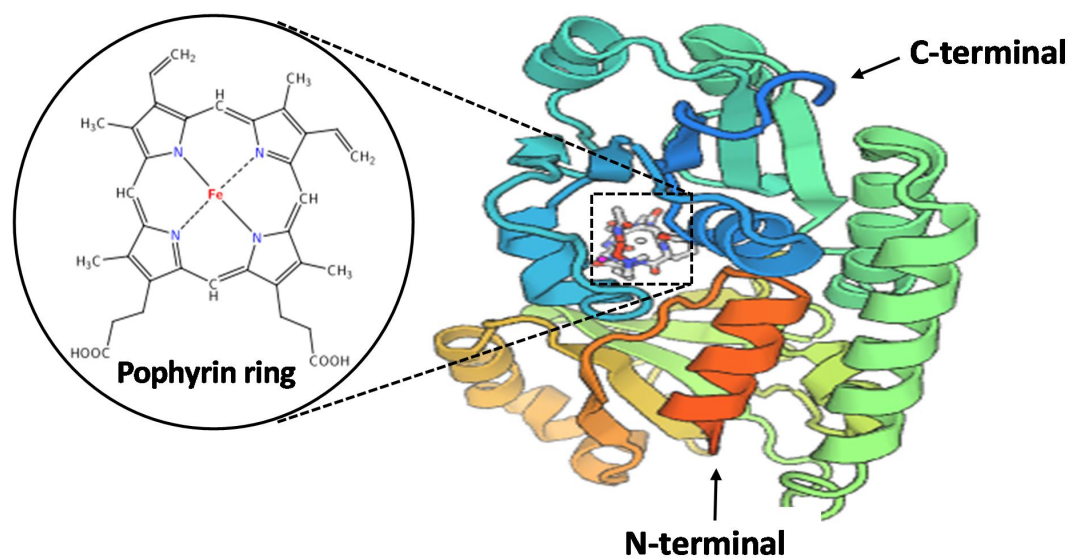
Figure 2.6: 3D model protein structure of CYP2D6 (formulated from SWISS model work space: https://swissmodel.expasy.org/interactive)
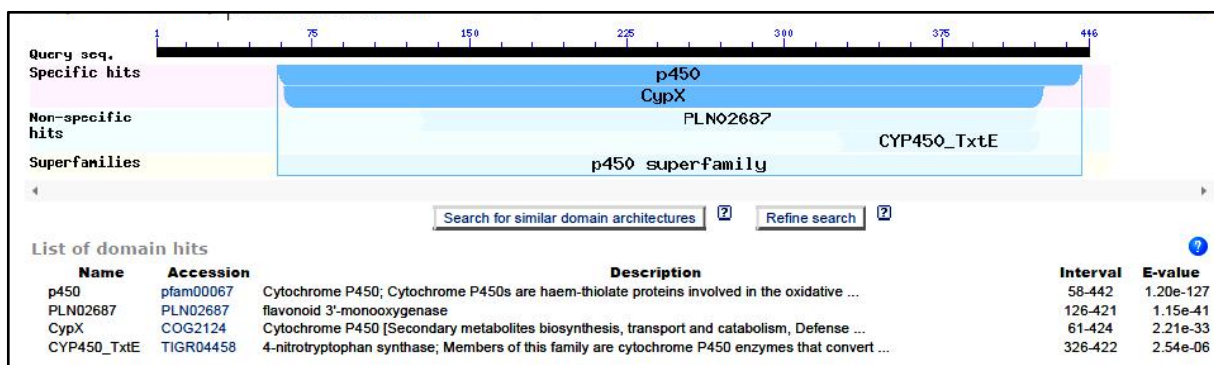
Figure 2.7: Conserved domains and the associated descriptions of CYP2D6 (formulated from NCBI conserved domain server: https://www.ncbi.nlm.nih.gov/Structure/cdd/wrpsb.cgi)

2.3.2 *In vitro* molecular characterisation of CYP2D6

The main aim of this chapter was to generate CYP2D6 expression construct in order to express large amounts of proteins for the future development of a biosensor, which will test the metabolism of tamoxifen in breast cancer patients at a low and effective cost as compared to commercial CYP2D6. This is due to the reason that commercial enzymes are available at small amounts/concentrations and are purchased at high cost contributing to the whole biosensor development as not cost effective.

2.3.2.1 CYP2D6 gene amplification

The amplification of CYP2D6 was done using gene specific primers as shown in Table 2.1, the successful results of PCR amplification are represented by lane 2 in Figure 2.8a, with the expected size of 1375 bp (represented by the black arrow). The amplified DNA of CYP2D6 was purified and further analysed on a 1 % agarose gel electrophoresis (Figure 2.8b).
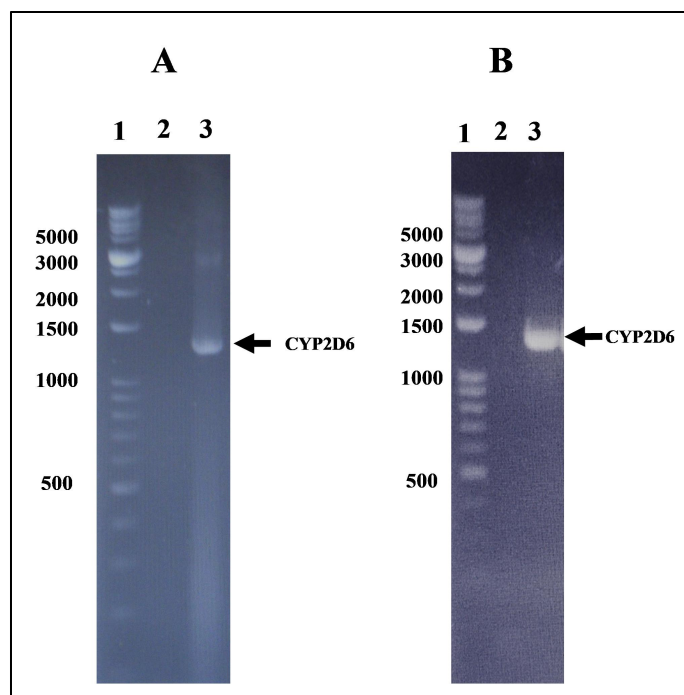
Figure 2.8: 1 % agarose gel electrophoresis analysis of CYP2D6 PCR product. (A) PCR amplification: Lane 1 – 1 Kb Kplus ladder RTU (Cat# DM011-R500, GeneDireX,Inc.); lane 2 – control and lane 3 – PCR amplification of CYP2D6 (B) purified CYP2D6 PRC product.

2.3.2.2 Cloning and screening of CYP2D6

In order to produce CYP2D6 expression construct, cloning was done as described in section 2.2.2.3. The cloning ligation mix was transformed into TOP10 competent cells and plated in LB agar plate containing 50 µg/ml (Figure 2.9a). In order to determine the positive clones, 5 colonies were screened using restriction double digestion as represented by the arrow in Figure 2.9b (in lane 5 and 6) that the gene of interest was released. In order to confirm the success of cloning, PCR amplification was also done with different combination of primers and the results are represented by lane 5 in Figure 2.9c, using CYP2D6 forward and pTrcHis reverse vector primers.
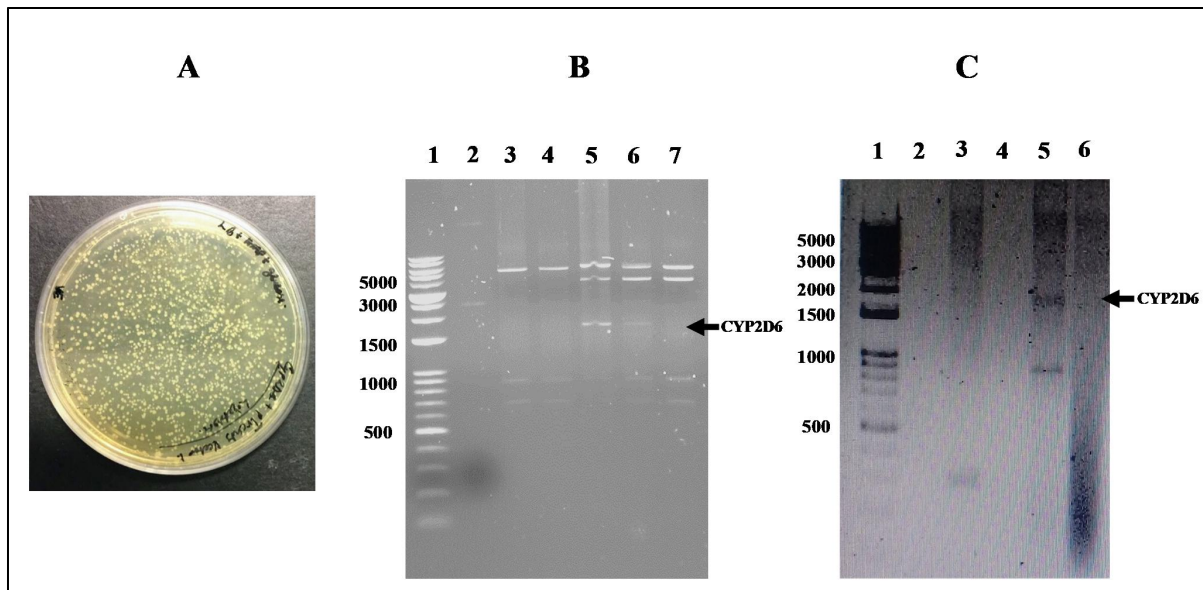
Figure 2.9: Confirmation of cloning using transformation, double digest, and PCR screening: (A) LB agar plate representing the TOP10 cells transformed with the ligation mixture. (B) Restriction doluble digest of pTrcHis-CYP2D6 with *BamH*I and *Xho*I: Lane 1 – Kplus ladder (1Kb); Lane-undigested TOPO plasmid (pTrcHis vector); Lane 3, 4 and – insert negative colonies; Lane 5 and 6 – insert positive colonies for pTrcHis vector + CYP2D6. (C) PCR screening: Lane 1 – Kplus ladder (1Kb); lane 2 – control and lane 3 – PCR amplification (using X press TOPO forward primer + pTrcHis reverse primer), lane 4 – control and lane 5 – PCR amplification (using CYP2D6 forward primer + pTrcHis reverse primer), and Lane 6 – negative amplification (using CYP2D6 forward primer + CYP2D6 reverse primers).

2.3.2.3 DNA sequencing

The clones were sent for sequencing at Inqaba Biotech laboratory (Pretoria, South Africa). According to their technicians, they were unable to amplify the 1450 bp CYP2D6 fragment; but a 300 bp fragment was always present. We also re-digested the CYP2D6 construct (Figure 2.10a) and reamplified the fragment using the combination of primers that target CYP2D6 and pTrcHis-TOPO® vector (Figure 2.10b). For PCR reamplification, there was a very clear band at 300 bp in all amplifications as it is shown by the black arrow. Lane 5 and 7 shows a positive amplification band at a correct size of 1450 bp, which is similar to the one observed during screening in section 2.3.2.2., although there were extra bands. For publication purposes, the sequencing process will be repeated.
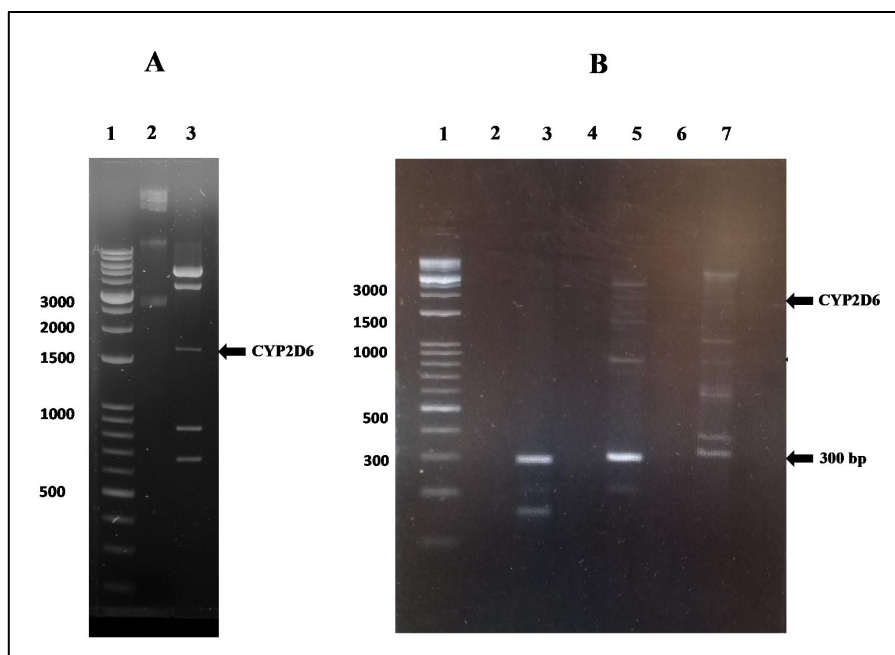
Figure 2.10: 1 % agarose gels indicating the 2nd screening of the pTrcHis-CYP2D6 positive clone (A) Repeated double digest of CYP2D6 screening: Lane 1 – Kplus ladder (1Kb); Lane 2 – undigested TOPO plasmid (pTrcHis vector); Lane 3 – positive release of CYP2D6 (black arrow). (B) PCR sequencing screening: Lane 1 – Kplus ladder (1Kb); lane 2, 4 and 6 – control of each primer set. Lane 3 – negative amplification (using X press TOPO forward primer + pTrcHis reverse primer), and lane 5 – PCR amplification (using CYP2D6 forward primer + pTrcHis reverse primer), and Lane 6 – PCR amplification (using CYP2D6 reverse primer + pTrcHis forward primer).

2.3.2.4 Expression of the recombinant pTrcHis-CYP2D6 construct

The expression of CYP2D6 was done under two different temperature conditions (30 ºC and 37 ºC) for the time course expression. Over-expression of the protein of interest was obtained at an expected size of ~68 kDa using pTrcHis-TOPO® vector (given that 50.05397 kDa correspond to CYP2D6 as predicted by physico-chemical parameters plus ~18 kDa of the plasmid sequence (~10 kDa), ~4 kDa 6x His-tag and ~4 kDa TOPO Xpress epitope), as shown in Figure 2.11a on lane 2, 4, 5, 8 in (black arrow). Large scale expression was done in order to obtain high amounts of recombinant CYP2D6 protein and this is represented in Figure 2.11b, lane 3 (black arrow). Proteins were extracted as described in section 2.2.2.7, lane 4 represent soluble fraction and lane 5 represent insoluble fraction.
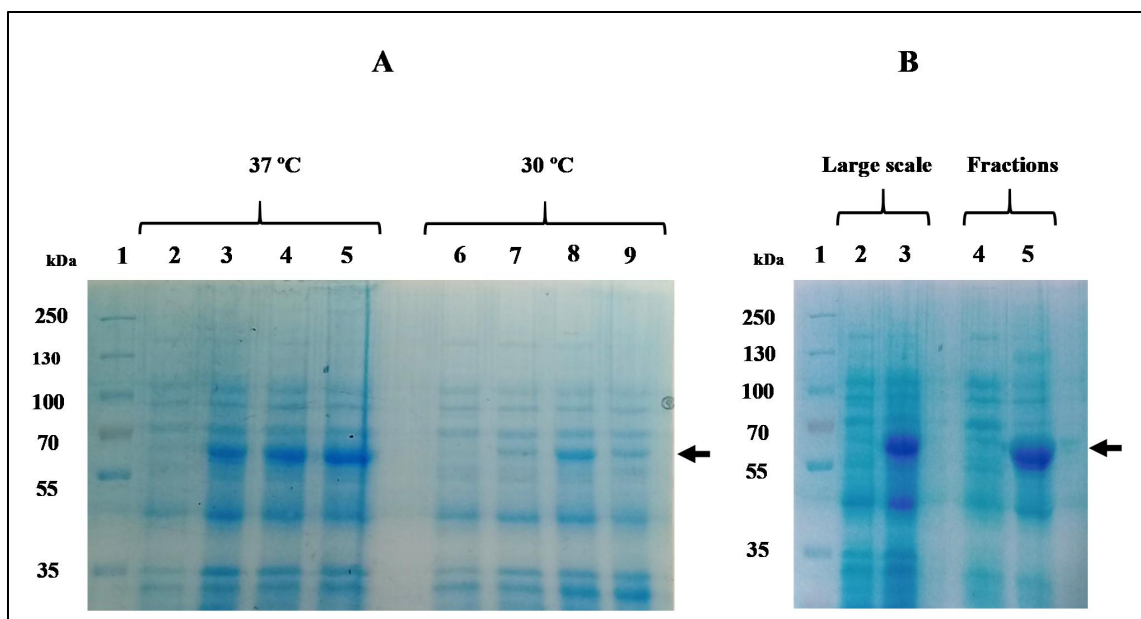
Figure 2.11: The 12 % SDS-PAGE analysis of the expression screen of CYP2D6. (A) Time course expression of CYP2D6 induction (small scale); Lane 1 – 250 kDa protein marker (Thermo Scientific, USA), Lane 2 – non-induced, Lane 3 to 5 represent 2, ,4, and 16 h (overnight) induction at 37 ºC respectively. Lane 6 – non-induced, Lane 7 to 9 represent 2, 4, and 16 h induction at 30 ºC respectively. (B) Large scale expression and protein extraction of CYP2D6. Lane 1 – 250 kDa protein marker; Lane 2 – uninduced; Lane 3 – induced, lane 4 –soluble faction (native conditions proteins) Lane 5 – Insoluble fraction (denatured proteins)**.**

2.3.2.5 Purification of recombinant CYP2D6

Both the expression screens and the large scale expression indicated that CYP2D6 is highly expressed in the insoluble fraction as a transmembrane protein, and it was therefore purified under denaturation conditions (in the presence of 8 M urea) using affinity chromatography as described in section 2.2.2.8. The purified protein is represented by a visible band of ~68 kDa (black arrow) in Figure 2.12.
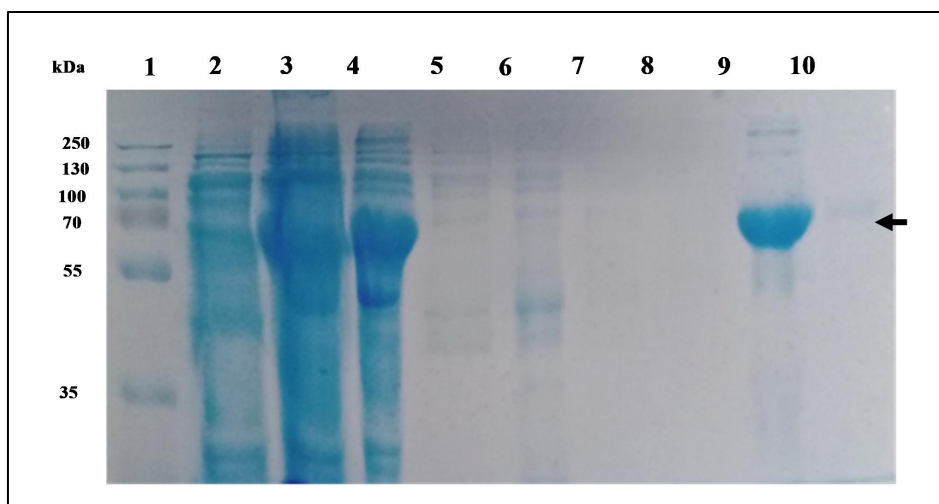
Figure 2.12: The 12 % SDS-PAGE analysis of the purification of CYP2D6 under denatured state. Lane 1 – 250 KDa protein marker, Lane 2 – uninduced, Lane 3 – induced, Lane 4 – flow through, Lane 5 – wash 1, Lane 6 – wash 2, Lane 7 – wash 3, Lane 8 –wash 4, Lane 9 – Elution 1, Lane 10 – elution 2.

2.3.2.5 Refolding of the Denatured Purified Recombinant CYP2D6 Protein

The CYP2D6 protein that was purified under denatured state was further purified with affinity chromatography, under renaturation state using the refolding buffer as described in section 2.2.2.9. The purified protein is represented by lanes 8 and 9 (Figure 2.13), for which it correspond to the protein band at ~68 kDa as shown by the black arrow.
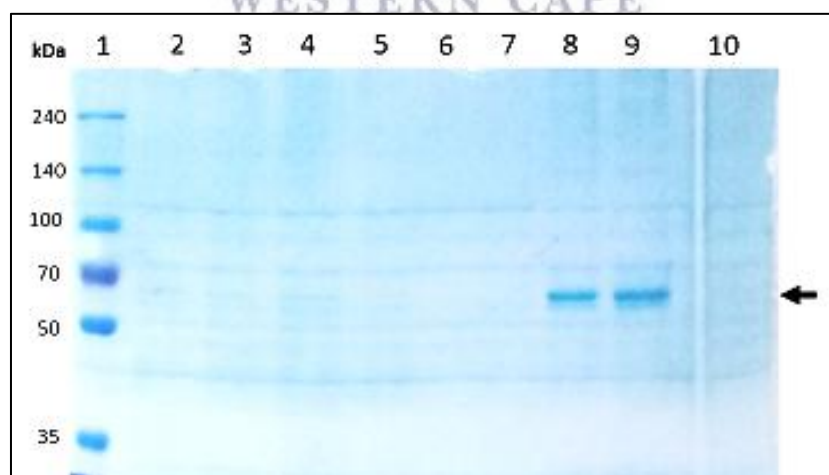
Figure 2.13: The 12 % SDS-PAGE purification gel of CYP2D6 under refolding state. Lane 1 – 250 KDa protein marker, Lane 2 – flow through 1, Lane 3 – flow through 2, Lane 4 to 7 – Washes using refolding buffer with zero urea. 4, Lane 8 to 9 – Elution 1 and 2, Lane 10 – NaCl wash.

2.3.2.6 Enzyme activity assay of CYP2D6 proteins.

The concentration of unfolded and folded CYP2D6 proteins were determined to be 505.7 µg/ml and 93.7 µg/ml by Bradford assay respectively. The activity of both unfolded and folded CYP2D6 was determined in the presence and absence of rifampicin as an inducer compound of CYP2D6 (Rae *et al.*, 2001), using P450-Glo™ CYP2D6 assay as described in section 2.2.2.10. As shown in Figure 2.14, the luminescence signal measured was 20104 RLU and 19643 RLU controls (1 and 2) in the absence and presence of Rifampicin respectively. About 20336.6 RLU and 20046.3 RLU were measured for the unfolded and folded CYP2D6 proteins. When rifampicin was added, an increase of 21776.67 RLU and 23333 RLU were observed for unfolded and folded CYP2D6 respectively
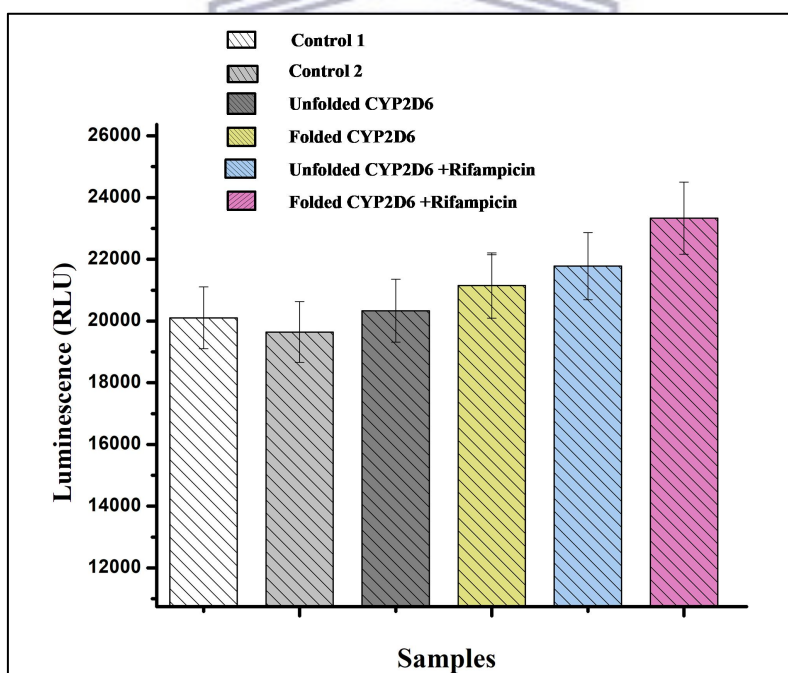
Figure 2.14: P450-GLO CYP2D6 activity assay. The controls had all the reagents except CYP2D6 proteins with or without rifampicin. The test assays were done in the presence CYP2D6 proteins with or without rifampicin as an inducer test compound of CYP2D6. n = 5, *Different from control $P < 0.05$, with a value P-value of 0,03355 (statistics computed using Origin software 7.0).

2.4 Discussion

The main aim of this chapter was to produce an expression construct in order to express large amounts of active recombinant CYP2D6 at a cheaper way. To achieve this goal, *in silico* characterisation of CYP2D6 gene was conducted using several bioinformatics tools in order to know the sequence and other parameters that might affect or influence expression, purification and enzyme activity assays. The physical properties of CYP2D6 were computed using Expasy ProtParam tool as represented in Table 2.6 and indicated that human CYP2D6 is composed of 446 amino acid residues with a molecular weight of 50.05397 kDa, and an isoelectric point (pI) of 6.21 for which is less than 7 and characterising the protein to be acidic. Therefore, it is important to consider pH or buffering condition of CYP2D6 during expression and post-expression use. The stability of the protein was studied by checking the instability index, aliphatic index and GRAVY. The instability index of 42.05 classified the protein as unstable in the test tube, since the value is above 40 (Guruprasad *et al.*, 1990), this finding is supported by the Soft berry results (Figure 2.7), which indicated that although five cysteines were identified in CYP2D6, none of them are SS-bonded meaning that the protein is unstable. The aliphatic index (AI) of 96.61 (between 44.47 and 104.88) means that CYP2D6 has a high volume that is occupied by aliphatic side chains and has increased thermal stability over a wide range of temperatures (Avci *et al.*, 2016). The positive GRAVY value of CYP2D6 indicates that it has no more surface accessibility to interact with water (Kramer *et al.*, 2012), and this character is in agreement with the SOSUI and SPPRED findings which predicted the protein as an insoluble transmembrane with a probability solubility percentage of 0.0% when over-expressed in *E. coli* (Figure 2.4). The half-life of CYP2D6 in the bacterial cell such as *E. coli* was estimated to be greater than 10 h, meaning protein synthesis will still be greater than protein degradation and stable in the bacterial system during expression after 10 h (Laalami *et al.*,2014).

Subcellular localisation of CYP2D6 prediction was conducted to determine all the locations where the protein is expressed in *E. coli*. The location of protein is important as it correlate with the protein function and understanding of its possibility in interacting with other proteins (Emanuelsson *et al*., 2002). The results have indicated that CYP2D6 is largely located in the endoplasmic reticulum (48%), followed by the extracellular space (41.3%), lysosome (51%), and small portions are located in the plasma membrane (4.5%) and Golgi apparatus (0.8%), however it is not found in the rest of the cell locations, including the cytoplasm. Taken together these results indicated that the expression of CYP2D6 in the prokaryotic system is possible however the protein will be expressed in the inclusion bodies as an insoluble fraction (Wang *et al*., 2014).

The sequence was also submitted into SWISS model workspace and NCBI conserved domain server to predict the protein model and identify the protein functional domains (Arnold *et al*., 2006; Marchler-Bauer *et al*., 2007). The results indicated that the structure of CYP2D6 (Figure 2.5) has a proper orientation running from the N-terminal to the C-terminal and it is characterised by 4 supercoiled lobes that forms a quaternary structure with the porphyrin ring bared at the centre. There were 4 main functional domains observed (2 specific and 2 non-specific hits) as shown in Figure 2.6: P450, for which categorises CYP2D6 as a member of the P450 Superfamily proteins that perform oxidative degradation of various compounds (Barnaba *et al*., 2017) and CypX which gives the protein secondary metabolites biosynthesis, transport and catabolism, and defence mechanisms abilities. None specific hits include PLN02687 for flavonoid 3'-monooxygenase; and CYP450 TxtE for enzymes that convert L-tryptophan into L-4-nitrotryptophan. Even though only the main non-specific hits are discussed in this section other non-specific hits domains are shown in full view at Appendix II. These results strongly suggest that CYP2D6 is indeed a redox protein and the presence of

the porphyrin ring with the heme bound in the structure strongly indicate that the metabolism of tamoxifen is possible.

The human CYP2D6 gene was successfully amplified and purified as indicated in Figure 2.8a and b, as shown by the expected size of CYP2D6 at 1375 bp. Cloning of CYP2D6 into pTrcHis-TOPO® vector was successfully achieved as shown by the results in Figure 2.9a, which shows a plate of recombinant colonies. Most of the colonies in the plate are likely to carry positive clones since they are said to have recombinant efficiency of 95% (Chaudhary *et al*., 2014). To confirm the success of cloning, the insert was verified by restriction double digestion, re-amplification and DNA sequencing using the recombinant isolated plasmid. Both double digestion and PCR showed a positive release and amplification of insert at the correct expected size respectively (Figure 2.9 b and c). Since there was a challenge with the gene-specific primers, thus the combination of gene specific primers were used and the successful amplification was obtained when CYP2D6 forward primer was combined with pTrcHis reverse primer and gave an expected amplicon of ~1450 bp which is the 1375 bp (CYP2D6 gene) plus the ~ 75 bp region between the insert and the end of the pTrcHis reverse priming site. There were also extra bands that were observed, which are expected when using TOPO TA cloning strategy as described previously (Chaudhary *et al*., 2014). Sequencing results as obtained from Inqaba indicated that the team were unable to amplify the gene for sequencing. Due to that challenge, we also reamplified the fragment using the combination of primers that target CYP2D6 and pTrcHis-TOPO® vector (Figure 2.10b), and there were faint bands corresponding to the amplicon size of CYP2D6 (1450 bp). This suggest that the faint bands might have been too low to be picked up by the signal during sequencing. The presence of very clear 300 bp band, might also have interfered with the analysis of the 1450

bp CYP2D6 band. However, in future for publication purposes the plasmid DNA samples will be sent again for re-sequencing.

The recombinant CYP2D6 was successfully over-expressed in *E. coli* TOP10 strain cells and the protein was found at the expected size of ~68 kDa on the SDS-PAGE (Figure 2.11a), corresponding to the 50.05397 kDa *in silico* predicted size plus ~18 kDa (for sequences that include the 6x His-tag (~4 kDa) and TOPO Xpress tag (~4 kDa) and ~10 kDa given by vector sequence) as given by the pTrcHis-TOPO® vector map. The large scale expression of CYP2D6 was done and the protein was successfully extracted as an insoluble fraction (Figure 2.11b) and purified using the Ni-NTA affinity chromatography under denaturing conditions (Figure 2.12) following refolding (Figure 2.13) as done by Santos e*t al.*, (2012). Refolding of extracellular proteins is possible (Vincentelli *et al.*, 2004; Willis *et al.*, 2005; Ruzvidzo *et al.*, 2013), however the protocol impose difficulty in purifying the refolded protein as it allows recovery of small fraction of the input protein (Gräslund *et al.*, 2008). Although, *E. coli* system was not the best system to express CYP2D6 as a soluble fraction, it was chosen due to its simplicity, reliable and affordability. The protein was successfully purified using the affinity chromatography since no any other protein bands were observed on the SDS PAGE, and there was no need for secondary step of purification. The protein concentration was determined using the Bradford assay and found to be adequate for further characterisation and functional assays.

To determine whether the recombinant protein was active and adequate for further application, its activity was determined using the P450-Glo™ CYP2D6 assay. The enzyme activity assay was done on both the unfolded (urea denatured) and folded (renatured) proteins. The unfolded CYP2D6 was used as a marker (control) in order to determine the level of

denaturation by urea, and the extent of refolding. The enzyme activities of both unfolded and folded CYP2D6 are represented by Figure 2.14. The luminescence relative light units (RLUs) signals measured showed an increase as compared to the negative controls which lacked the recombinant proteins. In the absence of rifampicin (as an inducer compound of CYP2D6), the unfolded CYP2D6 (2033.6 RLU) exhibited higher signal than folded CYP2D6 (20104 RLU). However, in the presence of rifampicin, the RLU signal for both proteins was higher as compared to that without rifampicin but the folded protein exhibited a higher signal (23333 RLU) than unfolded protein (21776.67 RLU). An increase was expected for induced folded CYP2D6 since rifampicin is an inducer compound of CYP2D6 (Rae *et al*., 2001), therefore, it is likely to be more functional than unfolded CYP2D6. The enzyme activity increase of CYP2D6 with an addition of rifampicin have proved that the effect of refolding CYP2D6 was necessary for the activity of CYP2D6 functionality, however, it is not certain that the protein was completely refolded. With regard to rifampicin-induction of CYP2D6 activity on compound metabolism, these results are consistent to the increased CYP2D6 activity in the P-glycoprotein metabolism previously described by Manda *et al*. (2015). CYP2D6 activity test in this study has shown that the p-value (p=0,03355) was considered to be statistically significant ($p < 0.05$). The enzyme activity results have proven that although sequencing was not possible, the protein is indeed a CYP2D6 since the substrate is specific for catalysis by CYP2D6. In addition, for publication purposes a western blot assay will be conducted using CYP2D6 specific primary antibody to confirm the protein.

CHAPTER 3: Electrochemical responses of CYP2D6-based sensor for tamoxifen

Abstract

Cytochrome P450 enzymes are heme-thiolated proteins that accomplish the reduction-oxidation electron exchange between the enzyme's active site and the drug. Cytochrome P450-2D6 (CYP2D6) is regarded to be a major form of cytochrome P450s that is responsible for tamoxifen (TAM) metabolism during breast cancer therapy. Ultraviolet-visible, fluorescence and electrochemical techniques such as cyclic and square wave voltammetry are the simplest, quick, sensitive and reliable methods for the determination of drug metabolism by enzymes. The main aim of this chapter was to develop an electrochemical biosensor in order to assay for tamoxifen metabolism. Tamoxifen metabolism by recombinant CYP2D6 using UV-Visible spectroscopy at ~216 nm for both unfolded and folded CYP2D6 was observed with a clear shift in wavelength (from 216 nm to ~212 nm) and decrease in absorbances (from 1.722 a.u to ~1.2 a.u) for folded CYP2D6 than unfolded CYP2D6. There was a shift in fluorescence spectra analysis of both recombinant CYP2D6 proteins at 432 nm. However, there was fluctuation upon tamoxifen additions of which might have been due to the redox state of CYP2D6 or high dose of tamoxifen. The electrochemical binding of tamoxifen to the heme site of CYP2D6 was monitored at a potential of -0.4 V with a clear shift in current for folded CYP2D6 than unfolded CYP2D6. The detection limit was 2.1567×10^{-4} ng/ml and 4.004×10^{-4} ng/ml for folded and unfolded CYP2D6 respectively, and is lower than the maximum tamoxifen plasma concentration of 40 ng/ul. The observed shifts were influenced by both tamoxifen binding to the heme and the CYP2D6 structure conformation (whether folded or unfolded).

Keywords: Biosensor, CYP2D6, Electrochemistry, Spectroscopy, Tamoxifen metabolism.
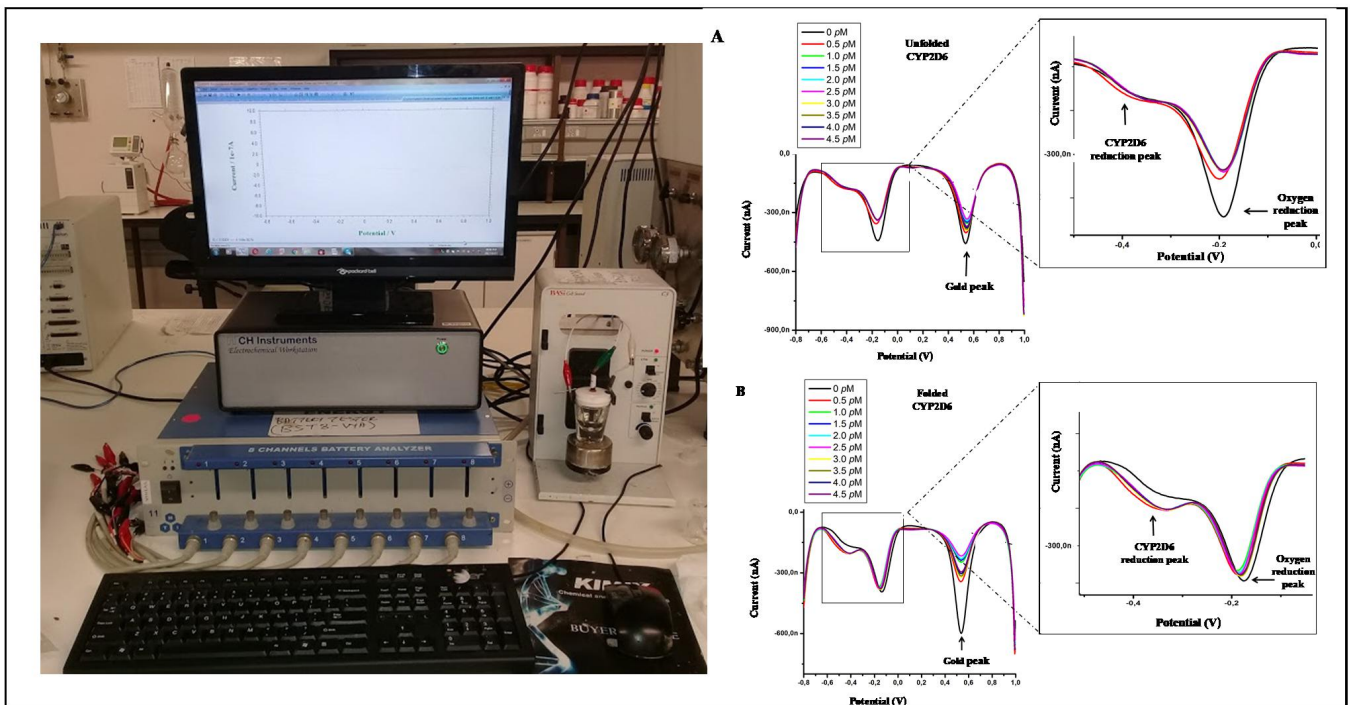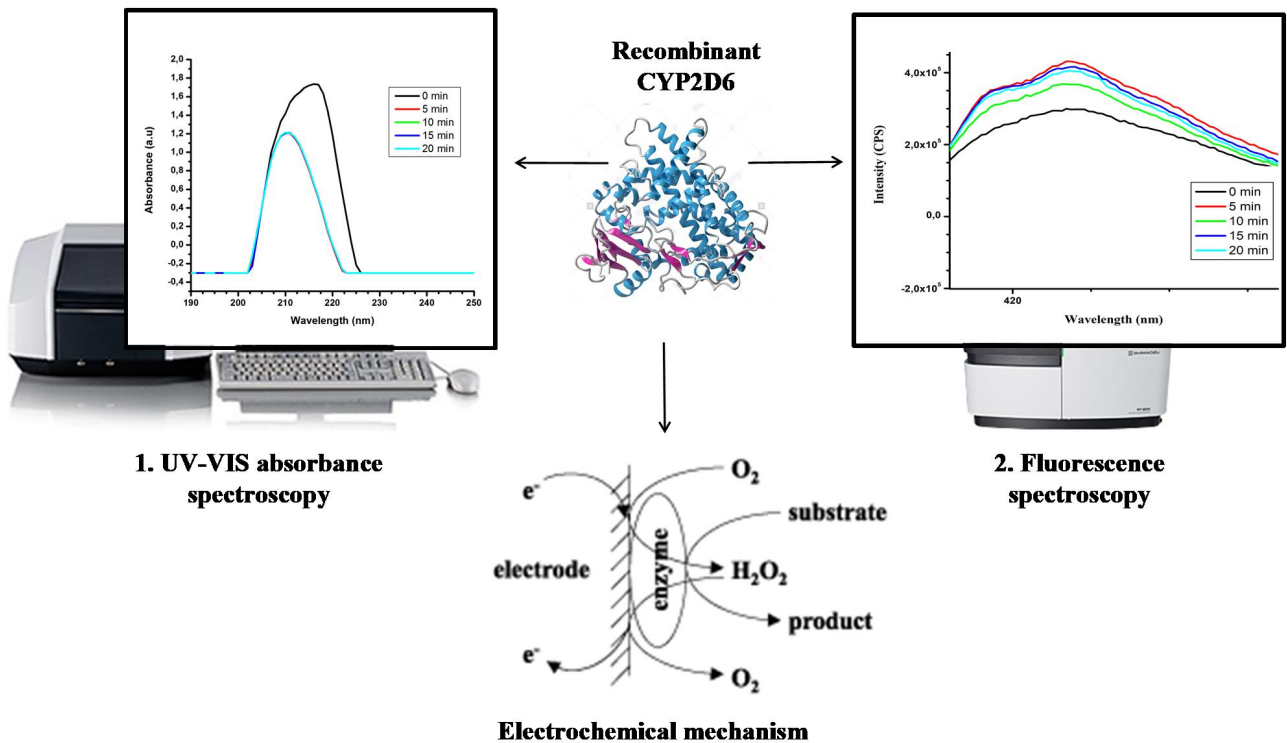
Figure 3.1: Graphical abstract of recombinant CYP2D6-tamoxifen metabolism. Metabolism was characterised using (1) UV-Visible, (2) fluorescence spectroscopy and (3) square wave voltammetry (Computed in Microsoft Power Point).

3.1 Introduction

Electrochemical techniques have been the mostly used methods for determining drug metabolism through cytochrome P450 enzymes, this is due to their relative simplicity, sensitivity and reliability amongst other methods (Yang *et al.,* 2009; Wang *et al.*, 2008). Tamoxifen metabolism by CYP2D6 into its active forms can be determined electrochemically by the use of redox reactions (Garrido e*t al* 2013; Shumyantseva *et al.*, 2015), and is of pharmacological importance particularly for oestrogen positive breast cancer therapy (Garrido *et al* 2013). Spectroscopy methods such as UV-Visible absorbance and Fluorescence spectroscopy, have been employed for drug testing and metabolism (Siddiqui *et al.*, 2013), and are based on natural UV absorption and chemical reactions (Gorog, 1995; Siddiqui *et al.*, 2013). These methods involve quantitative measurement of the reflection or transmission properties of a molecule to be tested as a function of wavelength (Siddiqui *et al.*, 2013). UV-Visible absorption spectroscopy involves measuring the absorbance of light by a molecule as a function of wavelength. While fluorescence spectroscopy occurs in the same wavelength range as UV-Visible, therefore it is a complementary technique to UV-Visible absorption and its results from an excited state are emitted than are absorbed (Penner, 2010; Abdelhalim *et al.*, 2013).

In an aqueous solution, the redox signal of cytochrome enzymes has been determined in the presence of drugs in order to test the electrochemical response of enzymes on drugs (Baj-Rossi *et al.*, 2012). Tamoxifen metabolism with a concern to develop breast cancer therapy was firstly demonstrated by Yarman and Scheller (2014). The possibility of cytochrome P450 enzymes to respond electrochemically, is due to the presence of heme (iron protoporphyrin IX ring) at a centre of the protein. The porphyrin ring is characterised by the ability to perform reduction and oxidation of organic compounds (Capece *et al.*, 2008). The

full system for heme protein involves a pathway where by O_2 is consumed into the organic substrate (RH) and converted into water. This reaction allows the enzyme to be reduced in the presence of NADPH as electron transfer partner and FAD as a reducing power. Due to gaining of electrons in the heme iron, the iron state changes from Fe^{3+} to Fe^{2+} (Banifacio *et al.*, 2008; Narasimhulu, 2010). The simple catalytic cycle and equation of this process is clearly represented below in Figure 3.2.

$$RH + NADPH + H^+ + O_2 \rightarrow ROH + NADP^+ + H_2O \ \dots\dots Eq\ 1.$$
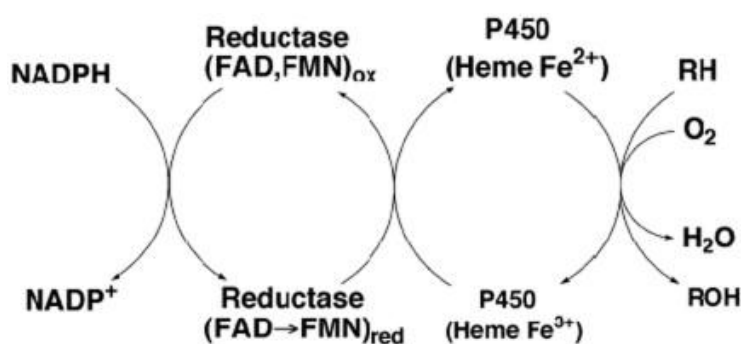
Figure 3.2: The simple catalytic cycle of CYP enzymes. (Adopted from Cederbaum, 2014).

In order to characterise the electrochemical response, cyclic voltammetry (CV) is a very popular, simple, rapid, and powerful method for characterising the electrochemical behaviour of analytes that can be electrochemically oxidised or reduced (Bilal, 2014). On the other hand, square wave voltammetry (SWV) has been widely used in recent years as it has high selectivity and sensitivity. It has been used for the development of electrochemical sensors and biosensors for various purposes including food analysis, environmental monitoring, diagnostics and enzyme sensing (Chen and Shah, 2014). Based on the characteristic features of CYP2D6 to undergo electron exchange with tamoxifen, this study was set out in order to develop a biosensor for breast cancer therapy. Furthermore, this study could contribute to decreasing the cost since the recombinant CYP2D6 is being prepared in the laboratory at a cheaper rate.

3.2 Materials and methods

3.2.1 Reagents and sample preparation

In order to characterise and understand the electrochemical metabolism of tamoxifen by recombinant CYP2D6, the protein was firstly analysed by UV-VIS and fluorescence spectroscopy to determine its absorbance and emission characteristics. Recombinant CYP2D6 protein was expressed as described in chapter 2, in preparation for future use in tamoxifen metabolism. About 50 mM sodium phosphate buffer solution, pH 7.4 was used for analysing the proteins in all experiments. A stock solution of 1 µM TAM was prepared in absolute ethanol from which a fresh standard solution of 1.6 nM TAM was prepared by diluting with 50 mM sodium phosphate buffer solution, pH 7.4. Both stock and standard TAM solutions were stored at 4 ºC until further use. Millipore ultrapure water (resistivity $\geq$ 18.2 MΩcm) was used throughout the experiments.

3.2.2 UV-Visible absorbance spectroscopy of CYP2D6

Ultraviolet–visible absorption measurements for the recombinant CYP2D6 were obtained using a Nicolet Evolution 100 UV-Visible spectrophotometer (Thermo Electron, UK), at a wavelength between 200 and 800 nm. Absorption spectra were determined in a 1 ml cuvette (1 cm path length) containing 0.0124 µM of each CYP2D6 proteins, 50 mM sodium phosphate buffer, and in the presence or absence of different concentration of tamoxifen (0.03 - 0.12 µM) through an optical resolution of 0.1. The baseline given by the PBS buffer was obtained to standardise the addition of other components and the measurements were conducted based on tamoxifen concentrations and time dependent manner. The cuvettes were cleaned before each use by sonication for 5 min in ethanol followed by rinsing with deionized water. All measurements were recorded at room temperature.

3.2.3 Fluorescence spectroscopy of CYP2D6

The photoluminescence (PL) spectra were recorded using a Nanolog, Horiba NanoLog™ 3-22-TRIAX (USA), with double grating excitation and emission monochromators, plus an imaging spectrograph for a second emission channel. Fluorescence spectra measurements were performed in a cuvette containing 1 ml of 50 mM sodium phosphate buffer pH 7.4, 0.03 µM each unfolded and folded CYP2D6 proteins, with the addition of tamoxifen to a final concentration of 0.04 mM. The measurements were employed for concentration-dependent and time basis. The cuvette was placed for detection of the tamoxifen metabolism on a HORIBA Jobin Yvon Fluorolog-3 model FL3 - 22 spectrofluorometer (HORIBA scientific, USA). Fluorescence measurements were taken over the wavelength of 300 nm and at 2 different excitation values (315 and 585 nm). All measurements were recorded at room temperature.

3.2.4 Electrochemical analysis of CYP2D6 in tamoxifen metabolism

3.2.4.1 Preparation of CYP2D6 bioelectrode system

The 3 mm diameter gold (Au) disk electrode used in this experiment was polished carefully with alumina slurry (1 µm, 0.3 µm down to 0.05 µm), on a polishing cloth and rinsed repeatedly with distilled water to obtain a mirror like surface. The electrode was then subjected to ultrasonic vibration in both absolute ethanol and Mili-Q water to remove residual alumina particles that might be trapped on the surface. About 3 µl of 0.03 µM CYP2D6 protein drop-casted on a gold electrode surface and then incubated at 4 ºC for 3 h, to allow the protein to be adsorbed on the Au electrode. The resulting CYP2D6/Au bioelectrode was rinsed gently with distilled H_2O to remove any physically adsorbed enzyme and was kept at 4 ºC in 50 mM sodium phosphate, pH 7.4 when not in use.

3.2.4.2 Bioelectrochemical analysis of tamoxifen metabolism using CYP2D6/Au

The electrochemical analysis of tamoxifen metabolism were conducted on a electrochemical cell consisting of three electrodes, working electrode CYP2D6/Au, Ag/AgCl as a reference electrode, and a coiled Pt wire as a counter electrode on the electrochemical workstation, CHI 760E (Shanghai CH Instrument Co., China). The electrochemical cell contained 50 mM sodium phosphate buffer (pH 7.4) as the electrolyte. The potentials were characterised at 800 Hz and 0.15 V amplitude voltage, sweeping from -0.1 V to +0.8V at different scan rates (mV/s) using cyclic voltammetry (CV) and square wave voltammetry (SWV). The bare electrode was firstly analysed alone in order to characterise the potentials of gold without the protein as a control for CVs and SWVs. The CVs and SWVs of both unfolded and folded CYP2D6 proteins were detected. Due to high sensitivity of SWVs than CVs (Lee *et al*., 2008) and that the protein redox characteristics were already known to be in the reduction state, tamoxifen metabolism was further conducted using SWVs at the best scan rate of 15 mV/s. Tamoxifen metabolism potentials were detected for concentration-dependent (using 0, 0.5, 1, 1.5, 2. 2.5, 3, 3.5, 4, and 4.5 *p*M) and time basis (0, 5, 10, 15, 20 and 25 min) on both proteins.
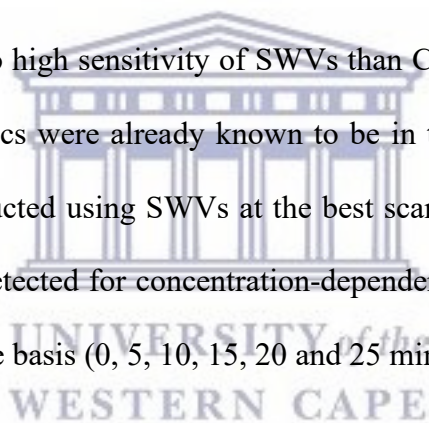
3.3 Results

The main aim of this chapter was to characterise tamoxifen metabolic response by both unfolded and folded recombinant CYP2D6 proteins using UV-Visible spectroscopy, florescence spectroscopy and electrochemical techniques, in order to determine the absorbance, emission spectra and redox potential characteristics respectively.

3.3.1 Optical properties of recombinant CYP2D6

The characteristic features of both unfolded and folded CYP2D6 in the absence and presence of tamoxifen were measured using the UV-Visible spectroscopy. As can be seen in Figure 3.3, both proteins exhibited a sorbet band at 216 nm with slight differences in absorbances (1.807 a.u for unfolded CYP2D6 and 1.722 a.u for folded CYP2D6). In the presence of 3 pM of tamoxifen concentration, the unfolded CYP2D6 protein had a slight shift in the absorbance band, but there was also a slight shift in wavelength as it is shown in Figure 3.4a and.c. Compared to the unfolded, folded CYP2D6 revealed a clear shift in wavelength from 216 nm to 212 nm and a decrease in absorbance from 1.722 a.u to ~1.2 a.u for both time dependent (0-25 min) and concentration dependent (0-12 pM) as shown in Figure 3.4b and d.
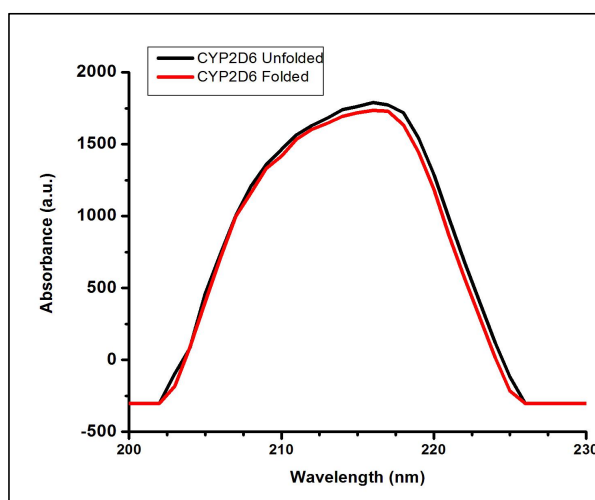
Figure 3.3: UV-Vis absorption spectra of the unfolded and folded CYP2D6 proteins. The absorbance spectra were measured at wavelength range of 200 - 800 nm.
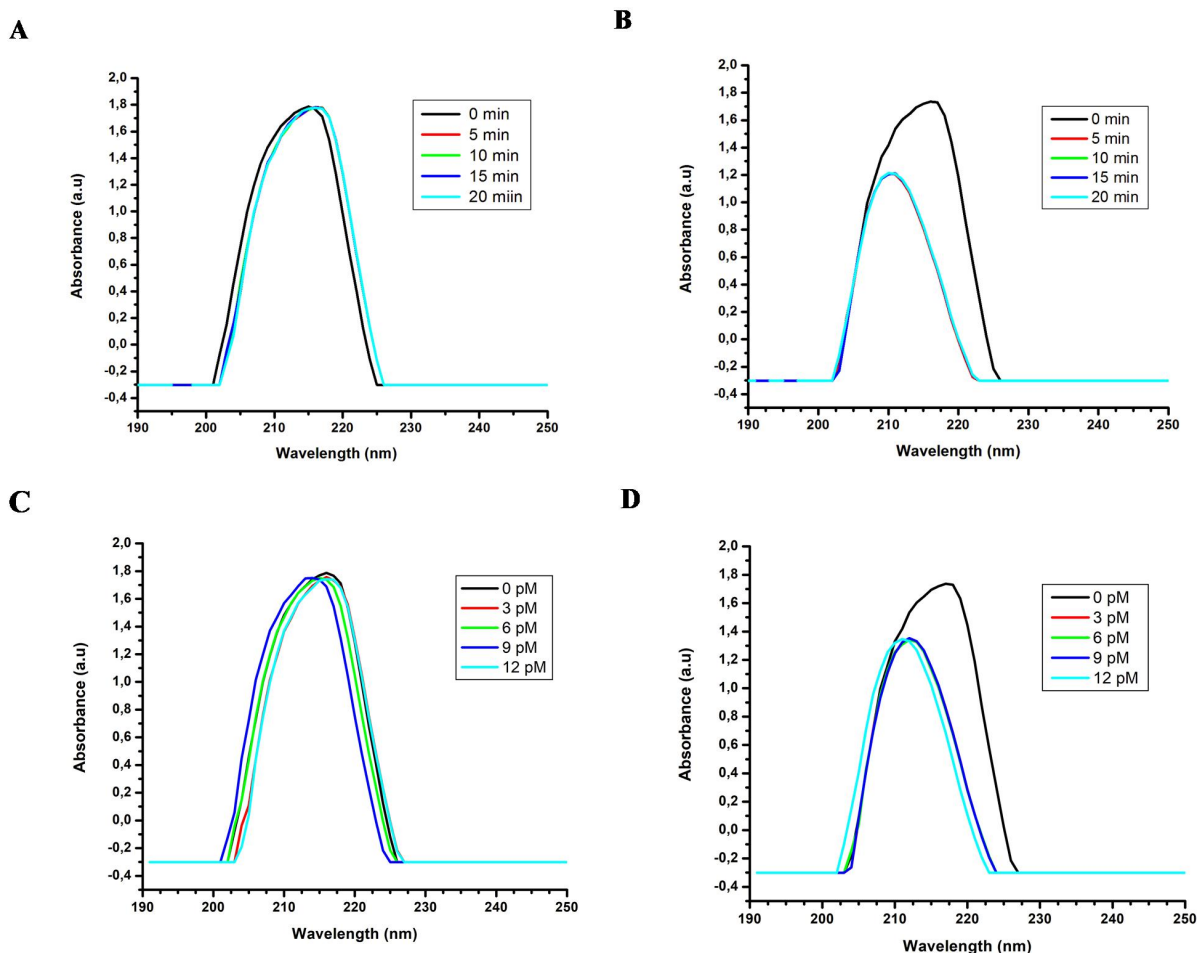
Figure 3.4: UV-Visible absorption spectra of CYP2D6-tamoxifen complex recorded in a 200-800 nm wavelength range in 50 mM sodium phosphate (pH 7.4): (A) Unfolded CYP2D6 and, (B) Folded CYP2D6 with 3 pM TAM at 0 - 25 min time dependent, (C) Unfolded CYP2D6 and (D) Folded CYP2D6 in the presence of TAM in a concentration dependent (0 - 12 pM).

4.3.2 Emission studies of recombinant CYP2D6

Fluorescence spectroscopy was employed to investigate CYP2D6-TAM interactions and presence of residues prior for fluorescent properties during tamoxifen metabolism. The emission spectra showing the optical properties of both unfolded and folded CYP2D6 and tamoxifen are illustrated in Figure 3.5. When excited at 315 nm, two maximum emission peaks were observed at 350 nm and 432 nm for unfolded and folded CYP2D6 respectively. Tamoxifen alone exhibited three emissions at 350 nm, 419 nm and 501 nm. In addition, the intensity obtained by the folded CYP2D6 was more enhanced than the unfolded CYP2D6.
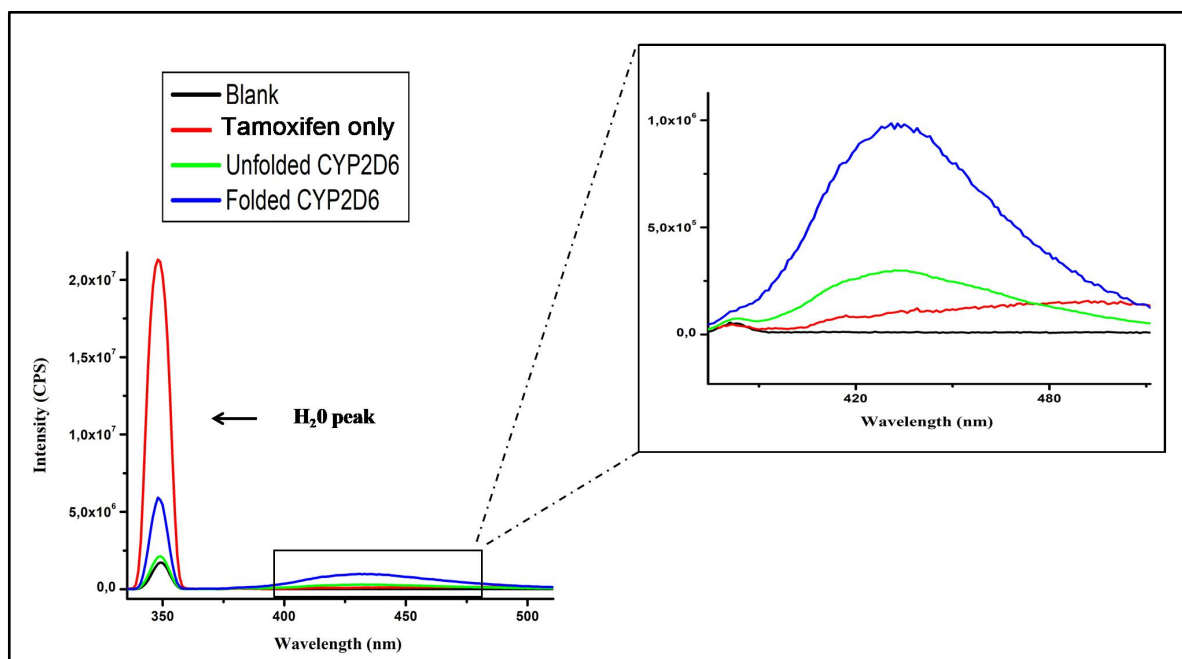
Figure 3.5: Fluorescence spectra of the CYP2D6 proteins alone and tamoxifen. Both recombinant CYP2D6 proteins emitted a peak at the wavelength of 432 nm and a drug was emitted at the wavelength of 419 nm and 501 nm. The emission of buffer has shown a peak at 350 nm wave length that depicts a peak of water.

Fluorescence spectra of both unfolded and folded CYP2D6 were further detected in the presence of TAM in a time and concentration dependent basis as illustrated in Figure 3.6. The intensity of emission peaks for unfolded and folded CYP2D6 proteins were unstable in the presence of 0.04 mM tamoxifen. In comparison, the fluorescent intensity of the unfolded CYP2D6 increased from 2.9479×10^6 CPS to 4.3181×10^6 CPS (Figure 3.6a), whereas that of folded CYP2D6 increased from 3.0121×10^6 CPS to 4.36148×10^6 CPS (Figure 3.6b). After the fluorescent intensity shifted, it began to fluctuates for both time and concentration dependent basis. For folded CYP2D6, the fluorescent intensity increased from 10.2668×10^6 CPS to 11.5820×10^6 CPS for time-dependent and then began to fluctuate (Figure 3.6c) and decreased from 9.8526×10^6 CPS to 9.2060×10^6 CPS for concentration-dependent and then began to fluctuates (Figure 3.6d).
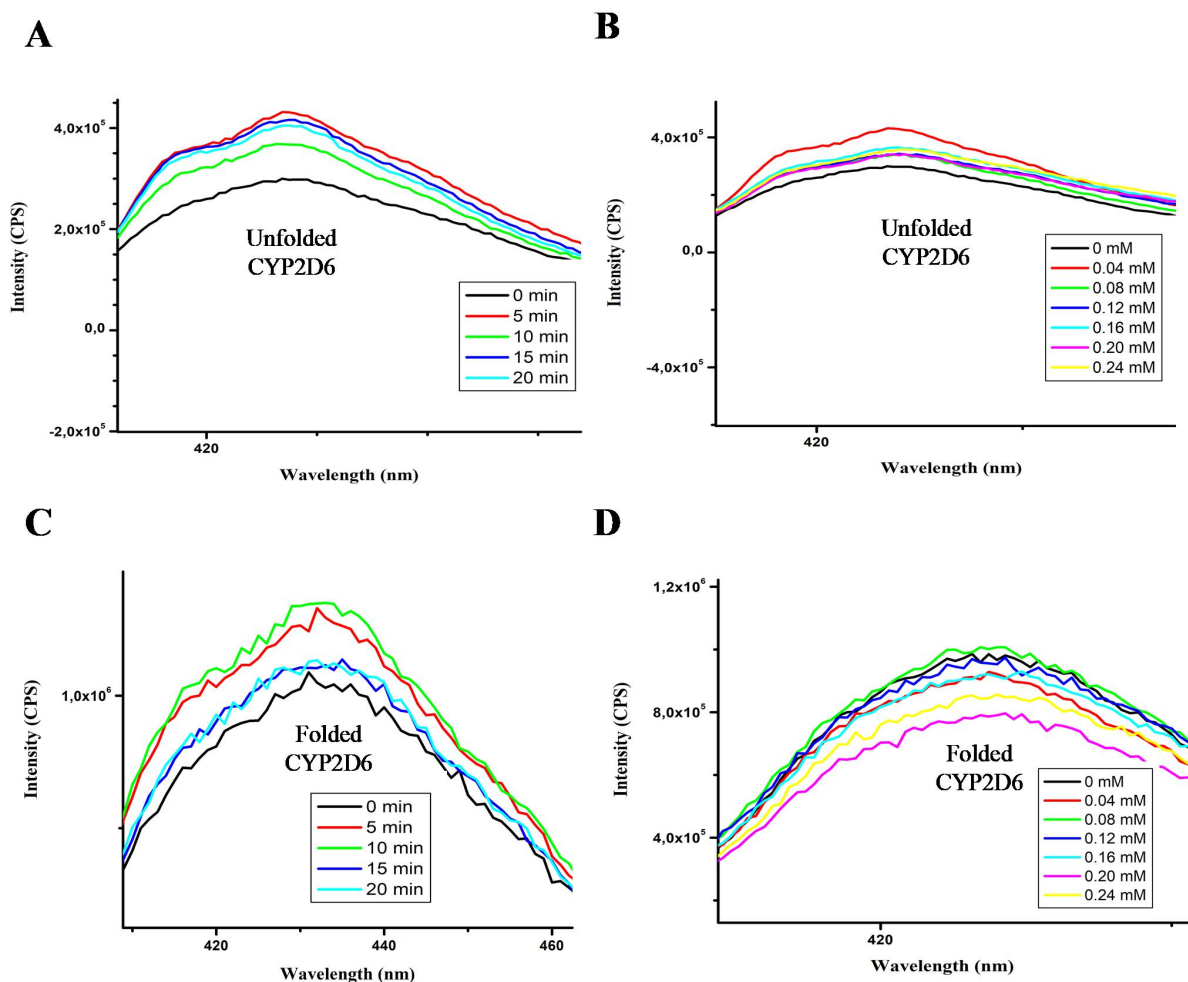
Figure 3.6: Fluorescence spectra of tamoxifen metabolism by recombinant CYP2D6. (A) Time-dependent tamoxifen metabolism by unfolded CYP2D6. (B) Concentration-dependent tamoxifen metabolism by unfolded CYP2D6. (C) Time-dependent tamoxifen metabolism by folded CYP2D6. (D) Concentration-dependent tamoxifen metabolism by folded CYP2D6.

3.3.3 Electrochemical analysis of recombinant CYP2D6

Firstly, the bare gold (Au) electrode was characterised using CV and SWV in order to determine its redox properties as a control. As shown in Figure 3.7a and b for both CV and SWV respectively, there was a clear reduction peak that depicts gold at ~0.6 V. For modified electrode (CYP2D6/Au), there was a clear reduction peak at -0.2 V using both CV and SWV that depict the reduction of O_2 to H_2O_2, for which it increased with an increase in scan rate up to 50 mV/s (Figure 3.7 c to f). For both unfolded (Figure 3.7c and d) and folded (Figure 3.7e

and f) CYP2D6 proteins, there was a peak that depict the recombinant CYP2D6 at approximately -0.4 V.
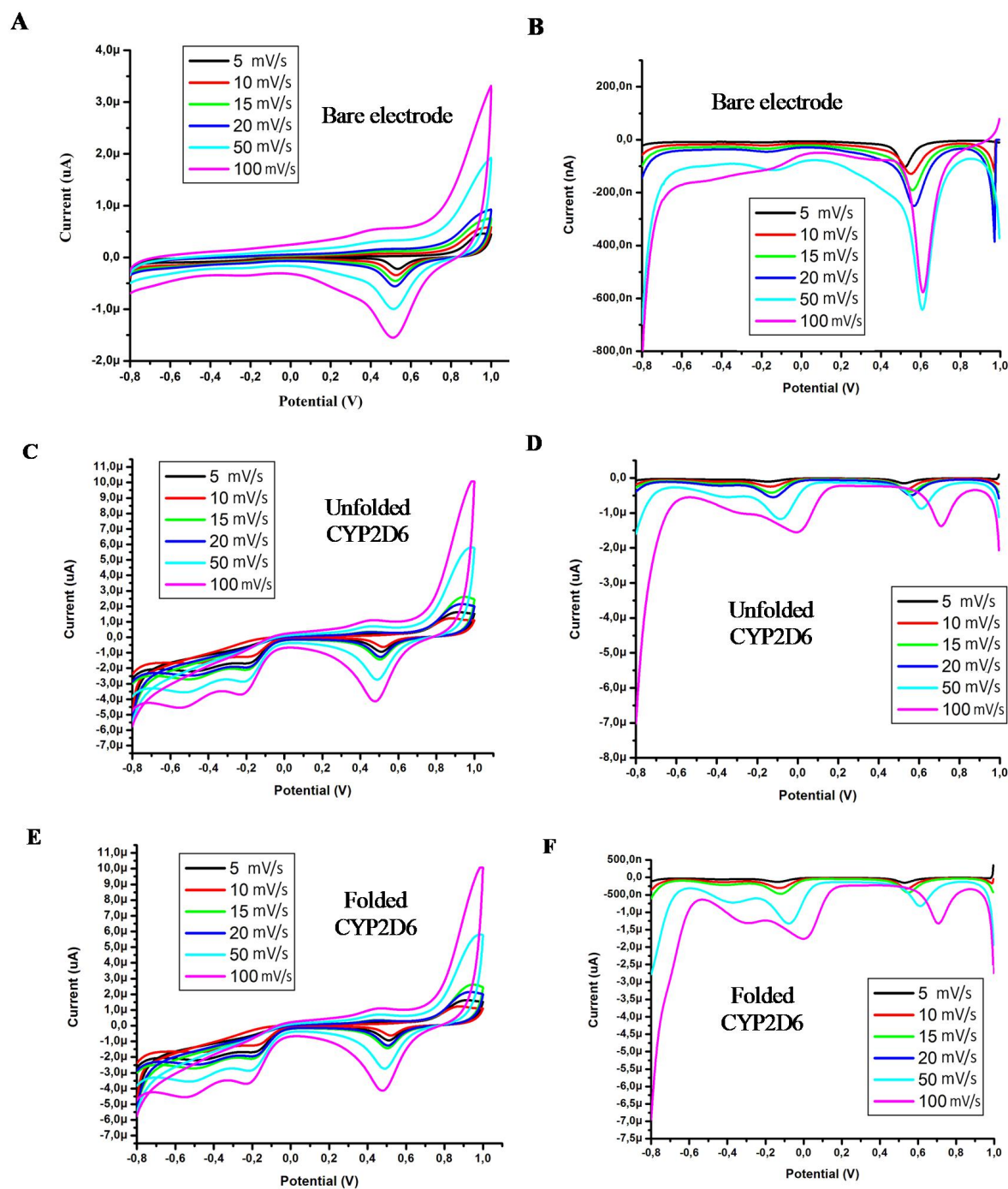
Figure 3.7: The CV and Square wave voltammograms of bare electrode and CYP2D6 proteins analysis in 50 mM sodium phosphate. (A) bare Au electrode. (B) SWV analysis of bare Au electrode. (C) CV analysis of unfolded CYP2D6/Au. (D) SWV analysis of unfolded CYP2D6/Au. (E) CV analysis of folded CYP2D6/Au. (F) SWV analysis of folded CYP2D6/Au.

The electro-catalysis of tamoxifen metabolism was further characterised in the presence of TAM in a concentration and time dependent as in shown in Figure 3.8 and Figure 3.9 respectively. For the concentration dependent studies with addition of (0 - 4.5 pM) TAM, the unfolded CYP2D6 showed a slight shift in current at a reduction peak of -0.4 V from -144.8 x 10^{-7} to -153.2 x 10^{-7} nA (Figure 3.8a) compared to folded CYP2D6 which showed a clear shift from -143.6 x10^{-7} to -206.2 x 10^{-7} nA (Figure 3.8b) A similar trend in current shift was also observed for time dependent (0-25 min), from -168.9 x 10^{-7} to -171 x10^{-7} nA for unfolded CYP2D6 (Figure 3.9a) compared to a clear shift of -164 x10^{-7} to -202.8 x 10^{-7} nA for folded CYP2D6 (Figure 3.9b).
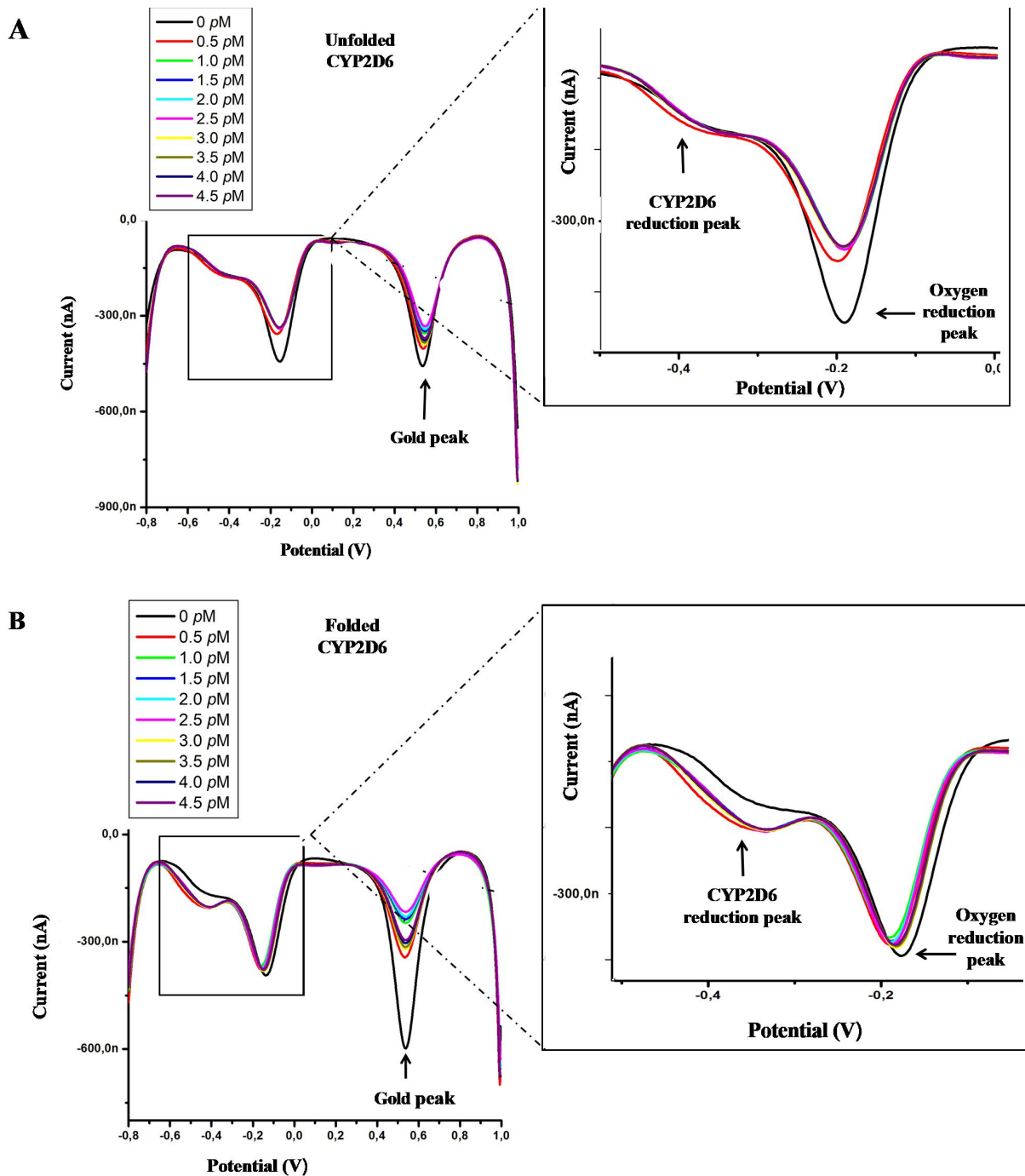
Figure 3.8: The concentration-dependent square wave voltammograms of CYP2D6 proteins. (A) SWV analysis of unfolded CYP2D6/Au in addition of different concentration of tamoxifen in 50 mM sodium phosphate buffer electrochemical cell. (B) SWV analysis of folded CYP2D6/Au in addition of different concentration of tamoxifen in 50 mM sodium phosphate buffer electrochemical cell.
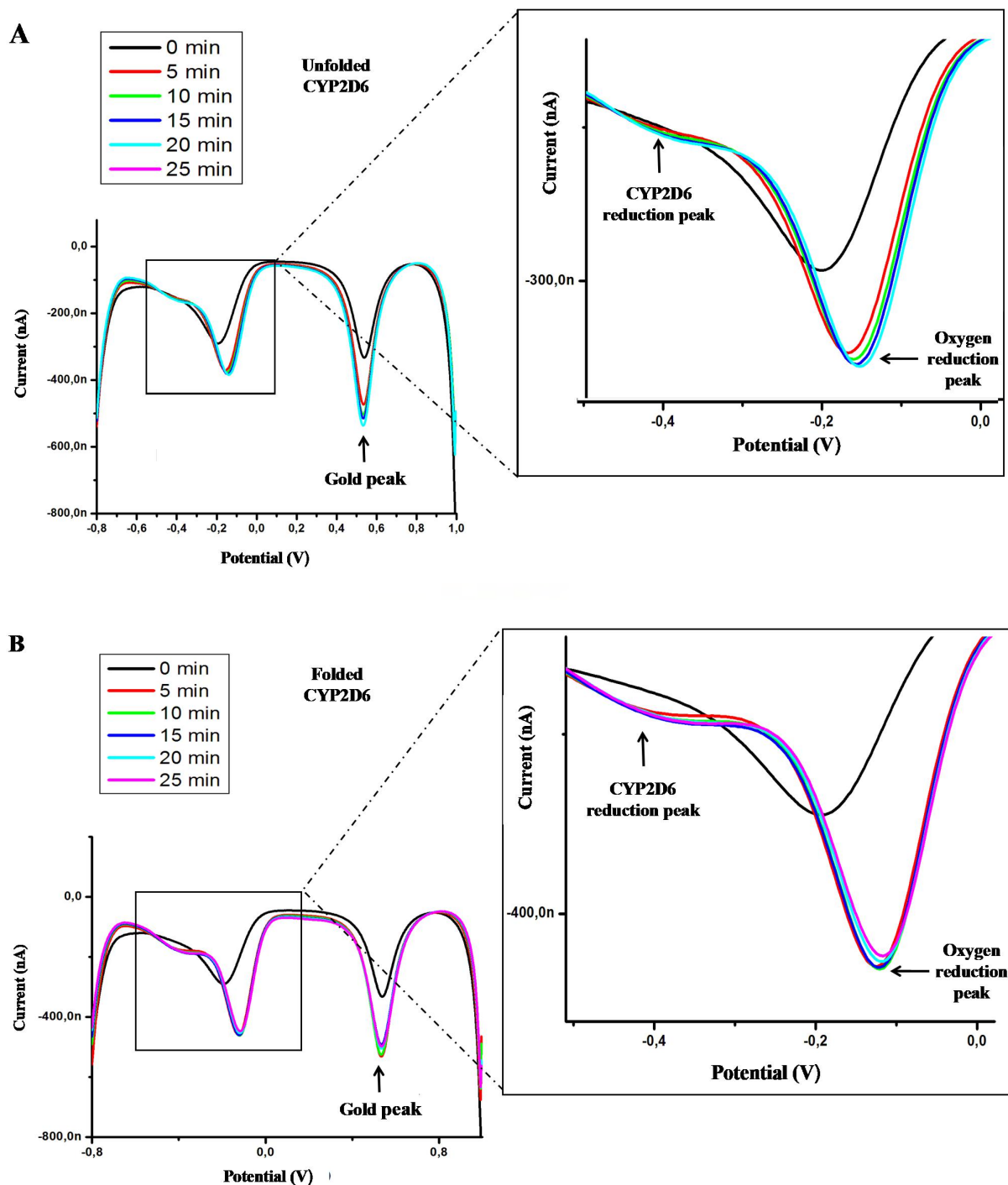
Figure 3.9: The time-dependent square wave voltammograms of CYP2D6 proteins. (A) SWV analysis of unfolded CYP2D6/Au upon addition of 0.5 pM of tamoxifen, with different time intervals in 50 mM sodium phosphate buffer. (B) SWV analysis of folded CYP2D6/Au upon addition of 0.5 pM of tamoxifen, with different time intervals in 50 mM sodium phosphate buffer.

The linear plot was performed in order to determine sensitivity and limit of detection of

tamoxifen catalysis using the protein current values versus different concentrations of

tamoxifen used against different current values of the blank protein peaks. The graphs gave linear calibration curves as shown in Figure 3.10. The sensitivity was determined as the slope of the calibration line which interpolates experimental data and the detection limit was calculated using the formula; limit of detection (LOD) = (3*standard deviation/sensitivity value). The electrochemical binding of tamoxifen and recombinant CYP2D6 proteins were sensitive up to 1.46667 nA/V with a detection limit of 4.2038×10^{-4} ng/ml (Figure 3.10a) and 1.69667 nA/V with a detection limit of 2.1567×10^{-4} ng/ml (Figure 3.10b) for unfolded and folded CYP2D6, respectively.
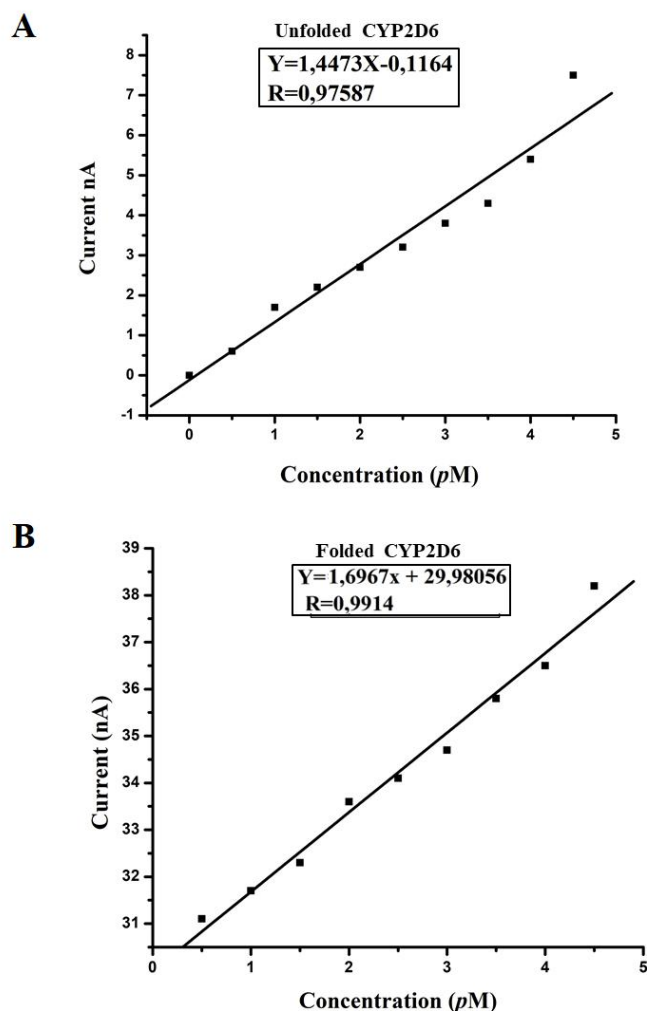
Figure 3.10: The calibration plot of recombinant CYP2D6 with different concentrations of tamoxifen at a potential of -0.4 V. (A) Unfolded CYP2D6 (current Vs. TAM concentration) (B) folded CYP2D6 (current Vs. TAM concentration).

3.3 Discussion

The aim of this chapter was to conduct the electrochemical binding of tamoxifen and recombinant CYP2D6 in order to develop a cheap and simple biosensor for assaying tamoxifen metabolism for breast cancer therapy. The UV-Visible absorbance, fluorescence spectroscopy and electrochemical analysis were conducted on both unfolded and folded recombinant CYP2D6. The spectroscopic analysis revealed that the absorbance band of both unfolded and folded recombinant CYP2D6 to be 1.807 a.u and 1.722 a.u at a wavelength of 216 nm (Figure 3.3) respectively. Such slight difference of 0.085 a.u between the two proteins is due to the presence of urea as a denaturant for unfolded CYP2D6 (Schmid, 2001). The time dependent results were conducted using constant tamoxifen concentration of 3 pM, with readings taken at different time intervals (0, 5, 10, 15, 20, and 25 min). The results showed that there was a slight shift of both the absorbance and wavelength for unfolded CYP2D6 (Figure 3.4a). Whereas for folded CYP2D6, there was a clear shift in absorbance from 1.722 a.u to ~1.2 a.u and a shift in wavelength from 216 nm to 212 nm (Figure 3.4b). A similar trend was observed with the addition of different tamoxifen concentrations of 3 - 12 pM, for both unfolded CYP2D6 (Figure 3.4c) and folded CYP2D6 (Figure 3.4d). The results suggest that there was an interaction between CYP2D6 and tamoxifen with the folded protein since a decrease in absorbances has followed a similar trend done by Baj-Rossi *et al*. (2012) in an electrochemical detection of anti-breast-cancer agents study.

The emission peaks of both CYP2D6 proteins were obtained at 432 nm with folded CYP2D6 emitted better that unfolded CYP2D6 (Figure 3.5). There was fluctuating fluorescent intensity of peaks for unfolded and folded CYP2D6 proteins with an addition of 0.04 mM tamoxifen. For unfolded CYP2D6, the fluorescent intensity increased from 3.0121×10^6 CPS to 4.36148×10^6 CPS and from 2.9479×10^6 CPS to 4.3181×10^6 CPS and then began to

fluctuates for both time and concentration-dependent respectively (Figure 3.6 a and b). For folded CYP2D6, the fluorescent intensity, increased from 10.2668 x 10^6 CPS to 11.5820 x 10^6 CPS (Figure 3.6c) for time-dependent while decreased from 9.8526 x 10^6 CPS to 9.2060 x 10^6 CPS (Figure 3.6d) for concentration-dependent, and then began to fluctuates. Such fluctuations in fluorescence intensity might have been influenced by the redox state of CYP2D6 as a cytochrome enzyme, upon tamoxifen additions and high dose of tamoxifen used in order to observe signal differences (Kumar *et al*., 2005).

The electrochemical analysis was conducted for bare electrode, both unfolded and folded CYP2D6-modified gold electrodes with different scan rates of 5, 10, 15, 20, 50, 100 mV/s using CV and SWV electrochemical techniques. The later approach was used alone since the direction of the redox potential of protein was already known to be in the reduction side and the fact that it is the most sensitive method than CV (Lee *et al*., 2008; Bagalkoti *et al.*, 2017). The SWV was measured on both unfolded and folded CYP2D6 using the single scan rate of 15 mV/s. An electrochemical analysis revealed that there was a different response between the bare electrode and the recombinant CYP2D6/Au modified gold electrodes as shown in Figure 3.7. The electrochemical results of bare electrode alone only showed a peak that depict the peak characteristics of gold in both CV (Figure 3.7a) and SWV (Figure 3.7 b) at a potential of approximately 0.6 V. Similar results of gold peak characterisation were previously reported by Rhieu and Reipa (2015) in their study, "Tuning the Size of Gold Nanoparticles with Repetitive Oxidation-reduction Cycles". In the immobilised electrodes, there were three peaks for which one depict the gold peak and the other two depicts the CYP2D6 protein and oxygen at the potential approximately -0.4 V and -0.18 V respectively.

In the presence of different tamoxifen concentrations of (0-4.5 *p*M) for concentration dependent and time dependent analysis (0, 5, 10 , 15 ,20, and 25 min) in the presence of

constant concentration of 0.5 pM, the SWV results showed an increase in the reduction peak that depicts CYP2D6. For unfolded CYP2D6 (Figure 3.8a), there was a slight shift in the current of the peak that depicts CYP2D6 from -168.9 nA to -171.8 nA at -0.4409 V, with increase in concentration. For folded CYP2D6 there was a clear shift in the current of protein peak from -164.6 nA to -202.8 nA (Figure 3.8b). For time dependent in the presence of 0.5 pM TAM there was a similar trend of shift in current for both proteins. There was a slight shift in current peak of unfolded CYP2D6 protein from -144.8 nA to -153.2 nA (Figure 3.9a) whereas for folded CYP2D6 protein there was a clear shift in current from -143.6 nA to -206.2 nA (Figure 3.9b). The gold peak with the time-dependent analysis also showed an increase shift in current for both unfolded and folded CYP2D6 proteins, while for concentration-dependent there was a decrease. Such a decrease in a concentration dependent experiment is due to saturation of tamoxifen drug as a substrate on the gold electrode surface (Shetti et al., 2015). Such shift in current for enzymes implies that the demand of electrons depends on the activity of the enzyme as seen with the folded CYP2D6 and can be directly correlated to the tamoxifen at the electrode interface. The results are consistent to the study reported by Cavallini (2013), which concluded that higher concentrations of tamoxifen as a substrate increases the electrons demand and therefore generates higher currents. Therefore, the increase in current is proportional to the amount of active tamoxifen metabolite, 4-hydroxytamoxifen as a product of tamoxifen metabolism by CYP2D6 (Garrido et al., 2011). The electrochemical binding of tamoxifen and recombinant CYP2D6 proteins was sensitive to 1.46667 nA/V with a detection limit of 4.004 X 10^{-4} ng/ml (Figure 3.10a) and 1.69667 nA/V with a detection limit of 2.1567 X 10^{-4} ng/ml (Figure 3.10b) for unfolded and folded CYP2D6 respectively. The linear calibration curves of tamoxifen determination are consistence with the results obtained by Reid et al. (2014), where the range was up to approximately 0.2 pM. The detection limit of tamoxifen metabolism for both recombinant

CYP2D6 proteins was less than the maximum tamoxifen plasma concentration (C_{max}) of 40 ng/ml (Reid *et al*., 2014). C_{max} is defined as the highest concentration of a drug in plasma (blood, cerebrospinal fluid) or target organ after a dose of drug is administered (https://medical-dictionary.thefreedictionary.com/Cmax). Low values detection limit implies that tamoxifen has been converted into a product, 4-hydroxytamixifen, according to the tamoxifen metabolism pathway with CYP2D6 alone.

CHAPTER 4: Conclusion and future prospects

The main aim of this study was to generate an expression construct in order to express large amounts of active recombinant CYP2D6 at a cheaper way in order to develop an electrochemical biosensor for tamoxifen metabolism test during breast cancer therapy. *In silico* characterisation of CYP2D6 gene provided parameters that are necessary for successful cloning, and purification of CYP2D6, particularly the size of CYP2D6 and its location when expressed in *E. coli* system. Cloning of CYP2D6 was much more efficient with the pTrcHis-TOPO® vector, producing approximately 95% of recombinant clone product (Yuvaraj, 2007). When CYP2D6 was expressed in *E. coli*, it needed to be extracted and purified under urea denaturing state followed by refolding to bring the protein to active functional state. The enzyme assay revealed that the recombinant CYP2D6 was active after it was refolded since there were high luminescence signals as expected for folded CYP2D6. However, the effect of refolding the protein did not reveal at what extent the protein was refolded or denatured (from or to its quaternary structure). It was also detected with purification that there is a possibility to purify denatured protein under refolding state, however the protocol allows small fraction to be recovered (Ruzvidzo *et al*., 2013; Gräslund *et al*., 2008). Our results proved with no doubt that the recombinant CYP2D6 protein that was expressed and refolded was active and adequate for electrochemical studies.

The tamoxifen metabolism based on the absorbance results showed that the metabolism was dependent to the structure of the protein whether folded on unfolded, since the folded protein showed a clear shift compared to unfolded CYP2D6 in the presence of TAM. The fluorescence results were also consistent with the UV-Visible absorbance spectroscopy, indicating an interaction between CYP2D6 and tamoxifen, although there were fluctuations.

These fluctuations might have been due to the redox state upon tamoxifen additions since the catalytic reaction of cytochrome P450 enzymes is a cycle or high dose of tamoxifen used in order to observe signal differences (Kumar *et al.*, 2005).

CYP2D6 based electrochemical sensor plays an important role in tamoxifen metabolism into its active metabolites. However, since the protein was firstly purified under denatured condition (as unfolded CYP2D6), only renatured protein (as folded CYP2D6) showed a definable shift in tamoxifen metabolism. Therefore, the phenotypic based sensor pose a promising application in developing a biosensor for assaying human tamoxifen metabolism during breast cancer therapy. The electrochemical analysis of tamoxifen metabolism revealed that the increase in current at the formal potential peak of CYP2D6 proteins was electrochemically-driven by electron exchange between the porphyrin ring of CYP2D6 and tamoxifen. According to the results obtained, tamoxifen metabolism was also dependent on the structural conformation of each protein whether it was unfolded or folded, and the folded CYP2D6 was able to convert TAM into 4-hydroxytamoxifen.

According to the pathway for tamoxifen metabolism, the catalysed tamoxifen in this study, did not produce the final product (endoxifen), since it has to work hand to hand with CYP3A4/5 but it produced 4-hydroxytamoxifen. Therefore, there is a need to characterise CYP3A4/5 also as the other main enzyme for tamoxifen metabolism, in order to complete the pathway of tamoxifen metabolism. Though there was a response with direct electrochemical characterisation of recombinant CYP2D6 in metabolising tamoxifen, there is still a need to use a molecular linker when immobilising the protein on gold electrode in order to improve the electron transfer in the electrochemical system. It will also be recommended to further study other techniques that support the electron exchange transfer detection between the tamoxifen and CYP2D6. For future work, we will culture and treat breast cancer cell line,

Michigan Cancer Foundation-7 (MCF-7), and conduct electrochemical analysis of tamoxifen. Lastly, we are aiming to develop a prototype, for rapid and simple detection of tamoxifen metabolism in breast cancer patients.

REFERENCES

Abdelhalim, M.A.K., Moussa, S.A.A., & Al-Mohy, Y.H. (2013). Ultraviolet-visible and fluorescence spectroscopy techniques are important diagnostic tools during the progression of atherosclerosis: diet zinc supplementation retarded or delayed atherosclerosis. *BioMed Research International*. https://doi.org/10.1155/2013/652604

Abraham, J.E, Maranian, M.J, Driver, K.E. (2011). CYP2D6 gene variants and their association with breast cancer susceptibility. *Cancer Epidemiol BiomarkersPrev.* 20: 1255-8

ACS (American Cancer Society). (2016). American Cancer Society's Cancer Statistics Center. Last medical review: 09/25/2014. Last revised: 02/22/2016. http://www.cancer.org/cancer/breastcancer/detailedguide/breast-cancer-key-statistics

Alonso-Lomillo, M.A., Gonzalo-Ruiz, J., Domínguez-Renedo, O., Muñoz, F.J., Arcos-Martínez Biosens, M.J. (2008). *Bioelectron.* 23: 1733-1737

Alvarez-Lueje, A., Zapata, C., & Perez, M. (2012). Electrochemical methods for the in vitro assessment of drug metabolism. *Topics on drug metabolism, Dr. James Paxton (Ed.), InTech.*.http://www.intechopen.com/books/topics-on-drug-metabolism/electrochemical-methods-for-the-in-vitro-assessment-of-drug-metabolism

Alwan, N.A., Al-Attar, W.M., Eliessa, R.A., Madfaie, Z.A. & Tawfeeq, F.N. (2012). 'Knowledge, attitude and practice regarding breast cancer and breast self-examination among sample of the educated population in Iraq'. *Eastern Mediterranean Health Journal.* 18: 337–345

Amann, E., Brosius, J., & Ptashne, M. (1983). Vectors bearing a hybrid trp-lac promoter useful for regulated expression of cloned genes in Escherichia coli. *Gene*. 25: 167-178. http://doi.org/10.1016/0378-1119: 90222-6

Anderson, K., Poulter, B., Dudgeon, J., Li, S.E., & Ma, X. (2017). A highly sensitive non enzymatic glucose biosensor based on the regulatory effect of glucose on electrochemical behaviours of colloidal silver nanoparticles on MoS2. *Sensors.* 17: 1807. https://doi.org/10.3390/s17081807

Arcos-Martínez, M. (2014). Cytochrome P450 2D6 based electrochemical sensor for the determination of codeine. *Talanta*. 129: 315-319. https://doi.org/10.1016/j.talanta.2014.05.053

Arnold, K., Bordoli, L., Kopp, J., & Schwede, T. (2006). The SWISS-MODEL workspace: A web-based environment for protein structure homology modelling. *Bioinformatics*. 22: 195–201. https://doi.org/10.1093/bioinformatics/bti770

Asturias-Arribas, L., Asunción Alonso-Lomillo, M., Domínguez-Renedo, O., & Alvarez-Lueje, A., Zapata, C., & Perez, M. (2012). Electrochemical methods for the *in vitro* assessment of drug metabolism. *Topics on drug metabolism.* 221–246. https://doi.org/10.5772/28647

ASDL (analytical Science Digital Library) (2016) Analytical chemistry: the basic concept http://www.asdlib.org/onlineArticles/ecourseware/Kelly_Potentiometry/PDF-14-EChem Cells.pdf. [Accessed: 12/06/2016]

Ausubel, F.M., Brent, R., Kingston, R.E., Moore, D.D., Seidman, J.G., Smith, J.A., & Struhl, K. (1994). Current protocols in molecular biology. New York: Greene Publishing Associates and Wiley-Interscience

Avci, M.K., Ayvaz, M., Uysal, H., Sevindik, E., Örenay Boyacioğlu, S., & Yamaner, Ç. (2016). Order-wide in silico comparative analysis and identification of growth-regulating factor proteins in malpighiales. *Turkish Journal of Biology.* 40: 26-42. https://doi.org/10.3906/biy-1502-23

Bagalkoti, J.T., Pattar, V.P., & Nandibewoor, S.T. (2017). Square wave and differential pulse voltammetric methods for the analysis of olivetol at gold electrode. *Journal of Electrochemical Science and Engineering.* 7: 77. https://doi.org/10.5599/jese.382

Balmain, A., Gray, J., & Ponder, B. (2003). The genetics and genomics of cancer. Nat. Genet. 33:238–244

Baj-rossi, C., Micheli, G. De, & Carrara, S. (2012). Electrochemical detection of anti-breast-cancer agents in human serum by cytochrome P450-coated carbon nanotubes. *Sensors (Switzerland).* 12: 6520–6537. https://doi.org/10.3390/s120506520

BCPI (Breast Cancer Prevention Institute) (2007). Link: http://www.bcpinstitute.org/onlinepub.htm[Accessed: 12/06/2016]

Bhalla, N., Jolly, P., Formisano, N., & Estrela, P. (2016). Introduction to biosensors. *Essays in Biochemistry*, *60*(June). 1-8. http://doi.org/10.1042/EBC20150001

Bistolas, N., Wollenberger, U., Jung, C., & Scheller, F.W. (2005). Cytochrome P450 biosensors—a review. *Biosensors and Bioelectronics*. 20: 2408-2423

Bisswanger, H. (2014). Enzyme assays. *Perspectives in science.* 1: 41-55. https://doi.org/10.1016/j.pisc.2014.02.005

Bjornsson, T.D., Callaghan, J.T., Einolf, H.J., Fischer, V., Gan L., Grimm, S.; Kao, J.; King, P.S.; Miwa, G.; Ni, L.; Kumar, G.; McLeod, J.; Obach, S.R.; Roberts S., Roe A., Shah A., Snikeris F., Sullivan J.T., Tweedie D., Vega J.M., Walsh J., Wrighton S.A.

(2003) The conduct of in vitro and in vivo drug-drug interaction studies: A pharmaceutical research and manufacturers of America (PhRMA) perspective. *Drug Metab.Dispos.* 31: 815-832

Blatt, N.L., Mingaleeva, R.N., Khaiboullina, S.F., Kotlyar, A., Lombardi, V.C., & Rizvanov, A.A. (2013). *In vivo* screening models of anticancer drugs. *Life Science Journal*. 10

Borges, S., Desta, Z., Li L., Skaar, T.C., Ward, B.A., Nguyen, A., Jin, Y., Storniolo, A.M., Nikoloff, D.M., Wu L., Hillman G., Hayes D.F., Stearns V., Flockhart D.A. (2006). Quantitative effect of CYP2D6 genotype and inhibitors on tamoxifen metabolism: implication for optimization of breast cancer treatment. *Clin Pharmacol Ther*. 80: 61-74

Bonifacio, A., Millo, D., Keizers, P.H.J., Boegschoten, R., Commandeur, J.N.M., Vermeulen, N. P. E., & Van Der Zwan, G. (2008). Active-site structure, binding and redox activity of the heme-thiolate enzyme CYP2D6 immobilized on coated Ag electrodes: A surface-enhanced resonance Raman scattering study. *Journal of Biological Inorganic Chemistry*. 13: 85-96. https://doi.org/10.1007/s00775-007-0303-1

Bradford, M. (1976) *Anal. Biochem.* 72: 248

Brandt, W.E., Chiewsilp, D., Harris, D.L., & Russell, P.K. (1970). Thermo scientific pierce protein purification technical handbook version 2. *The Journal of immunology.* 105

Brauch, H., Mürdter, T.E., Eichelbaum, M., & Schwab, M. (2009). Pharmacogenomics of tamoxifen therapy. *Clinical Chemistry*, 55: 1770-1782. http://doi.org/10.1373/clinchem.2008.121756

Brauch, H., & Schwab, M. (2014). Prediction of tamoxifen outcome by genetic variation of CYP2D6 in post-menopausal women with early breast cancer. *British Journal of Clinical Pharmacology.* 77: 695-703. https://doi.org/10.1111/bcp.12229

Briesemeister, S., Rahnenführer, J., & Kohlbacher, O. (2010). YLoc-an interpretable web server for predicting subcellular localisation. *Nucleic Acids Research.* 38: 497-502. https://doi.org/10.1093/nar/gkq477

Brosius, J., Erfle, M., & Storella, J. (1985). Spacing of the -10 and -35 regions in the tac promoter. J. *Biol. Chem.* 260: 3539-3541

Brunelle, E., Huynh, C., Alin, E., Eldridge, M., Le, A.M., Halámková, L., & Halámek, J. (2018). Fingerprint analysis: moving toward multi-attribute determination via individual markers. *Analytical Chemistry.* 90: 980-987. https://doi.org/10.1021/acs.analchem.7b04206

Busti, A.J. (Ed) (2015). Genetic polymorphisms of the CYP3A4 enzyme and potential influence on drug efficacy and/or safety. *ebmconsult.com*. https://www.ebmconsult.com/articles/genetic-polymorphisms-cytochrome-p450-cyp3a4-enzyme

Burstein, H.J., Griggs, J.J., Prestrud, A.A., Temin, S. (2010). American society of clinical oncology clinical practice guideline update on adjuvant endocrine therapy for women with hormone receptor-positive breast cancer. *J Oncol Pract*. 6: 243-6. PubMed PMID: 21197188

Cali, J. J., Ma, D., Sobol, M., Good, T., Liu, D., & Corporation, P. (2006). P450 - GLO ™ CYP2C19 and CYP2D6 assays and screening systems: The method of choice for *in vitro* P450 assays, bioluminescent CYP2D6 and CYP2C19 Assays. *Cell Notes*. 14: 2-6.

Cali, J. J., Ma, D., Wood, M. G., Meisenheimer, P.D., & Klaubert, D. H. (2012). Bioluminescent assays for ADME evaluation: Dialing in CYP selectivity with luminogenic substrates, *Expert opinion on drug metabolism & toxicology*. 8: 9, 1115-1130. https://doi.org/10.1517/17425255.2012.695345.

Capece, L., Estrin, D. A., & Marti, M. A. (2008). Dynamical characterization of the heme NO oxygen binding (HNOX) domain. Insight into soluble guanylate cyclase allosteric transition. *Biochemistry*. 47: 9416-9427. https://doi.org/10.1021/bi800682k

Cavallini, A. (2013). An implantable biosensor array for personalized therapy applications. *5819*

Cederbaum, A. I. (2014). Methodology to assay CYP2E1 mixed function oxidase catalytic activity and its induction. *Redox Biology*. 2: 1048-1054. https://doi.org/10.1016/j.redox.2014.09.007

Chang, M. (2012). Tamoxifen resistance in breast cancer. *Biomolecules & Therapeutics*. 20: 256-267. https://doi.org/10.4062/biomolther.2012.20.3.256

Chaudhary, V.K., Shrivastava, N., Verma, V., Das, S., Kaur, C., Grover, P., & Gupta, A. (2014). Rapid restriction enzyme-free cloning of PCR products: A high-throughput method applicable for library construction. *PLoS ONE*. 9: 1-11. https://doi.org/10.1371/journal.pone.0111538

Chen, C., Mireles, R.J., Campbell, S.D., Lin, J., Mills, J.B., Xu, J. J., & Smolarek, T.A. (2004). Differential interaction of HMG-CoA reductase inhibitors with ABCB1, ABCC2, and OATP1B1. *drug Metab dispos*. 33: 537-546. https://doi.org/10.1124/dmd.104.002477

Chen, A., & Shah, B. (2013). Electrochemical sensing and biosensing based on square wave voltammetry. *Analytical Methods*. 5: 2158. https://doi.org/10.1039/c3ay40155c

Cheng, J., Randall, A. Z., Sweredoski, M. J., & Baldi, P. (2005). SCRATCH: A protein structure and structural feature prediction server. *Nucleic Acids Research.* 33: 72-76. https://doi.org/10.1093/nar/gki396

Crocetti, S., Beyer, C., Schade, G., Egli, M., Fröhlich, J., & Franco-Obregón, A. (2013). Low intensity and frequency pulsed electromagnetic fields selectively impair breast cancer cell viability. *PLoS ONE.* 8, e72944. https://doi.org/10.1371/journal.pone.0072944

Daly, A.K. (1996) Nomenclature for human CYP2D6 alleles. *Pharmacogenetics.*   6:193-201

Damia, G. & M. D'Incalci, 2009. Contemporarypre-clinical development of anticancer agents--what are the optimal preclinical models? *Eur. J. Cancer*. 45: 2768-2781

Deng, H.T. & Van Berkel, G.J. (1999). A thin-layer electrochemical flow cell coupled on-line with electrospray-mass spectrometry for the study of biological redox reactions. *Electroanalysis,* 11: 857-865

de Leon, J., Susce, M.T., Johnson M., Hardin, M., Maw, L., Shao, A., Allen, A.C., Chiafari, F.A., Hillman, G., Nikoloff, D.M. (2009). DNA microarray technology in the clinical environment: the AmpliChip CYP450 test for CYP2D6 and CYP2C19 genotyping. *CNS Spect.*, 14:19-34.

Dean, L., Pratt, V., & McLeod, H. (2016). Tamoxifen therapy and CYP2D6 genotype. *Medical Genetics Summaries.*1–11

Dehal, S. S., & Kupfer, D. (1999). Cytochrome P-450 3A and 2D6 catalyse ortho hydroxylation of 4- hydroxytamoxifen and 3-hydroxytamoxifen (droloxifene) yielding tamoxifen catechol: Involvement of catechols in covalent binding to hepatic proteins. *Drug Metabolism and Disposition.* 27: 681-688

Dehal, S. S., & Kupfer, D. (1997). CYP2D6 catalyses tamoxifen 4-hydroxylation in human liver. *Cancer Research.* 57: 3402-3406. https://doi.org/10.1126/science.8493571.15

Desta, Z., Ward, B.A., Soukhova, N.V. & Flockhart, D.A. (2004). Comprehensive evaluation of tamoxifen sequential biotransformation by the human   cytochrome   P450 system in vitro: prominent roles for CYP3A and CYP2D6. *The Journal of Pharmacology and Experimental Therapeutics.* 310: 1062-75

Dixon, B.M., Lowry, J. P., & O'Neill, R.D. (2002). Characterisation *in vitro* and *in vivo* of the oxygen dependence of an enzyme/polymer biosensor for monitoring brain glucose. *Journal of Neuroscience Methods*. 119: 135-142

Ding, S., Vardy A., Elcombe, C.R., & Wolf, C.R. (2017). An *in vitro* model for the prediction of chemical metabolism and toxicity. *CXR Biosciences Ltd.* Dundee, Scotland. http://www.conceptlifesciences.com/wp-content/uploads/2017/04/An-in-vitro-model-for-the-prediction-of-chemical-metabolism-and-toxicity.pdf

Ekwall, B., Silano, V., Paganuzzi-Stammati, A., & Zucco F. (1990). Toxicity tests with mammalian cell cultures in short-term toxicity tests for non-genotoxic effects (Eds Bourdeau, P.H, Somers, E.,Richardson, G.M. & Hickman, J.H. *SCOPE, John Wiley k Sons Ltd.* 75-7

Evan, G.I., Lewis, G.K., Ramsay, G., & Bishop, V.M. (1985). Isolation of monoclonal antibodies specific for c-myc proto-oncogene product. *Mol. Cell. Biol.* 5:3610-3616

Dean, L., Pratt, V., & McLeod, H. (2016). Tamoxifen therapy and cyp2d6 genotype. *Medical Genetics Summaries*, (Md). 1-11.

Dodgen, T.M., Hochfeld, W.E., Fickl, H., Asfaha, S.M., Durandt, C., Rheeder, P., & Pepper, M.S. (2013). Introduction of the AmpliChip CYP450 Test to a South African cohort: a platform comparative prospective cohort study. *BMC Medical Genetics*. 14: 20. http://doi.org/10.1186/1471-2350-14-20

Fakruddin, M., Mohammad Mazumdar, R., Bin Mannan, K. S., Chowdhury, A., & Hossain, M. N. (2013). Critical factors affecting the success of cloning, expression, and mass production of enzymes by recombinant *E. coli*. *ISRN Biotechnology*. 3: 1-7. https://doi.org/10.5402/2013/590587

Fantozzi, A., & Christofori, G. (2006). Mouse models of breast cancer metastasis. *Breast Cancer Research*. 8: 212

Fasinu, P., Bouic, P.J., Rosenkranz, B. (2012). Liver-based in vitro technologies for drug biotransformation studies - a review. *Curr Drug Metab*. 13: 215-224

FDA (Food and Drug Association) (2006). Tamoxifen. https://www.fda.gov/ohrms/dockets/ac/06/briefing/2006-4248B1-01-FDATamoxi fen%2 0Background%20Summary%20Final.pdf. [Accessed: 13/06/2016]

Ferlay, J, Soerjomataram, I, Ervik, M, Dikshit, R, Eser, S, Mathers, C, Rebelo, M, Parkin, DM, Forman, D, Bray, F. and GLOBOCAN (2012). Cancer incidence and mortality worldwide: IARC Cancer Base. 1: 11 [Internet]. Lyon, France: International Agency for Research on Cancer; 2012.http://globocan.iarc.fr, [Accessed: 13/06/2016]

Ferraldeschi, R., & Newman, W. G. (2010). The impact of CYP2D6 genotyping on tamoxifen treatment. *Pharmaceuticals*. 3: 1122-1138

Fleeman, N., Martin Saborido, C., Payne, K., Boland, A., Dickson, R., Dundar, Y., & Walley, T. (2011). The clinical effectiveness and cost-effectiveness of genotyping for CYP2D6 for the management of women with breast cancer treated with tamoxifen: a systematic review. *Health Technology Assessment (Winchester, England).* 15: 1-102. https://doi.org/10.3310/hta15330

Cowan, C., & Hoskins, R. (2007). Information preferences of women receiving chemotherapy for breast cancer. *European Journal of Cancer Care.* 16: 543-550. https://doi.org/10.1111/j.1365-2354.2007.00782

Folkerd, E. J., & Dowsett, M. (2010). Influence of sex hormones on cancer progression. *Journal of Clinical Oncology*. 28: 4038-4044. http://doi.org/10.1200/JCO.2009.27.4290

Franceschi, M., Scarcelli, C., Niro, V., Seripa, D., Pazienza, A.M., Pepe, G., Colusso, AM., Pacilli, L., & Pilotto, A. (2008). Prevalence, clinical features and avoidability of adverse drug reactions as cause of admission to a geriatric unit: a prospective study of 1756 patients. *Drug Saf*. 31: 545-56

Frere, C., Cuisset, T., Morange, P.E., Quilici, J., Camoin-Jau, L., Saut, N., & Alessi, M.C. (2008). Effect of Cytochrome P450 Polymorphisms on Platelet Reactivity After Treatment With Clopidogrel in Acute Coronary Syndrome. *American Journal of Cardiology.* 101:, 1088-1093. https://doi.org/10.1016/j.amjcard.2007.11.065

Frew, J.E., & Hill, H.A.O. (1988). Direct and indirect electron transfer between electrodes and redox proteins. *European Journal of Biochemistry.* 172: 261-269. https://doi.org/10.1111/j.1432-1033.1988.tb13882

Gaedigk, A., Bradford, L.D., Marcucci, K.A., & Leeder, J.S. (2002). "Unique CYP2D6 activity distribution and genotype-phenotype discordance in black Americans".*Clin. Pharmacol.Ther.* 72: 76–89. https://doi:10.1067/mcp.2002.125783. PMID 12152006

Garrido, J. M. P. J., Manuela, E., Garrido, P. J., Oliveira-Brett, A. M., & Borges, F. (2011). An electrochemical outlook on tamoxifen biotransformation: current and future prospects. *Current Drug Metabolism.* 12: 372-382. https://doi.org/BSP/CDM/E-Pub/000140

Garrido, J.M. P.J., Quezada, E., Fajín, J.L.C., Cordeiro, M.N.D.S., Garrido, E.M.P.J., & Borges, F. (2013). Electrochemical oxidation of tamoxifen revisited. *International Journal of Electrochemical Science*. 8: 5710-5723

Gasteiger, E., Hoogland, C., Gattiker, A., Duvaud, S., Wilkins, M. R., Appel, R. D., & Bairoch, A. (2005). Protein identification and analysis tools on the ExPASy Server. *The Proteomics Protocols Handbook.* 571-607. https://doi.org/10.1385/1592598900

Gill, S.C., & Von Hippel, P.H. (1989). Calculation of protein extinction coefficients from amino acid sequence data. *Analytical Biochemistry*. https://doi.org/10.1016/0003-2697(89)90602-7

Goetz, M., Kamal, A., &Ames, M. (2008). Tamoxifen Pharmacogenomics: The role of CYP2D6 as a predictor of drug response. C*linical Pharmacology and Therapeutics*. 83: 160-166. http://doi.org/10.1038/sj.clpt.6100367

Gonzalez, F.J & Yu, A.M (2006). Cytochrome P450 and xenobiotic receptor humanized mice. *Annu Rev Pharmacol Toxicol*. 46: 41-64

Goss, P.E.; Ingle, J.N., Martino, S., Robert, N.J., Muss, H.B., Piccart, M.J., Castiglione, M., Tu, D., Shepherd, L.E., Pritchard, K.I., Livingston, R.B., Davidson, N.E. Norton, L., Perez, E.A.; Abrams, J.S.; Cameron, D.A.; Palmer, M.J., & Pater, J.L. (2005). Randomized trial of letrozole following tamoxifen as extended adjuvant therapy in receptor-positive breast cancer: updated findings from NCIC CTG MA.17. J. *Natl. Cancer Inst*. 97: 262-1271

Grabski, A.C., & Burgess, R.R. (2001). Preparation of protein samples for SDS-polyacrylamide gel electrophoresis: procedures and tips. *In Novations*, 13: 10-12

Gräslund, S., Nordlund, P., Weigelt, J., Hallberg, B.M., Bray, J., Gileadi, O., & Gunsalus, K. C. (2008). Protein production and purification. *Nature Methods*. 5: 135-146. https://doi.org/10.1038/nmeth.f.202

Grieshaber, D., MacKenzie, R., Vörös, J., & Reimhult, E. (2008). Electrochemical biosensors sensor principles and architectures. *Sensors*. 8: 1400-1458. https://doi.org/10.3390/s80314000

Guruprasad, K., Reddy, B.V.B., & Pandit, M.W. (1990). Correlation between stability of a protein and its dipeptide composition: a novel approach for predicting *in vivo* stability of a protein from its primary sequence. *Protein Engineering, Design and Selection*. 4: 155-161. https://doi.org/10.1093/protein/4.2.155

Hacker, M., Messer W.S. & Bachmann K.A. (2009). Pharmacology: Principles and Practice. *Academic Press*. 216-217

Hamadeh, I.S., Langaee, T.Y., Dwivedi, R., Garcia, S., Burkley, B.M., Skaar, T. C., Chapman,A.B., Gums, J.G., Turner, S.T., Gong, Y., Cooper-DeHoff R.M. & Johnson, J.A. (2014). Impact of *CYP2D6* polymorphisms on clinical efficacy and tolerability of metoprolol tartrate. *Clinical Pharmacology & Therapeutics*. 96:175-181. https://doi: 10.1038/clpt.2014.62

Hardison, R. (1999). The Evolution of Hemoglobin: Studies of a very ancient protein suggest that changes in gene regulation are an important part of the evolutionary story.*American Scientist*. 87: 126

Hirokawa, T., Boon-Chieng, S., & Mitaku, S. (1998). SOSUI: classification and secondary structure prediction system for membrane proteins. *Bioinformatics* 14: 378-379. https://doi.org/10.1093/bioinformatics/14.4.378

Horn, J.R., & Hansten, P.D. (2008). Get to know an enzyme: CYP2C9. Available from: http://www.pharmacytimes.com/publications/issue/2008/2008-03/2008-03-8462.[Accessed: 11/06/2016]

Hoskins, J.M., Carey, L.A., & McLeod, H.L. (2009). CYP2D6 and tamoxifen: DNA matters in breast cancer. *Nat Rev Cancer*. 9: 576-586

Ikai, A. (1980). Thermostability and aliphatic index of globular proteins. *Journal of Biochemistry.* 1898: 1895-1898. https://doi.org/10.1017/CBO9781107415324.004

Ingelman-Sundberg M. (2004). Pharmacogenetics of cytochrome P450 and its applications in drug therapy: the past, present and future. *Trends Pharmacol Sci*. 25:193-200.

Ingelman-Sundberg, M., Sim, SC., Gomez, A., & Rodriguez-Antona, C. (2007). Influence of cytochrome P450polymorphisms on drug therapies: pharmacogenetic, pharmacoepigenetic and clinical aspects. *Pharmacol. Ther*. 116: 496-526

Isozymes, C. (2009). Short Communication ABSTRACT, 37: 1-4. https://doi.org/10.1124/dmd.108.023663

Iwuoha, E.I., Joseph, S., Zhang, Z., Smyth, M.R., Fuhr, U. & Ortiz, de Montellano, P.R. (1998). Drug metabolism biosensors: electrochemical reactivities of cytochrome P450cam immobilised in synthetic vesicular systems. *Journal of Pharmaceutical and Biomedical Analysis*. 17: 1101-1110

Jacob, F., & Monod, J. (1961). Genetic regulatory mechanisms in the synthesis of proteins. *Journal of Molecular Biology*. 3: 318-356. http://doi.org/https://doi.org/10.1016/S0022-2836(61)80072-7

Ji, L., Pan S., Marti-Jaun, J., et al (2002). Single-step assays to analyse CYP2D6 gene polymorphisms in Asians: allele frequencies and a novel *14B allele in mainland Chinese. *Clin Chem*. 48: 983-88

Jin, Y., Desta, Z., Stearns, V., Ward, B., Ho, H., Lee, K.H., Skaar, T., Storniolo, A.M., Li, L., Araba, A., Blanchard R., et al. (2005) CYP2D6 genotype, antidepressant use,

and	tamoxifen metabolism during adjuvant breast cancer treatment. *J. Natl. Cancer Inst*. 97:	30-39

Johansson, T.; Weidolf, L.; Jurva, U. (2007). Mimicry of phase I drug metabolism –novel methods for metabolite characterisation and synthesis. *Rapid Commun. Mass	Spectrom*. 21: 2323-2331

Johansson, I. & Ingelman-Sundberg, M. (2011). Genetic polymorphism and toxicology-with emphasis on cytochrome p450. *Toxicol Sci*. 120: 113

Johnson, J.A., & Lima, J.J. (2003). Drug receptor/effector polymorphisms and pharmacogenetics: current status and challenges. *Pharmacogenetics* .13: 525-34

Johnson, K.E., Forward, J.A., Tippy, M.D., Ceglowski, J.R., El-Husayni, S., Kulenthirarajan, R., & Battinelli, E.M. (2017). Tamoxifen directly inhibits platelet angiogenic potential and platelet-mediated metastasis. *Arteriosclerosis, Thrombosis, and Vascular Biology*. 37: 664-674. http://doi.org/10.1161/ATVBAHA.116.308791

Kalvass, J.C.; Tess, D.A., Giragossian, C., Linhares, M.C., Maurer, T.S. (2001). Influence of microsomal concentration on apparent intrinsic clearance: implications for scaling in vitro data. *Drug Metab.Dispos*. 29*:* 1337-1342

Khanjani, N., Noori, A. & Rostami, F. (2012). The knowledge and practice of breast cancer	screening among women in Kerman, Iran. *Al Ameen Journal of Medical Science* 5: 177-182

Kimple, M.E., Brill, A.L. and Pasker, R.L. (2013). Overview of affinity tags for protein purification. *Current	Protocols	in	Protein	Science*.	73:	9.9.1-9.9.23. https://doi.org/10.1002/0471140864.ps0909s73

Kitagishi, Y., Kobayashi, M., & Matsuda, S. (2013). Defective DNA repair systems and the development of breast and prostate cancer (Review). *International Journal of Oncology*. 42: 29-34. https://doi.org/10.3892/ijo.2012.1696

Koyun, A., Ahlatcolu, E., & Koca, Y. (2012). Biosensors and their principles. *A Roadmap of Biomedical Engineers and Milestones*. http://doi.org/10.5772/48824

Kramer, R.M., Shende, V.R., Motl, N., Pace, C.N., & Scholtz, J.M. (2012). Toward a molecular understanding of protein solubility: Increased negative surface charge correlates with increased solubility. *Biophysical Journal.* 102: 1907-1915. https://doi.org/10.1016/j.bpj.2012.01.060

Lamb, D.C., Lei, L., Warrilow, A.G.S., Lepesheva, G.I., Mullins, J.G.L., Waterman, M.R., & Kelly, S.L. (2009). The first virally encoded cytochrome P450. *Journal of Virology.* 83: 8266-8269. https://doi.org/10.1128/JVI.00289-09

Li, S.C., Squires, C.L., & Squires, C. (1984). Antitermination of *E. coli* rRNA transcription is caused by a control region segment containing lambda nut-like sequences. *Cell.* 38: 851-860

Lodish, H.F & National Library of Medicine. (2000). *Molecular cell biology* (4th ed). W.H. Freeman, New York

Lukong, K. E. (2017). Understanding breast cancer – The long and winding road. *BBA Clinical.* 7: 64-77. https://doi.org/10.1016/j.bbacli.2017.01.001

MacGregor, J.I. & Jordan, V.C. (1998). Basic guide to the mechanisms of antiestrogen action. *Pharmacol. Rev*. 50: 151-196

Mani, C. & Kupfer, D. (1991). Cytochrome P-450-mediated activation and irreversible binding of the antioestrogen tamoxifen to proteins in rat and human   liver: Possible involvement of flavin-containing monooxygenases in tamoxifen activation. *Cancer Res.* 51: 6052-6058

Manda, V., Avula, B., Dale, O., Chittiboyina, A., Khan, I., Walker, L., & Khan, S. (2015). Studies on Pharmacokinetic Drug Interaction Potential of Vinpocetine. *Medicines.* 2: 93-105. https://doi.org/10.3390/medicines2020093

MacGregor, J. I., & Jordan, V. C. (1998). Basic guide to the mechanisms of antiestrogen action. *Pharmacological Reviews*. 5: 151-196

Marchler-Bauer, A., Bo, Y., Han, L., He, J., Lanczycki, C. J., Lu, S., & Bryant, S. H. (2017). CDD/SPARCLE: Functional classification of proteins via subfamily domain architectures. *Nucleic Acids Research.* 45: 200-203. https://doi.org/10.1093/nar/gkw1129

Martins, D.M.F., Vidal, F.C.B., Souza, R.D.M., Brusaca, S.A., & Brito, L.M.O. (2014). Determination of CYP2D6 *3, *4, And *10 frequency in women with breast cancer in São Luís, Brazil, and its association with prognostic factors and disease-free survival. *Brazilian Journal of Medical and Biological Research.* 47*:* 1008-1015. https://doi.org/10.1590/1414-431X20143761

Martinkova, P., & Pohanka, M. (2016). Voltammetric biosensor based on a modified chitosan membrane enzyme peroxidase. *International Journal of Electrochemical Science.* 11: 10391-10406. https://doi.org/10.20964/2016.12.64

Mathew, S. (2010). An overview on the allelic variant of CYP2D6 genotype. *African Journal of Biotechnology*. 9: 9096-9102

McGraw, J., & Waller, D. (2012). Cytochrome P450 variations in different ethnic populations. *Expert Opinion on Drug Metabolism & Toxicology*. 8: 371-382. http://doi.org/10.1517/17425255.2012.657626

Meyer, U.A., & Zanger, U.M. (1997). Molecular mechanisms of genetic polymorphisms of drug metabolism. *Annu Rev Pharmacol Toxicol*. 37: 269-296

Miles, D., Chan, A., Romieu, G., et al (2008). Randomized, double-blind, placebo-controlled, phase III study of bevacizumab with docetaxel or docetaxel with placebo as first-line therapy for patients with locally recurrent or metastatic breast cancer (mBC): AVADO. *Proc Am Soc Clin Oncol*. 26

Mohanty, B.K., Raina, V., Gogia, A., Deo, S.V.S., and Shukla, N.K. (2012). Young patients with breast cancer (< 35 years): Single-institution study of 194 patients from India. *JClinOncol e11013*

Mohanty, C. (2017). Improvement of cancer therapy by nanotechnology.

Morrow, P.K., Serna, R., Broglio, K., Pusztai, L., Nikoloff, D.M., Hillman, G.R., Gonzalez-Angulo, A. M. (2012). Effect of CYP2D6 polymorphisms on breast cancer recurrence. *Cancer*. 118: 1221-1227. https://doi.org/10.1002/cncr.26407

Müller-Hill, B., Crapo, L., & Gilbert, W. (1968). Mutants that make more lac repressor. proc. *Natl. Acad. Sci. USA* 59. 1259-1262

Müller, M., Agarwal, N., & Kim, J. (2016). A cytochrome P450 3A4 biosensor based on generation 4.0 PAMAM dendrimers for the detection of caffeine. *Biosensors*. 6 http://doi.org/10.3390/bios6030044

Mulligan, M. E., Brosius, J., & Clure, W. R. (1985). Characterization in vitro of the effect of spacer length on the activity of *E. coli* RNA polymerase at the tac promoter. J. Biol. Chem. 260: 3539-3538

Nambiar, S., & Yeow, J.T.W (2011). Conductive polymer-based sensors for biomedical applications biosensors and bioelectronics 26: 1825-1832

Narasimhulu, S. (2010). New cytochrome P450 mechanisms: implications for understanding molecular basis for drug toxicity at the level of the cytochrome. *Expert Opinion on Drug Metabolism & Toxicology*. 6: 1-15. https://doi.org/10.1517/17425250903329095

NCCN Guidelines (National Comprehensive Cancer Network clinical practice guidelines in oncology) (2014). Breast Cancer Version 3. Available from: http://www.nccn.org/ [Last accessed: 31 May 2017]

NCI (National Cancer Institute) (2015 August 26) "Tamoxifen Citrate". http://www.cancer.gov/aboutcancer/treatment/drugs/tamoxifencitrate [Retrieved 29 April 2016]

Negi, B., Salvi, P., Bhatt, D., Majee, M., & Arora, S. (2017). Molecular cloning, in-silico characterization and functional validation of monodehydroascorbate reductase gene in Eleusine coracana. *PLoS ONE*. 12: 1-29. http://doi.org/10.1371/journal.pone.0187793

Nelson, D. (2009). Cytochrome P450 homepage. *Human Genomics*. 4: 59-65

Newman, W.G., Hadfield, K.D., Latif, A., Roberts, S.A., Shenton, A., McHague, C., Lalloo, F., Howell, S., & Evans, D.G. (2008) Impaired tamoxifen metabolism reduces survival in familial breast cancer patients. *Clin Cancer Res.* 14: 5913-5918.

Niiranen, L., Espelid, S., Karlsen, C. R., Mustonen, M., Paulsen, S. M., Heikinheimo, P., & Willassen, N. P. (2007). Comparative expression study to increase the solubility of cold adapted Vibrio proteins in *Escherichia coli*. *Protein Expression and Purification* 52: 210-218. https://doi.org/10.1016/j.pep.2006.09.005

Novillo, A., Romero-Lorca, A., Gaibar, M., Rubio, M., & Fernández-Santander, A. (2017). Tamoxifen metabolism in breast cancer treatment: Taking the focus off the CYP2D6 gene. *Pharmacogenomics Journal.* 17: 109-111. https://doi.org/10.1038/tpj.2016.73

Olins, P.O., Devine, C.S., Rangwala, S.H., and Kavka, K.S. (1988). T7 phage gene10 leader RNA, a ribosome-binding site the dramatically enhances the expression of foreign genes in *Escherichia coli*. *Gene.* 73: 227-235

Omotara, B., & Yahya, S. (2012). Awareness, attitude and practice of rural women regarding breast cancer in northeast Nigeria. *Journal of Community Medicine & Health Education*. 2: 2-5. http://doi.org/10.4172/2161-0711.1000148

Orosz, A., Boros, I., and Venetianer, P. (1991). Analysis of the complex transcription termination region of the *Escherichia coli* rrnB Gene. *Eur. J. Biochem*. 201: 653-659

Parkin, D.M., & Fernández, L. M.G. (2006). Use of statistics to assess the global burden of breast cancer. *Breast Journal.* 12: 70-80. https://doi.org/10.1111/j.1075-122X.2006.00205

Parker, K., Aasebø, W., Haslemo, T., & Stavem, K. (2016). Relationship between cytochrome P450 polymorphisms and prescribed medication in elderly haemodialysis patients. *SpringerPlus*. 5: 2-7. http://doi.org/10.1186/s40064-016-1986-y

Pawlik, A., Słomińska-Wojewódzka, M., & Herman-Antosiewicz, A. (2016). Sensitization of oestrogen receptor-positive breast cancer cell lines to 4-hydroxytamoxifen by isothiocyanates present in cruciferous plants. *European Journal of Nutrition.* 55: 1165-1180. https://doi.org/10.1007/s00394-015-0930-1

Penner, M.H. (2010). Food analysis. In Food Analysis, ed. SS Nielsen. 375-385. Boston, MA, USA: Springer

Pinto, N., & Dolan, M.E. (2011). Clinically relevant genetic variations in drug metabolizing enzymes. *Current Drug Metabolism.* 12: 487-497. https://doi.org/10.1016/j.pestbp.2011.02.012.Investigations

Popping, B., & Diaz-Amigo, C. (2014). The probability of obtaining: A correct and representative result in allergen analysis. *Agro Food Industry Hi-Tech.* 25: 29-31. http://doi.org/10.1007/978-1-4419-1478-1

Pratt, V., McLeod, H., Dean, L., Malheiro, A., & Rubinstein, W. (2012). Medical genetics summaries. *Medical Genetics Summaries*, Clopidogrel therapy and CYP2C19 genotype. https://doi.org/10.1007/s00439-006-0262-6

Rae, J.M., Sikora, M.J., Henry, N.L., Li L., Kim, S., Oesterreich, S., Skaar, T.C.,Nguyen, A.T., Desta. Z., Storniolo, A.M., Flockhart, D.A., Hayes, D.F., Stearns, V. (2009). Cytochrome P450 2D6 activity predicts discontinuation of tamoxifen therapy in breast cancer patients. *Pharmacogenomics J.* 9: 258-264

Reid, J. M., Goetz, M.P., Buhrow, S. A., Walden, C., Safgren, S.L., Kuffel, M.J. & Ames, M.M. (2014). Pharmacokinetics of endoxifen and tamoxifen in female mice: implications for comparative in vivo activity studies. *Cancer Chemotherapy and Pharmacology.* 74: 1271-1278. http://doi.org/10.1007/s00280-014-2605-7

Ramathuba, D.U., Ratshirumbi, C.T., & Mashamba, T.M. (2015). Knowledge, attitudes and practices toward breast cancer screening in a rural South African community. *Curationis.* 38: 1-8

Ranganatha, N., & Kuppast, I.J. (2012) A review on alternatives to animal testing methods in drug development. *Int. J. Pharm. Pharm. Sci.* 4: 28-32

Rawson, F.J., Downard, A.J., & Baronian, K.H. (2014). Electrochemical detection of intracellular and cell membrane redox systems in Saccharomyces cerevisiae. *Scientific Reports.* 4: 1-9. https://doi.org/10.1038/srep05216

Rehm, B.H.A. (2001). Bioinformatic tools for DNA/protein sequence analysis, functional assignment of genes and protein classification. *Applied Microbiology and Biotechnology.* 57: 579-592. https://doi.org/10.1007/s00253-001-0844-0

Roberts, R.L., & Kennedy, M.A. (2006). Rapid detection of common cytochrome P450 2D6 alleles in Caucasians. *Clin Chmi Acta.* 366: 348-51

Roche, (2016). Amplichip® CYP450 Test product monograph. Available from: http://www.roche.com/products/productdetails.htm?type=product%26id=17 [Accessed: 06/062016]

Rosano. G.L., & Ceccarelli, E.A. (2014). Recombinant protein expression in *Escherichia coli*: advances and challenges. *Frontiers in Microbiology.* 5: 172. http://doi.org/10.3389/fmicb.2014.00172

Rothbauer, U., Zolghadr, K., Muyldermans, S., Schepers, A., Cardoso, M. C., & Leonhardt, H. (2008). A Versatile Nanotrap for Biochemical and Functional Studies with Fluorescent Fusion Proteins. *Molecular & Cellular Proteomics*. 7: 282–289. http://doi.org/10.1074/mcp.M700342-MCP200

Roy, S.S & Vadlamudi, R.K (2012). Role of oestrogen receptor signalling in breast cancer metastasis. *International Journal of Breast Cancer.* 1-8. https://doi:10.1155/2012/654698

Ruzvidzo, O., Dikobe, T., Kawadza, D., H. Mabadahanye, G., Chatukuta, P., & Kwezi, L. (2013). Recombinant expression and functional testing of candidate adenylate cyclase domains. *Methods in molecular biology (Clifton, N.J.).* 1016. http://doi.org/10.1007/978-1-62703-441-8_2

Schoner, B.E., Belagaje, R.M., & Schoner, R.G. (1986). Translation of a synthetic two-cistron mRNA in *Escherichia coli*. Proc. *Natl. Acad. Sci. USA.* 83: 8506-8510

Shuman, S. (1994). Novel approach to molecular cloning and polynucleotide synthesis using vaccinia DNA topoisomerase. *J. Biol. Chem.* 269: 32678-32684

Sambrook, J., Fritsch, E.F., & Maniatis, T. (1989). Molecular cloning: A laboratory manual. 2nd Ed. Plainview, New York: Cold Spring Harbor Laboratory Press

Samer, C.F., Lorenzini, K.I., Rollason, V., Daali, Y., & Desmeules, J. A. (2013). Applications of CYP450 testing in the clinical setting. *Molecular Diagnosis & Therapy.* 17: 165-184.

Sassolas, A, Blum, L.J, Leca-Bouvier, B.D. (2011). Immobilization strategies to develop enzymatic biosensors. *Biotechnology Advances*. 30: 489-571

Schmid, F. (2001). Biological Macromolecules : UV-visible spectrophotometry. *Encyclopedia of Life Sciences.* 1-4. https://doi.org/10.1038/npg.els.0003142/abstrac

Schneider, E., & Clark, D.S. (2013). Cytochrome P450 (CYP) enzymes and the development of CYP biosensors. *Biosensors and Bioelectronics*. 39: 1-13. http://doi.org/10.1016/j.bios.2012.05.043

Shetti, N.P., Malode, S.J., & Nandibewoor, S.T. (2015). Electro-oxidation of captopril at a gold electrode and its determination in pharmaceuticals and human fluids. *Analytical Methods*, 7: 1-10. https://doi.org/10.1039/c5ay01619c

Shumyantseva, V., Bulko, T., Sigolaeva, L., Kuzikov, A., Shatskaya, M., & Archakov, A. (2015). Electrosynthesis and binding properties of molecularly imprinted poly-o-phenylenediamine as artificial antibodies for electroanalysis of myoglobin. *Doklady Biochemistry and Biophysics.* 464. http://doi.org/10.1134/S1607672915050038

Siddiqui, M. A., Alhadlaq, H. A., Ahmad, J., Al-Khedhairy, A. A., Musarrat, J., & Ahamed, M. (2013). Copper oxide nanoparticles induced mitochondria mediated apoptosis in human hepatocarcinoma cells. *PLOS ONE*. 8: 69534. Retrieved from https://doi.org/10.1371/journal.pone.0069534

Siddiqui, M.R., Al-Othman, Z.A., & Rahman, N. (2017). Analytical techniques in pharmaceutical analysis: A review. *Arabian Journal of Chemistry.* 10: 1409-1421. https://doi.org/10.1016/j.arabjc.2013.04.016

Singer, J.M. (1998). The pharmacokinetics and metabolism of ifosfamide during bolus and infusional administration: A randomized cross-over study. *Br. J. Cancer.* 77: 978-984.

Singh, A., Bhat, T.K., Sharma, O.P. (2011). Clinical Biochemistry of Hepatotoxicity. *J Clinic Toxicol.* 4: 001. https://doi:10.4172/2161-0495.S4-001

Singh, K.P., Dhruva, A.A., Flowers, E., Kober, K.M., & Miaskowski, C. (2018). A review of the literature on the relationships between genetic polymorphisms and chemotherapy-induced nausea and vomiting. *Critical Reviews in Oncology/Hematology*, 121: 51-61. https://doi.org/10.1016/j.critrevonc.2017.11.012

Smith, L.L Brown, K., Carthew, P., Lim, C.K., Martin, E.A., Styles, J., & White, I.N.H. (2000). Chemoprevention of breast cancer by tamoxifen: risks and opportunities. *Crit. Rev. Toxicol*. 30: 571-594

Souza, E. De, Giselle, G., & Melo, R. De. (2010). Electrochemical biosensors in pharmaceutical analysis. *Brazilian Journal of Pharmaceutical Sciences.* 46: 1-19. https://doi.org/10.1590/S1984-82502010000300002

Stem Cell Technology. (2016). Mouse mammary stem cells. Available from: https://www.stemcell.com [Accessed 15/07/2016]

Subehan, U.T., Kadota, S. & Tezuka, Y. (2006) Mechanism-based inhibition of human liver microsomal cytochrome P450 2D6 (CYP2D6) by alkamides of Pipernigrum. *Planta Med*. 72: 527-532

Sugerman, D. (2013). Tamoxifen update. *JAMA*. 310: 866. Retrieved from http://dx.doi.org/10.1001/jama.2013.58662

Sun, D., Cai, C., Xing, W., & Lu, T. (2004). Immobilization and direct electrochemistry of copper-containing enzymes on active carbon. *Chinese Science Bulletin.* 49: 2452-2454. https://doi.org/10.1360/04wb0070

Surekha, D., Sailaja, K., Rao, D.N. (2010). CYP2D6*4 polymorphisms and breast cancer risk. *Biology and Medicine*. 2: 49-55

Travis, R. C., & Key, T. J. (2003). Oestrogen exposure and breast cancer risk. *Breast Cancer Research*, 5:239-247. http://doi.org/10.1186/bcr628

Taylor, P. (2007). Cytochrome P450 2D6 (CYP2D6) bioelectrode for fluoxetine. 37-41. https://doi.org/10.1081/AL-120030288

Travis, R. C., & Key, T. J. (2003). Oestrogen exposure and breast cancer risk. *Breast Cancer Research.* 5: 239-247. https://doi.org/10.1186/bcr628

Torre, L.A., Siegel, R.L., Ward, E.M., & Jemal, A. (2016). Global cancer incidence and mortality rates and trends - An update. *Cancer Epidemiology Biomarkers & Prevention.* 25: 16-27. https://doi.org/10.1158/1055-9965.EPI-15-0578

Turanli-Yildiz C., Alkim Z., & Cakar P. (2012). Protein engineering methods and applications, protein engineering, Kaumaya, P (Ed.). ISBN: 978-953-51-0037-9. http://www.intechopen.com/books/protein-engineering/protein-engineering-methods-and -applications [Access: 13/13/2018]

Vincentelli, R., Canaan, S., Campanacci, V., Valencia, C., Maurin, D., Frassinetti, F. & Bignon, C. (2009). High-throughput automated refolding screening of inclusion bodies. *Protein Science.* 13: 2782-2792. https://doi.org/10.1110/ps.04806004

Vigneshvar, S., Sudhakumari, C.C., Senthilkumaran, B., & Prakash, H. (2016). Recent advances in biosensor technology for potential applications - An overview. *Frontiers in Bioengineering and Biotechnology.* 4: 11. http://doi.org/10.3389/fbioe.2016.00011

Vuignier, K.., Veuthey, J.-L., Carrupt, P.-A., & Schappler, J. (2013). Global analytical strategy to measure drug–plasma protein interactions: From high-throughput to in-depth analysis. *Drug Discov. Today*. 18: 030-1034

Wang, Z., Zou, Q., Jiang, Y., Ying, J., Xiangxiang, Z. (2014). Review of protein subcellular localization prediction. *Curr. Bioinf.* 9: 331-342

Wang, D., Papp, A.C., & Sun, X. (2015). Functional characterization of CYP2D6 enhancer polymorphisms. *Human Molecular Genetics.* 24: 1556-1562. https://doi.org/10.1093/hmg/ddu566

Willis, M.S., Hogan, J.K., Prabhakar, P., Liu, X., Tsai, K., Wei, Y., & Fox, T. (2005). Investigation of protein refolding using a fractional factorial screen: A study of reagent effects and interactions. *Protein Science.* 14: 1818-826. https://doi.org/10.1110/ps.051433205

Yang, Z., Zhang, L., Zhang, Y., Zhang, T., Feng,Y., Lu X., … Wang X. (2011). Highly efficient production of soluble proteins from insoluble inclusion bodies by a Two-Step-Denaturing and refolding method. *PLoS ONE.* 6: 1-8. https://doi.org/10.1371/journal.pone.0022981

Yang, Z., & Xiong, H.-R. (2012). Culture conditions and types of growth media for mammalian cells. In L. Ceccherini-Nelli and B. Matteoli (ed.), *Biomedical Tissue Culture.* 3-18. InTech. ISBN 978-953-51-0788-0. http://dx.doi.org/10.5772/3071

Yarman, A., & Scheller, F. W. (2014). The first electrochemical MIP sensor for tamoxifen. *Sensors (Switzerland)*, 14: 7647-7654. http://doi.org/10.3390/s140507647

Yoo, E.H., & Lee, S.Y. (2010). Glucose biosensors: An overview of use in clinical practice. *Sensors.* 10: 4558-4576. https://doi.org/10.3390/s100504558

Yuan, T. (2017). Nanostructured gold: applications in the study of drug metabolism [Groningen]: University of Groningen

Yuvaraj, S., & Comalada, M. (2007). Repertoire of IgA and IgG in inflamed and non-inflamed ileum of Crohn's. *and Disease.* Retrieved from http://dissertations.ub.rug.nl/FILES/faculties/medicine/2007/s.yuvaraj/thesis.pdf#page=85. [Accessed; 22/03/2018]

Zanger, U.M., Raimundo,S. & Eichelbaum, M. (2004). Cytochrome P450 2D6: overview and update on pharmacology, genetics, and biochemistry. *Naunyn Schmiedebergs Arch Pharmacol.* 369: 23-37

Zhang, X.H.F., Wang, Q., Gerald, W., Hudis, C.A., Norton, L., Smid, M., & Massagué, J. (2009). Latent bone metastasis in breast cancer tied to Src-dependent survival signals. *Cancer Cell.* 16: 67-78

Zhou, S.F. (2009). Polymorphism of human cytochrome P450 2D6 and its clinical significance: Part I. *Clin Pharmacokinet.* 48: 689-723.

Zhou, L.P., Luan, H., Dong, X.H., Jin, G.J., Man, D.L., & Shang, H. (2012). Genetic variants of CYP2D6 gene and cancer risk: A huge systematic review and meta-analysis. *Asian Pacific Journal of Cancer Prevention.* 13: 3165-3172. https://doi.org/10.7314/APJCP.2012.13.7.3165

Appendix

Appendix I: Chemicals, stock solutions, buffers, bacterial strains, and preparation of gels

A. Stock solutions, buffers and media

2 X SDS sample buffer: 4 % SDS, 0.125 M Tris pH 6.8, 15 % glycerol, 1 mg/ml Bromophenol Blue, 2 M DTT stored at -20 °C.

Ammonium persulphate (APS): 10 % stock was prepared by dissolving 1g of APS in 10 ml distilled water.

Ampicillin 50 mg/ml: 50 mg/ml ampicillin in distilled water.

Bacterial strains: TOP10 competent cells

Bovine Serum albumin (BSA)

Coomassie Brilliant Blue staining buffer: 2g Coomassie blue R-250, 45 % methanol and 10 % glacial acetic acid.

Destain solution: 30 % methanol, 10 % glacial acetic acid made up with distilled water.

Dithiothreitol (DTT): 0.5 M DTT was dissolved in distilled water.

Electrophoresis buffer: 10 % stock solution prepared by dissolving 30 g Tris-Cl, 144 g Glycine, 10 g SDS, made up to 1000 ml with distilled water.

Elution buffer: 50 mM NaH_2PO_4, 300 mM NaCl, 250 mM Imidazole, and pH adjusted to 8.0 with NaOH.

Glucose 20 %: 20 g of glucose in distilled water.

IPTG (Isopropyl-1-thio- (D-galactoside)): 0.1 M stock solution prepared by dissolving 1.19 g IPTG dissolved in 50 ml water. Solution divided into 5 ml aliquots, sterilized by filtration and stored at -20 °C. Stable for 2 to 4 months.

Luria Broth (LB) medium: 10 g pancreatic digest, 5 g yeast extract, 5 g NaCl.

LB agar: LB medium containing 15 g/l Bacteriological Agar.

Lysis buffer: 0.1 M sodium buffer (0.1 M sodium monobasic and 0.1 M sodium dibasic), 1x Triton-X100, 1 mM dithiolthreitol (DTT), 100 μg/ml of lysozyme, 1 mM phenylmethylsulfonyl fluoride (PMSF).

Phenylmethylsulfonyl fluoride (PMSF): 1 mM PMSF in distilled water.

Primers: 100 μM stock solutions stored at -20 °C.

SDS loading dye 2X: 10 % SDS, 0.2 M Tris, p H 6.8, 20 % glycerol, 0.05 % Bromophenol Blue, 10 mM DTT.

SDS running buffer 10X: 30 g Tris base, 144 g glycine, and 10 g SDS were in distilled water, and the volume was filled to 1000 ml.

SDS: 10 % stock solution prepared by dissolving 100 g of SDS was dissolved in 900 ml water, heated to 68 °C to dissolve the crystals, and the volume made up to 1000 ml. Stored at room temperature

Separating buffer: 1.5 M Tris pH 8.8, stored at 4 °C.

Sodium phosphate buffer 50 mM: 0.2 M sodium phosphate dibasic anhydrous and 0.2 M sodium phosphate monobasic anhydrous were dissovled in distilled water to pH 8.0 and the diluted to 50 mM.

SOC media: 1.5 % yeast extract, 1 % Bacto-Tryptone, 10 mM NaCl, 2 mM KCl, 10mM MgCl$_2$, 20 mM glucose.

Stacking buffer: 0.5 M Tris pH 6.8, stored at 4 °C.

Tris/Borate/EDTA (TBE) 10X: 108 g Tris base, 55 g boric acid, and 705 g EDTA were dissolved in distilled water, and filled into 1000 ml.

Tris-Cl: 1 M stock solution prepared by dissolving 121.4 g in 500 ml of distilled water, pH adjusted with HCl and the volume made up to 100 ml.

Urea lysis buffer: 200 mM NaCl, 50 mM Tris-Cl; pH 8.0, 500 mM glucose, 0.05 % (w/v) PEG, 20 mM β-mercaptoethanol, 8 M urea, 10 mM imidazole

Wash buffer 1: 300 mM NaCl, 50 mM sodium buffer, pH 8.

Wash buffer 2: 300 mM NaCl, 50 mM sodium buffer, 10 mM Imidazole, pH 8.0.

Wash buffer 3: 300 mM NaCl, 50 mM sodium buffer, 20 mM Imadazole, pH 8.0.

Wash buffer 4: 300 mM NaCl, 50 mM sodium buffer, 50 mM Imidazole pH 8.0.

B. The preparation of 1 % agarose gel and DNA samples:

In order to prepare a 1 % agarose gel, 1g of agarose was weighed out and dissolved in 100 ml of 1x TBE. The mixture was microwaved for 1.5 min for the gel to dissolve. After heating, it was allowed to cool such that it still allows for pouring into the casting tray with the comb for wells making. The comb was removed once the agarose solidified. About 2 µl of the loading dye was mixed with 10 µl of the DNA samples each time loading is done . The samples were then electrophoresed at 100V for 1 h.

C. SDS-PAGE gel preparation

The stacking gel of 5 % and separating gel of 12 % acrylamide were prepared as shown in Table 1. The separating gel was prepared first, poured between the spacer plates and enough space was left for the stacking gel. Isopropanol was placed on top the separating gel and the gel was left to set for 20 min at room temperature. Once solidified the isopropanol was

thrown off on paper towel and the stacking gel was prepared and loaded on top off the separating gel. This was followed by immediately placing 1 mm well combs between the spacer plates to form wells.

Table 1: Preparation of 12 % SDS-PAGE gel

Gel type	Stacking gel	Separating gel
Acrylamide %	5%	12%
30 % Polyacrylamide (ml)	0.67	4
0.5 M Tris, pH 6.8 (ml)	1.25	-
1.5 M Tris, pH 8.8 (ml)	-	2.6
10 % Ammonium persulfate (ml)	0.05	0.1
10% SDS (ml)	0.05	0.1
TEMED (ml)	0.006	0.01
dH$_2$O (ml)	2.975	3.2
Total volume (ml)	5	10

D. Protein sample preparation

The protein lysates or pellets of cells carrying recombinant CYP2D6 were mixed with 2 X SDS-loading dye (10 % SDS, 0.2 M Tris, p H 6.8, 20 % glycerol, 0.05 % Bromophenol Blue, 10 mM DTT) followed by incubation at 95 °C for 5 min. The samples were then loaded on a 12 % 1D SDS-PAGE gel and ran at the voltage of 100 V in 1X SDS running buffer (25 mM Tris, 192 mM glycine, 0.1 % glycine, 0.1 % SDS). Following electrophoresis, the gels were stained with Coomassie Brilliant Blue staining buffer (2g Coomassie blue R-250, 45 % methanol and 10 % glacial acetic acid) for 20 min and then destained with a destaining solution (30 % methanol, 10 % glacial acetic acid made up with distilled water).

Appendix II: Prediction of protein parameters for the CYP2D6 protein

```
              10          20          30          40          50
        MGLEALVPLA MIVAIFLLLV DLMHRRQRWA ARYPPGPLPL PGLGNLLHVD FQNTPYCF

              70          80          90         100         110        1
        LRRRFGDVFS LQLAWTPVVV LNGLAAVREA LVTHGEDTAD RPPVPITQIL GFGPRSQG

             130         140         150         160         170        1
        FRPNGLLDKA VSNVIASLTC GRRFEYDDPR FLRLLDLAQE GLKEESGFLR EVLNAVPV

             190         200         210         220         230        2
        HIPALAGKVL RFQKAFLTQL DELLTEHRMT WDPAQPPRDL TEAFLAEMEK AKGNPESS

             250         260         270         280         290        3
        DENLCIVVAD LFSAGMVTTS TTLAWGLLLM ILHPDVQRRV QQEIDDVIGQ VRRPEMGD

             310         320         330         340         350        3
        HMPYTTAVIH EVQRFGDIVP LGVTHMTSRD IEVQGFRIPK GTTLITNLSS VLKDEAVW

             370         380         390         400         410        4
        PFRFHPEHFL DAQGHFVKPE AFLPFSAGRR ACLGEPLARM ELFLFFTSLL QHFSFSVP

             430         440
        QPRPSHHGVF AFLVTPSPYE LCAVPR
```

References and documentation are available.

_____

Number of amino acids: 446

Molecular weight: 50053.97

Theoretical pI: 6.21

Amino acid composition: [CSV format]

Ala (A)	34	7.6%	
Arg (R)	33	7.4%	
Asn (N)	10	2.2%	
Asp (D)	23	5.2%	
Cys (C)	5	1.1%	
Gln (Q)	20	4.5%	
Glu (E)	26	5.8%	
Gly (G)	29	6.5%	
His (H)	15	3.4%	
Ile (I)	15	3.4%	
Leu (L)	60	13.5%	
Lys (K)	10	2.2%	
Met (M)	11	2.5%	
Phe (F)	30	6.7%	
Pro (P)	37	8.3%	
Ser (S)	18	4.0%	
Thr (T)	24	5.4%	
Trp (W)	5	1.1%	
Tyr (Y)	5	1.1%	
Val (V)	36	8.1%	
Pyl (O)	0	0.0%	
Sec (U)	0	0.0%	
(B)	0	0.0%	
(Z)	0	0.0%	
(X)	0	0.0%	

Total number of negatively charged residues (Asp + Glu): 49
Total number of positively charged residues (Arg + Lys): 43

Atomic composition:

```
Carbon      C        2275
Hydrogen    H        3552
Nitrogen    N         620
Oxygen      O         622
Sulfur      S          16
```

Formula: $C_{2275}H_{3552}N_{620}O_{622}S_{16}$
Total number of atoms: 7085

Extinction coefficients:

Extinction coefficients are in units of M^{-1} cm^{-1}, at 280 nm measured in water

```
Ext. coefficient    35200
Abs 0.1% (=1 g/l)   0.703, assuming all pairs of Cys residues form cystines
```

```
Ext. coefficient    34950
Abs 0.1% (=1 g/l)   0.698, assuming all Cys residues are reduced
```

Estimated half-life:

The N-terminal of the sequence considered is M (Met).

The estimated half-life is: 30 hours (mammalian reticulocytes, in vitro).
                           >20 hours (yeast, in vivo).
                           >10 hours (Escherichia coli, in vivo).

Instability index:

The instability index (II) is computed to be 42.05
This classifies the protein as unstable.

Aliphatic index: 96.61

Grand average of hydropathicity (GRAVY): 0.001

Figure 1: The full data of CYP2D6 protein parameters. (Computed using ProtParam Expasy tool).

## Appendix III: Prediction of functional domains CYP2D6 protein
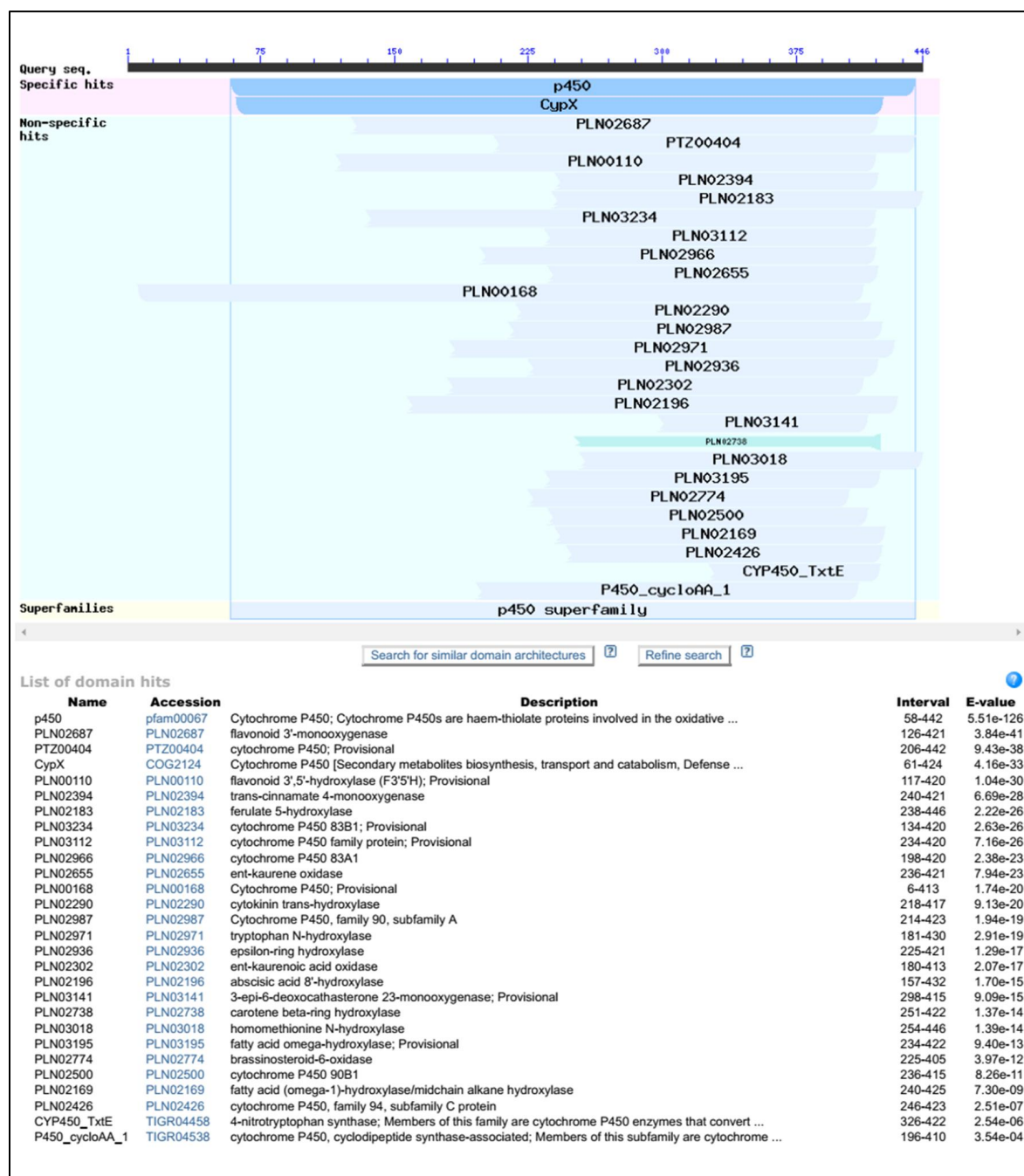
Figure 2: The full data of detailed functional domains of CYP2D6 protein. (computed using NCBI conserved domains server).

Appendix IV: Data for the determination of protein concentration using Bradford assay

Bradford assay

In order to determine protein concentration, the Bradford assay (Bradford, 1979) was performed using a 96 well microplate. The standard protein, Bovine serum albumin (BSA) was diluted in separate Eppendorf tubes starting with 2 mg/ml as seen in Table 2. Na-phosphate buffer (300 mM NaCl, 50 mM sodium buffer, 40 mM Imidazole) was used as the diluent. The various dilutions of BSA along with a 1:5 and 1:10 dilution of the protein sample were transferred to a 94 well microplate as seen in Table 3. The 1x Bradford reagent was added to the samples and the plate was placed on a mixer. The plate was then incubated at room temperature for 5 min and the samples were read at A_{595nm}. A standard curves were then plotted.in order to determine the concentration of unknown recombinant CYP2D6 protein concentrations (Figure 3).

Table 2: Microplate Bradford standard Assay

Tube number	Standard volume (µl)	Source of standard (BSA)	Diluent Buffer 4 (µl)	Final protein conc. (mg/ml)
1	20	2 mg/ml	0	2
2	30	2 mg/ml	10	1.5
3	20	2 mg/ml	20	1
4	20	Tube 2	20	0.75
5	20	Tube 3	20	0.5
6	20	Tube 5	20	0.25
7	20	Tube 6	20	0.125
8 (blank)	-	-	20	0

Table 3: Bradford reagent and protein standard volumes to be added to a microplate.

Assay	Volume of standard and sample	Volume of 1x Dye reagent
Microplate	5 µl	250 µl
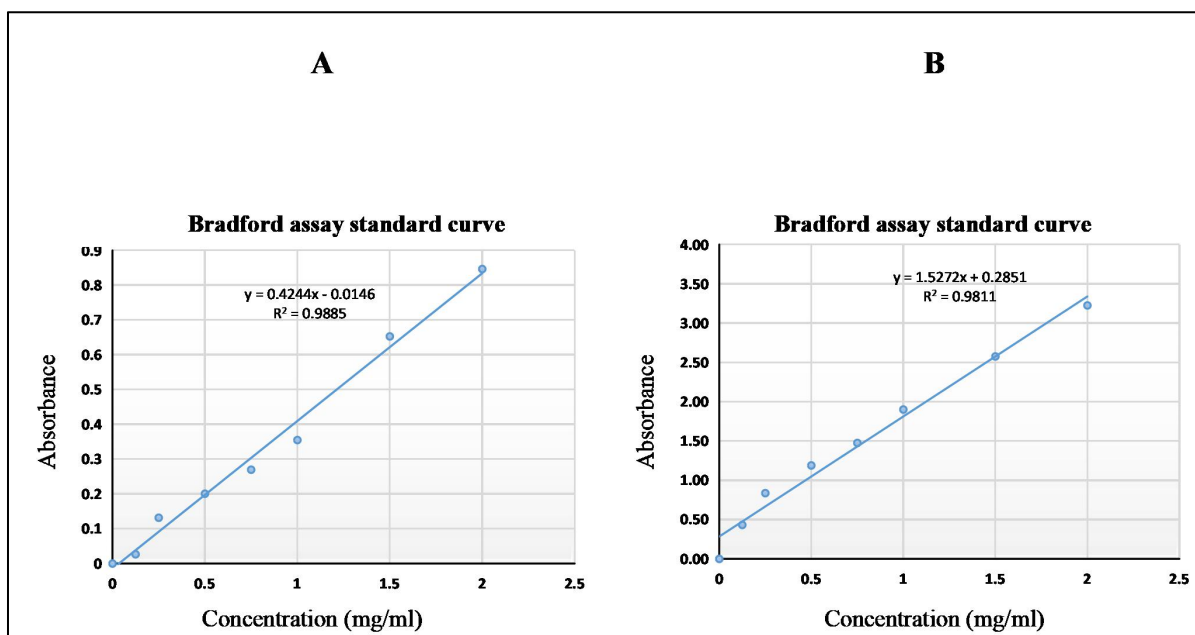
Figure 3: Standard curve of the BSA for the Bradford assay to determine the concentration of recombinant CYP2D6. A595 values corresponding to different standard (BSA) concentrations are plotted against concentration (mg/ml). The unknown concentration of CYP2D6 protein was determined using the measured absorbance values at 1:5 and 1:10 dilution factors. The values corresponding to the concentration are calculated using the formula corresponding to the straight line fitted to the data. (A) and (B) represent the standard curve unfolded and folded CYP2D6 respectively.